

Battery Storage Applications for Enterprise Users

Vasileios Papadopoulos

Doctoral dissertation submitted to obtain the academic degree of
Doctor of Electrical Engineering

Supervisors

Prof. Jan Desmet, PhD - Prof. Jos Knockaert, PhD
Department of Electromechanical, Systems and Metal Engineering
Faculty of Engineering and Architecture, Ghent University

July 2024



Battery Storage Applications for Enterprise Users

Vasileios Papadopoulos

Doctoral dissertation submitted to obtain the academic degree of
Doctor of Electrical Engineering

Supervisors

Prof. Jan Desmet, PhD - Prof. Jos Knockaert, PhD

Department of Electromechanical, Systems and Metal Engineering
Faculty of Engineering and Architecture, Ghent University

July 2024



ISBN 978-94-6355-855-6

NUR 959

Wettelijk depot: D/2024/10.500/60

Members of the Examination Board

Chair

Prof. Em. Luc Taerwe, PhD, Ghent University

Other members entitled to vote

Prof. Thierry Coosemans, PhD, Vrije Universiteit Brussel

Prof. Emmanuel De Jaeger, PhD, Université catholique de Louvain

Prof. Chris Develder, PhD, Ghent University

Prof. Dirk Van Hertem, PhD, KU Leuven

Prof. Lieven Vandevelde, PhD, Ghent University

Supervisors

Prof. Jan Desmet, PhD, Ghent University

Prof. Jos Knockaert, PhD, Ghent University

Battery Storage Applications for Enterprise Users

Abstract

The energy sector is undergoing a significant change on global scale. The climate change is pushing humanity away from conventional fossil fuel based energy sources; green energy technologies are becoming the new norm. Countries all over the world have committed to reduce their carbon footprint by investing massively in renewable energy sources such as wind power and photovoltaics (PV). Nevertheless, the growth of renewables comes at a price. The intermittent nature of wind and PV poses serious challenges to the electric grid. As forecasting uncertainty continues to rise, the grid must become more flexible. In response to this need, different market players are currently undertaking several actions.

Transmissions System Operators (TSOs) are uniting in Europe under a common pan-European framework with the aim to standardize the electricity balancing market and allow the most efficient transaction of balancing reserves. In the meantime, in the energy wholesale market, energy trading is shifting closer to the delivery date through spot markets (day-ahead and intraday); also here, major initiatives have been taken to increase flexibility and allow a more cost-effective market operation by creating the pan-European Single Day-Ahead Coupling (SDAC) and Single Intraday Coupling (SIDC). Furthermore, as Distribution System Operators (DSOs) are rolling out digital meters to enable energy monitoring and invoicing closer to real time, end users are incentivized to adapt their consumption and reduce electricity costs through dynamic pricing contracts.

To facilitate the green energy transition, system operators need to adopt a “prosumer” centric approach. The once typically passive end user is now interacting with the grid through decentral generation and flexible assets such as batteries, electric vehicles, heat pumps, etc. Among these technologies, especially battery storage can play a crucial role. Over the past decade, we have seen globally a tremendous research effort to valorize battery storage applications for prosumers. What is the value of battery storage for households, buildings or an industrial site? What kind of applications are available for the user? How should a battery be dimensioned or be controlled to provide a certain application? What are the options to combine different applications together for improving profitability?

In this PhD thesis, we address battery storage applications mainly from an enterprise user's perspective located in Belgium. Back in 2018, when this thesis was conceptualized, we set as ultimate goal the development of a software tool that will serve as a guide in battery storage projects. We imagined a master Energy Management System (EMS) that would conduct optimizations considering different applications concurrently e.g., increasing the self-sufficiency of the PV installation, peak demand reduction, ancillary services. This concept, maximizing the profitability by combining multiple revenue streams from diverse applications, is what we call "value stacking" and it is regarded by many as the holy grail for unleashing mainstream adoption of battery storage systems.

In a first step, we dedicated our research on exploring the electricity market in Belgium. In Chapter 2, we provide a bird's eye view on how the electricity market in Belgium works. How the market is structured in terms of the electricity unit traded (capacity or energy), the contract horizon, the products and the existing trading platforms and market operators. Next, we explain how these market mechanisms open up opportunities for battery storage. Finally, we decide to focus on three major applications that exhibit good potential for widespread adoption: (i) increasing the self-sufficiency of renewable energy systems, (ii) peak shaving, (ii) pricing arbitrage

In Chapter 3, we continue with a case study on increasing the self-sufficiency of a hybrid renewable energy installation comprising wind, PV, a hydrogen electrolyzer and batteries. We compare different battery technologies and assess their techno-economic impact. Afterwards, in Chapter 4, we carry out a study on the impact of the time resolution of the data inputs. We compare results conducted from two different scenarios (i) 10 min and (ii) 1 sec averaged power flow simulations in a hybrid battery-wind powered industrial site. In Chapter 5, we shift our focus on peak shaving. Here, we conduct a comparative techno-economic study on peak shaving for 40 different end users after introducing an analytic power flow model and an optimization method for dimensioning the battery storage system. Finally, Chapter 6 presents an optimization framework for day-ahead pricing arbitrage applications under peak shaving, considering a fully representative electricity invoicing model (in Flanders) and forecasting uncertainty in the load and power source.

In Chapter 7, we summarize some important conclusions and make suggestions for future research in the field. A major bottleneck in the development of a multi-objective EMS is certainly the unstable regulatory framework but also the inherent uncertainty caused by fluctuating prices and auction based trading platforms. From an investor's point of view, it is difficult to draw financial projections on the long term (5–10 years). A battery EMS is not like

a wind or PV installation that once it is commissioned simply injects power to the grid for the next decade. Conversely, a battery EMS needs to be sufficiently flexible to adapt according to the latest market evolutions whatever this might be e.g., electricity tariff model, balancing market rules, changes on the user's load infrastructure, forecasting analytics on power and price data. This poses serious challenges to project developers since it requires additional effort for maintaining and updating the software over its entire lifetime.

Our initial goal to build a master EMS that operates the battery in value stacking mode has not been accomplished as we imagined. Nevertheless, this thesis has generated valuable deliverables and insights for future research towards this direction. From our experience, we strongly recommend to approach the problem as a two-step optimization process. In a first step the EMS operates at daily resolution; every day the EMS decides which applications will be considered for the next day based on a kind of priority ranking e.g., (i) peak shaving, (ii) increasing self-sufficiency, (iii) ancillary services. In the second step, the EMS carries out repetitive intraday optimizations given the latest forecast data and current state of the user's infrastructure. Finally, we note that, over the past 2 years (2022–2024), this PhD thesis has been the foundation for the development of a software prototype (FlexLab – Flexible Laboratory, see Annex). FlexLab is a web application that provides a suite of energy tools designed for the non-expert end user covering a variety of interest areas such as visualization widgets, forecast analytics, alerts, optimization tools and more. The prototype is currently in valorization phase.

Beknopte samenvatting

De energiesector ondergaat op wereldschaal aanzienlijke veranderingen. De klimaatverandering duwt de mensheid weg van conventionele, op fossiele brandstoffen gebaseerde energiebronnen; Groene energietechnologieën worden de nieuwe norm. Landen over de hele wereld hebben zich ertoe verbonden hun ecologische voetafdruk te reduceren door massaal te investeren in hernieuwbare energiebronnen zoals windenergie en fotovoltaïsche zonne-energie (PV). Niettemin heeft de groei van hernieuwbare energiebronnen een prijs. Het intermitterende karakter van wind- en zonne-energie zorgt voor een aantal serieuze uitdagingen voor het elektriciteitsnet. Nu de onzekerheid over de voorspellingen blijft toenemen, moet het elektriciteitsnet flexibeler worden. Als antwoord op deze behoefte ondernemen verschillende marktspelers momenteel verschillende acties.

Transmissienetbeheerders (TNBs) verenigen zich in Europa onder een gemeenschappelijk pan-Europees raamwerk met als doel de balanceringsmarkt te standaardiseren en de meest efficiënte transactie van balanceringsreserves mogelijk te maken. Ondertussen verschuift de energiehandel op de groothandelsmarkt voor energie via spotmarkten (day-ahead en intraday) steeds dichterbij de leveringsdatum; ook hier zijn belangrijke initiatieven genomen om de flexibiliteit te vergroten en een meer kosteneffectieve marktwerking mogelijk te maken door het creëren van de pan-Europese Single Day-Ahead Coupling (SDAC) en Single Intraday Coupling (SIDC). Bovendien worden eindgebruikers, nu distributienetbeheerders (DNBs) digitale meters uitrollen om energiemonitoring en facturering dichterbij realtime mogelijk te maken, gestimuleerd om hun verbruik aan te passen en de elektriciteitskosten te verlagen door middel van dynamische prijscontracten.

Om de transitie naar groene energie te vergemakkelijken, moeten systeembeheerders een “prosumenten”-gerichte aanpak hanteren. De ooit typisch passieve eindgebruiker heeft nu interactie met het elektriciteitsnet via decentrale opwekking en flexibele middelen zoals batterijen, elektrische voertuigen, warmtepompen enz. Van deze technologieën kan vooral batterijopslag een cruciale rol spelen. De afgelopen tien jaar hebben we wereldwijd een enorme onderzoeksinspanning gezien om batterijopslagtoepassingen voor prosumenten te valoriseren. Wat is de waarde van batterijopslag voor huishoudens, gebouwen of een industrieterrein? Wat voor soort toepassingen zijn er beschikbaar voor de gebruiker? Hoe moet een batterij gedimensioneerd of aangestuurd worden om een bepaalde toepassing te kunnen bieden? Wat zijn de mogelijkheden als het gaat om het combineren van verschillende applicaties om de winstgevendheid van de use case te verbeteren?

In dit doctoraat behandelen we toepassingen voor batterijopslag voornamelijk vanuit het perspectief van een zakelijke gebruiker in België. In 2018, toen dit proefschrift werd geconceptualiseerd, stelden we als uiteindelijk doel de ontwikkeling van een softwaretool die als leidraad zal dienen bij batterijopslagprojecten. We stelden ons een master energiebeheersysteem (EMS) voor dat optimalisaties zou uitvoeren, rekening houdend met gelijktijdige verschillende toepassingen, b.v. het vergroten van de zelfvoorziening van de PV-installatie, vermindering van de piekvraag, ondersteunende diensten. Dit concept, dat de winstgevendheid maximaliseert door meerdere inkomstenstromen uit diverse toepassingen te combineren, is wat wij 'value stacking' noemen en wordt door velen beschouwd als de heilige graal voor het ontketenen van de mainstream adoptie van batterijopslagsystemen.

In een eerste stap hebben we ons onderzoek gewijd aan het verkennen van de elektriciteitsmarkt in België. In hoofdstuk 2 geven we een overzicht in vogelvlucht van hoe de elektriciteitsmarkt in België werkt. Hoe is de markt gestructureerd in termen van de verhandelde elektriciteitsseenheid (capaciteit of energie), de contracthorizon, de producten en de bestaande handelsplatformen en marktpartijen. Vervolgens leggen we uit hoe deze marktmechanismen kansen bieden voor batterijopslag. Ten slotte besluiten we ons te concentreren op drie belangrijke toepassingen die goede mogelijkheden bieden voor brede adoptie (i) het vergroten van de zelfvoorziening van hernieuwbare energiesystemen, (ii) peak shaving, (ii) prijsarbitrage

In hoofdstuk 3 gaan we verder met een case studie over het vergroten van de zelfvoorziening van een hybride hernieuwbare energie-installatie bestaande uit wind, PV, een waterstofelektrolyzer en batterijen. We vergelijken verschillende batterijtechnologieën en beoordelen hun techno-economische impact. Daarna voeren we in hoofdstuk 4 een onderzoek uit naar de impact van de tijdsresolutie van de gegevensinvoer. We vergelijken de resultaten van twee verschillende scenario's (i) 10 min en (ii) 1 sec gemiddelde power flow simulaties in een hybride batterij-windaangedreven industriële locatie. Later in hoofdstuk 5 verleggen we onze focus naar peak shaving. Hier voeren we een vergelijkend techno-economisch onderzoek uit naar peak shaving voor 40 verschillende eindgebruikers na de introductie van een analytisch power flow model en een optimalisatiemethode voor het dimensioneren van het batterijopslagsysteem. Ten slotte presenteren we in hoofdstuk 6 een optimalisatiekader voor day-ahead prijsarbitrage-toepassingen onder peak shaving, waarbij we een volledig representatief elektriciteitsfactureringsmodel (in Vlaanderen) in ogenschouw nemen en voorspellingsonzekerheid in de belasting en energiebron.

In hoofdstuk 7 vatten we enkele belangrijke conclusies samen en doen we suggesties voor toekomstig onderzoek op dit gebied. Een belangrijk knelpunt bij de ontwikkeling van een EMS met meerdere doelstellingen is zeker het onstabiele regelgevingskader, maar ook de inherente onzekerheid die wordt veroorzaakt door fluctuerende prijzen en op veilingen gebaseerde handelsplatforms. Vanuit het perspectief van een belegger is het moeilijk om financiële projecties op de lange termijn (5-10 jaar) te maken. Een batterij-EMS is niet zoals een wind- of PV-installatie die, zodra deze in gebruik is genomen, eenvoudigweg stroom aan het elektriciteitsnet injecteert voor de komende tien jaar. Omgekeerd moet een batterij-EMS voldoende flexibel zijn om zich aan te passen aan de laatste marktevoluties, wat deze ook mogen zijn. tariefmodel voor elektriciteit, balancingmarktregels, veranderingen in de infrastructuur van de gebruiker, voorspellingsanalyses van stroom- en prijsgegevens. Dit brengt serieuze uitdagingen met zich mee voor projectontwikkelaars, omdat het extra inspanningen vergt voor het onderhouden en updaten van de software gedurende de gehele levensduur ervan.

Ons oorspronkelijke doel om een master-EMS te bouwen dat de batterij in value stacking bedient, is niet bereikt zoals we ons hadden voorgesteld. Niettemin heeft dit proefschrift waardevolle resultaten en inzichten opgeleverd voor toekomstig onderzoek in deze richting. Vanuit onze ervaring raden we ten eerste aan om het probleem te benaderen als een optimalisatieproces dat uit twee stappen bestaat. In een eerste stap werkt het EMS op dagelijkse resolutie; elke dag beslist het EMS welke toepassingen de volgende dag in behandeling zullen worden genomen op basis van een soort prioriteitsrangschikking, b.v. (i) peak shaving, (ii) vergroten van de zelfvoorziening, (iii) ondersteunende diensten. In de tweede stap voert het EMS repetitieve intraday-optimalisaties uit op basis van de nieuwste voorspellingsgegevens en de huidige status van de infrastructuur van de gebruiker. Tenslotte merken we op dat dit proefschrift de afgelopen 2 jaar (2022-2024) de basis heeft gelegd voor de ontwikkeling van een softwareprototype (FlexLab – Flexibel Laboratorium, zie bijlage). FlexLab is een webapplicatie die een reeks energietools biedt die zijn ontworpen voor de niet-deskundige eindgebruiker en die een verscheidenheid aan interessegebieden bestrijkt, zoals visualisatiewidgets, voorspellingsanalyses, waarschuwingen, optimalisatietools en meer. Het prototype bevindt zich momenteel in de valorisatiefase.

Acknowledgements

Back in 2016, I was a young electrical engineer working in the industry when I noticed an interesting vacancy at Ghent university. I didn't believe at all that I stood a chance to get the job. Nevertheless, I gave it a shot and finally was hired! I couldn't believe how much my life would change from that moment.

Soon, my career at Ghent university will end, I have to move on and open a new chapter in my life. I am sure I will be thinking nostalgically back to those 8 years of "beautiful" working experiences. But why would that trip be remembered as "beautiful" ? Was it the team, my colleagues, the place, the working conditions, the projects I was involved in, the tasks I did, the meetings and the barbecues ? I would say that it was the combination of all those things together that synthesized a series of "beautiful" moments.

And as in every orchestration process there is always a main composer, so was it in my case. The chance for a PhD student having a supervisor like prof. Jan Desmet is the 1 in 1,000,000 times (*"and I certainly have some data to support this statement"*). I want to thank Jan simply for being the best boss I could imagine. When you have a personal problem, he is the very first person at work you want to talk with, always available to help and even if he doesn't have time, he will make time for you too. When the team needs some time to disconnect from the hard work, he will take us out to breathe, talk, eat and laugh, as simple as that but certainly highly uncommon for the typical boss, supervisor or prof. When you need guidance, he is the most resourceful mentor and when you need flexibility (work from home, come later at the office, postpone plans) he will give it to you because he trusts you. Finally, I want to thank Jan for believing in me. I am very happy and proud for what I am today, because of the things I accomplished in the past, the knowledge I built, the technical skills, the people I have met, my experiences and the way my mentality and perception has been shaped over time. I wouldn't be here without his invaluable support.

Finally, I want to thank my family, especially my wife Mideia for supporting me through all those years of hard work, for sacrificing her personal time and taking care of everything so that I can have the necessary time to focus on my work and thrive as a professional (*"elaborating on my wife's support would run the printer out of ink."*)

Vasileios Papadopoulos,
PhD researcher at Ghent university

Abbreviations and Acronyms

aFRR	Automatic Frequency Restoration Reserve
AMR	Automatic Meter Reading
BESS	Battery Energy Storage System
BRP	Balancing Responsibility Party
BSP	Balancing Service Provider
CAES	Compressed Air Energy Storage
CAPEX	Capital Expenditures
CHP	Combined Heat and Power
CCMD	Consumer Centric Market Design
CRM	Capacity Remuneration Mechanism
DAM	Day-Ahead Monthly
DoD	Depth of Discharge
DSO	Distribution System Operator
EBGL	Electricity Balancing Guideline
EMS	Energy Management System
EoL	End of life
ESCO	Energy Service Company
EV	Electric Vehicle
FCR	Frequency Containment Reserve
FFN	Feed Forward Network
IGCC	International Grid Control Cooperation
LFP	Lithium iron phosphate (LiFePO ₄)
LV	Low Voltage
MCP	Marginal Clearing Price
MCV	Marginal Clearing Volume
MDP	Markov Decision Process
MDP	Marginal Decremental Price
MIP	Marginal Incremental Price
mFRR	Manual Frequency Restoration Reserve
OPEX	Operating expenditures
OTC	Over-The-Counter
PPA	Power Purchase Agreement
PV	Photovoltaics
RES	Renewable Energy Systems
ROI	Return of Investment

SDAC	Single Day-Ahead Coupling
SIDC	Single Intraday Coupling
SoC	State of Charge of the battery
SR	Strategic Reserve
ToU	Time of User
TSO	Transmission System Operator
UPS	Uninterruptible Power Supply
VRB	Vanadium Redox Flow

Terminology

Aggregator	A service provider that integrates different decentralized units (e.g., EVs, heat pumps, batteries) into a single flexible asset that can be upwards (power generation) or downwards (power consumption) activated.
C rate	Rate of time at which the battery is charged or discharged.
ENTSO-E	European Network of Transmission System Operators for Electricity. ENTSO-E is an organization that promotes the closer collaboration of the TSOs in Europe. It consists of 39 TSOs across 35 countries.
Imbalance Netting	Imbalance Netting is the process agreed between TSOs of two or more Load Frequency Control (LFC) areas that allows avoiding the simultaneous activation of frequency restoration reserves in opposite directions. The TSO members of the IGCC perform imbalance netting on the aFRR.
NEMO	Nominated Electricity Market Operator. NEMOs are the organizations mandated to run the day-ahead and intraday integrated market coupling. Examples are EPEX SPOT, Nord Pool, OTE, Nasdaq
OTC	OTC refers to financial instruments traded directly between two parties, rather than on an organized exchange.
Power Exchange	A trading platform where different parties come together to buy and sell electricity. Examples are ICE Endex, EEX, EPEX Spot.

Nomenclature

Symbols	Definition	Unit
a	Hellman exponent	
a_m	Action m in Markov decision process	
A	Action space in Markov decision process	
A_{incr}	Consumption increase	%
$A_{\text{peak red}}$	Peak reduction percentage	%
C_{p1}	Capacitance of 1 st parallel element in LFP battery cell electric model	F
C_{p2}	Capacitance of 2 nd parallel element in LFP battery cell electric model	F
C_{Ah}	Battery capacity in Ah	Ah
C_{kWh}	Battery capacity in kWh	kWh
C_{MWh}	Battery capacity in MWh	MWh
CP_{pv}	Capacity factor of PV	%
CP_{wind}	Capacity factor of wind	%
C_{rate}	Battery C rate	
Cost_{bat}	Battery CAPEX per unit	€/kWh
$E_{\text{dis tot}}$	Total energy discharged by the battery	kWh
$E_{\text{load tot}}$	Total load energy demand	kWh
$E_{\text{grid tot}}$	Total energy delivered to load by the grid	kWh
$E_{\text{q activated}}$	Activated energy volume for quarter q	MWh
ER_{tot}	Total self-sufficiency error	%
ER_{bat}	Battery utilization error	%
$ER_{\text{inst}}(t)$	Instantaneous self-sufficiency error	%
$E_{\text{load inst}}(t)$	Instantaneous load consumption at time t	kWh
$E_{\text{grid inst}}(t)$	Instantaneous energy delivered to the load by the grid at time t	kWh
h	Height	m
OCV	Open Circuit Voltage	V
$P_a(s, s')$	Probability of Markov decision process that action a in state s at time step t will lead to state s' at time step $t+1$	
P_{bat}	Power of the battery	kW
$P_{\text{capacity bid}}$	Power of the capacity bid	MW
P_{inv}	Power of the DC/AC inverter	kW

P_{nom}	Nominal power of the DC/AC inverter	kW
$P_{battery\ max}$	Upper charging power limit of the battery	kW
$P_{battery\ min}$	Lower discharging power limit of the battery	kW
P_{elect}	Electricity price	€/kWh
$P_{battery\ AC\ output}(t)$	Power of the battery storage system (AC output) at time t	kW
$P_{grid}(t)$	Power of the electric grid at time t	kW
$P_{load}(t)$	Power of the load at time t	kW
$P_{wind}(t)$	Power of the wind turbine at time t	kW
$Pr_{q\ energy\ bid}$	Energy bid price for quarter q	€/MWh
$Pr_{capacity\ bid}$	Capacity bid price	€/MW/h
$q_{t,m}$	Real power measurement $P_{load} - P_{pv}$ in the quarter m of time step t	
$Q(S_t, A_t)$	State action value function at time step t	
R	Total internal resistance of LFP battery cell	Ω
R_0	Resistance of series element in LFP battery cell electric model	Ω
$R_a(s, s')$	Expected immediate reward received after transitioning from state s to s' to action a	
$R_{capacity}$	Remuneration for reserved power capacity	€
R_{energy}	Remuneration for activated energy volume	€
R_{p1}	Resistance of 1 st parallel element in LFP battery cell electric model	Ω
R_{p2}	Resistance of 2 nd parallel element in LFP battery cell electric model	Ω
$R_{peakred-to-cap}$	Ratio peak reduction to capacity	
R_t	Reward in Markov decision process at time step t	
Rev	Peak compensation revenue	€/kW/h
S	State space in Markov decision process	
S_{tot}	Total self-sufficiency of the installation	%
$SoC_{act\ time}$	Average percentage of time during the simulation that the battery is deployed for peak shaving	%
$SoC(t)$	Battery State-of-Charge at time t	%
$S_{inst}(t)$	Instantaneous self-sufficiency of the installation at time t	%
T_{step}	Time step of the simulation	s
$U_{battery}$	Battery utilization	%
U_{PEM}	Electrolyzer utilization	%
v	Wind speed	m/s

v_{10}	Wind speed at 10 meters height	m/s
ΔP_{peak}	Peak reduction	kW
γ	Discount factor in calculation of MDP reward	
η_{battery}	Round trip efficiency of the battery	%
$\eta_{\text{DC/AC}}$	Efficiency of the DC/AC converter	%
η_{total}	Total efficiency of the battery storage system	%

List of Figures

Figure 1: Battery storage applications.....	2
Figure 2: Flowchart - Relation between the different chapters.....	6
Figure 3: Thesis contributions by chapter.....	6
Figure 4: Market players.....	10
Figure 5: Electricity market structure in Belgium.....	12
Figure 6: Evolution of prices in 2022 for a delivery in 2023, 2024 and 2025 [12].....	13
Figure 7: Evolution of Belpex for Jan 2023 [12].....	14
Figure 8: Market Clearing Price in Day-Ahead auction [14].....	15
Figure 9: Evolution of Day-Ahead volumes traded in EPEX SPOT [15].....	16
Figure 10: Time frame of Day-ahead auctions [15].....	16
Figure 11: Countries participating in Single Day-Ahead Coupling [16].....	17
Figure 12: Timeframe of Intraday trading in EPEX SPOT [15].....	18
Figure 13: Evolution of Intraday volumes traded in EPEX SPOT [15].....	19
Figure 14: Evolution of SIDC in 4 major waves [18].....	20
Figure 15: Activation sequence of balancing reserves in Europe.....	22
Figure 16: Sequence of capacity auctions in the balancing market [19].....	22
Figure 17: Merit order curve in aFRR and mFRR energy bids.....	23
Figure 18: FCR activation method: Frequency droop control.....	23
Figure 19: Imbalance pricing settlement.....	26
Figure 20: Trading example combining forwards/futures, day-ahead and intraday contracts.....	27
Figure 21. System topology.....	43
Figure 22: Wind speed distribution.....	45
Figure 23: XANT L-33: Power-to-speed curve.....	45
Figure 24: Electrolyzer capital expenditures.....	48

Figure 25: Power flow model (pseudocode).....	51
Figure 26: Economic evaluations: Payback period of scenario C with Lithium NMC.....	58
Figure 27: Economic evaluations: Additional accumulated profit of scenario C with Lithium NMC, having as reference of comparison scenario B.....	58
Figure 28: System topology.....	65
Figure 29: Scatter plot of wind speed and wind power at 1 s and 10 min resolution for the 2 months period: 1 June 2017 12:00:00–1 August 2017 11:59:59.....	66
Figure 30: 2nd order RC equivalent for LFP cell.....	68
Figure 31: Voltage discharge curves for C/25, C/3 and 1C according to Ref. [80].....	69
Figure 32: Comparison of voltage to time curves between simulation and reference with optimized parameters.....	70
Figure 33: Power flow model: The entire model was implemented using basic Simulink blocks. The bottom part of the figure shows the interior of blocks 1, 2, 3 and 4.....	73
Figure 34: Power capability curves of a single LiFePO ₄ cell, considering different C rate limitations. The indexes for the charging and discharging curves are “Chg” and “Dis” respectively.....	75
Figure 35: Total self-sufficiency at 1 s resolution (red), total self-sufficiency error (black).....	80
Figure 36: Battery utilization at 1 s resolution (red), battery utilization error (black).....	82
Figure 37: Instantaneous self-sufficiency error on 8 June 2017 without battery storage (Capacity is zero, C rate irrelevant) and load ratio 1/6.....	83
Figure 38: Bivariate probability mass function at 10 min resolution considering: (i) variable X: instantaneous ratio P_{load}/P_{wind} , (ii) variable Y: instantaneous self-sufficiency error, (iii) battery capacity is zero (C rate irrelevant), load ratio is 1/20.....	84
Figure 39: Univariate probability mass function at 10 min resolution considering: (i) variable X: instantaneous ratio P_{load}/P_{wind} , (ii) battery capacity is zero (C rate irrelevant), (iii) load ratio is 1/20.....	85
Figure 40: System topology.....	93
Figure 41: Boxplots, 40 load profiles: (a) Mean power (left), (b) Ratio: Peak-to-mean power (right).....	95

Figure 42: DC/AC efficiency, $Y = f(x)$ 96

Figure 43: Power flow model for peak shaving designed in Matlab/Simulink 98

Figure 44: Flow chart—Dichotomy method: (a) Pseudocode (left), (b) Midpoint evolution (right)..... 99

Figure 45: Simulation results: (a) Peak reduction-to-capacity (left), (b) peak reduction (right).....102

Figure 46: Simulation results: (a) SoC active time (left), (b) Battery utilization (middle), (c) Consumption increase (right).....103

Figure 47: Peak shaving—results of economic feasibility study. At each point $[x, y]$, the color represents the total number of users whose peak reduction-to-capacity exceeds the y value. The yellow and green dashed lines represent the profitability thresholds 0.43 106

Figure 48: Thermal image, predictable load profile 108

Figure 49: Thermal image, unpredictable load profile 109

Figure 50: System topology 115

Figure 51: MDP in day-ahead optimization 117

Figure 52: Feed Forward Neural Network 122

Figure 53: Weekly load profile 123

Figure 54: Scenario A - optimization output 126

Figure 55: Scenario B – optimization output 127

Figure 56: Scenario C – optimization output 127

Figure 57: Scenario D – optimization output 128

Figure 58: Scenario E – optimization output 128

List of Tables

Table 1: Examples of pricing formulas in energy supply contracts.....	29
Table 2: Wind turbine: Technical specifications	46
Table 3: Electrolyzer: Technical specifications.....	47
Table 4: Battery: Technical specifications.....	50
Table 5: Energetic results.....	52
Table 6: Economic evaluations: Parameters & Variables	56
Table 7: Economic evaluations: Scenario B.....	57
Table 8: Wind turbine: Technical specifications.....	66
Table 9: LFP cell characteristics [80].....	68
Table 10: Parameters of the 2nd order RC model using Matlab's optimization toolbox. The values refer to a single LFP cell.....	70
Table 11: Comparison of performance metrics for two cases derived from Figure 35	81
Table 12: LFP Cell Characteristics, according to [80]	94
Table 13: Peak Shaving, Parameters for Economic Feasibility.....	105
Table 14: Action space.....	119
Table 15: Pseudocode of Day-Ahead optimization problem.....	121
Table 16: BESS specifications.....	123

Contents

1	<u>INTRODUCTION.....</u>	1
1.1	CONTEXT AND MOTIVATION	1
1.2	QUESTIONS AND CHALLENGES.....	2
1.3	CONTRIBUTIONS.....	4
1.4	LIST OF PUBLICATIONS	7
2	<u>ELECTRICITY MARKET & OPPORTUNITIES FOR BATTERY STORAGE.....</u>	8
2.1	ELECTRICITY MARKET IN BELGIUM.....	8
2.1.1	INTRODUCTION.....	8
2.1.1.1	Market structure.....	10
2.1.2	FORWARD AND FUTURE MARKET	12
2.1.3	DAY-AHEAD	14
2.1.4	INTRADAY	17
2.1.5	BALANCING MARKET.....	20
2.1.6	IMBALANCE PRICING	25
2.1.7	RETAIL MARKET.....	27
2.2	BATTERY STORAGE APPLICATIONS	30
2.2.1	INTRODUCTION.....	30
2.2.2	RES SELF-SUFFICIENCY	30
2.2.3	PEAK SHAVING	31
2.2.4	PRICING ARBITRAGE.....	31
2.2.5	POWER QUALITY.....	33
2.2.6	BALANCING MARKET.....	33
2.2.7	OTHER GRID SERVICES	34
2.2.8	CONCLUSIONS AND DISCUSSION	35
3	<u>INCREASING THE SELF-SUFFICIENCY IN RENEWABLE ENERGY SYSTEMS.....</u>	37

3.1	INTRODUCTION	37
3.2	METHODOLOGY.....	43
3.2.1	PHOTOVOLTAIC PARK.....	43
3.2.2	WIND TURBINES.....	44
3.2.3	ELECTROLYZER.....	46
3.2.4	BATTERY STORAGE SYSTEM.....	49
3.2.5	POWER FLOW MODEL.....	51
3.3	RESULTS	52
3.3.1	ENERGETIC ASSESSMENTS.....	52
3.3.2	ECONOMIC EVALUATIONS.....	55
3.4	CONCLUSIONS	59
4	<u>THE IMPACT OF TIME RESOLUTION IN SELF-SUFFICIENCY STUDIES.....</u>	<u>61</u>
4.1	INTRODUCTION	61
4.2	METHODOLOGY.....	66
4.2.1	DATA INPUTS – WIND POWER AND LOAD POWER.....	66
4.2.2	BATTERY MODEL	67
4.2.2.1	Dynamic model	67
4.2.2.2	Evaluation of the dynamic response	71
4.2.2.3	Power flow model.....	71
4.2.2.3.1	Process 1 – DC/AC efficiency and minimum power threshold	74
4.2.2.3.2	Process 2 – Limitation imposed by power capability	74
4.2.2.3.3	Process 3 - Limitation imposed by resolution scale	76
4.2.3	DEFINITION OF PERFORMANCE METRICS.....	77
4.3	RESULTS	79
4.3.1	TOTAL SELF-SUFFICIENCY	79
4.3.2	TOTAL SELF-SUFFICIENCY ERROR.....	80
4.3.3	BATTERY UTILIZATION	81
4.3.4	BATTERY UTILIZATION ERROR	82
4.3.5	INSTANTANEOUS SELF-SUFFICIENCY ERROR.....	83
4.4	CONCLUSIONS	85
4.5	DISCUSSION	87
5	<u>PEAK SHAVING.....</u>	<u>89</u>

5.1	INTRODUCTION	89
5.2	METHODOLOGY.....	94
5.2.1	DATA.....	94
5.2.2	POWER FLOW MODEL.....	95
5.2.3	DICHOTOMY METHOD.....	99
5.2.4	DEFINITION OF PERFORMANCE METRICS.....	100
5.3	RESULTS	101
5.3.1	ENERGETIC ASSESSMENTS.....	102
5.3.2	ECONOMIC EVALUATIONS.....	104
5.4	CONCLUSIONS	107
5.5	DISCUSSION	108
6	<u>DAY-AHEAD PRICING ARBITRAGE & PEAK SHAVING.....</u>	<u>110</u>
6.1	INTRODUCTION	110
6.2	METHODOLOGY.....	115
6.2.1	INTRODUCTION TO MARKOV DECISION PROCESS (MDP).....	115
6.2.2	SOLUTION – DEEP Q NETWORK.....	120
6.3	RESULTS	122
6.4	CONCLUSIONS	129
7	<u>FINAL THOUGHTS, DISCUSSION FOR FUTURE WORK.....</u>	<u>130</u>
8	<u>ANNEX – FLEXLAB.....</u>	<u>133</u>

1 Introduction

1.1 CONTEXT AND MOTIVATION

Energy storage has been at the forefront of the renewable energy landscape for many years. It is regarded by many experts as an indispensable part of the solution towards a 100 % green energy world. In general, energy storage technologies can be divided into 3 categories depending on how long the energy is stored: (i) long-term storage, from months to years (e.g., CAES, hydrogen storage), (ii) medium-term storage, from days to weeks (e.g., batteries, pumped hydro), (iii) short-term storage, from seconds to minutes (e.g., batteries, supercapacitors, flywheels). Among these technologies, battery storage is by far the most popular mainly due to the fact that batteries, at least until now, are still the most cost-effective technology to be adopted for mainstream use.

With respect to battery storage applications, we make a distinction between mobile and stationary applications. Mobile applications refer to the use of batteries in transportation such as electric vehicles, trucks, buses, bikes etc. In stationary applications, batteries are basically part of the electric grid infrastructure e.g., homes, grid interactive PV systems, ancillary services to TSOs etc. As of 2024, battery storage has seen some growth in mobile applications, while the adoption of the technology for stationary applications is still in its early stages due to a variety of reasons as explained in the next paragraph.

First of all, one would argue that there is some serious lack of stability in long term market rules. The increased penetration of renewables is changing the way we think of electricity. The forecasting uncertainty of renewables is impacting the wholesale and retail markets. Energy trading is shifting closer to the delivery date to hedge against risks. The once taken for granted fixed pricing contracts are not the norm anymore. To mitigate forecasting errors, energy suppliers opt to expose the end user to variable or even dynamic pricing contracts, which impacts negatively investments in green technologies such as batteries with long payback horizons (more than 5 years). What is more, on DSO level, as renewables grow, the tariff structure is also experiencing major reviews; additional costs are imposed on the connection capacity and peak demand of the installation. Furthermore, on TSO level, the balancing market is being reshaped through pan-European integration initiatives for the FCR, aFRR and mFRR reserve. Consequently, the electricity market is in continuous transition that creates challenges and doubt especially for the typical non-expert end user who is nevertheless the final decision maker when it comes to the implementation and final technology valorization.

On the other hand, battery storage exhibits a lot of potential for creating value to different market players (see [Figure 1](#)). (i) Prosumer (commonly known as behind-the-meter), (ii) DSO, (iii) TSO¹. Behind-the-meter battery systems can technically provide the largest number of applications. The further downstream the system is installed on the electric grid, the more applications it can provide to the whole system. Depending on the use case, the battery can be deployed either for a single standalone application or for a combination of multiple applications to benefit from different revenue streams; the latter is commonly known as “value-stacking”.

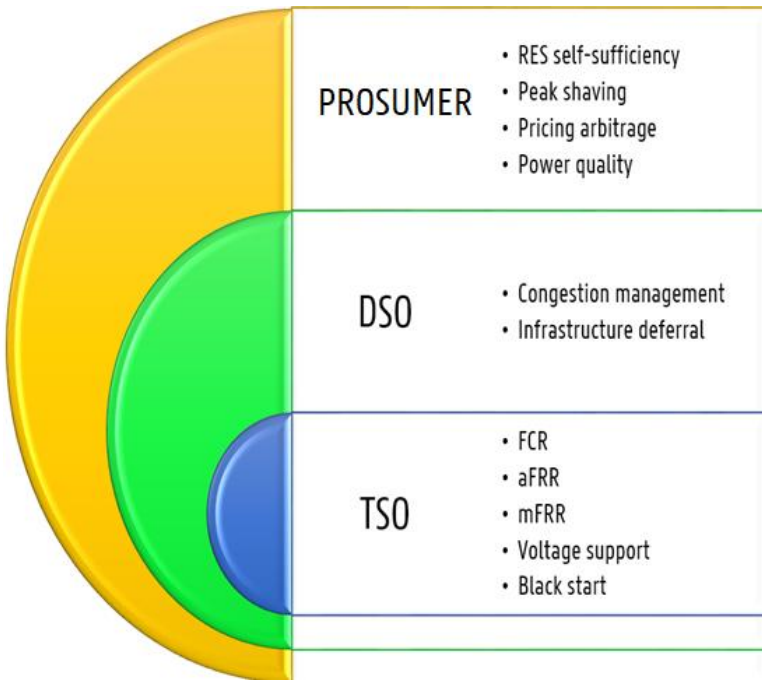


Figure 1: Battery storage applications

1.2 QUESTIONS AND CHALLENGES

The present research work can be regarded as a contribution to behind-the-meter battery storage applications. Here, we distinguish two main user groups: households and enterprises. This thesis focuses primarily on enterprises rather than households since enterprises have generally speaking the biggest potential to benefit from value stacking and deliver services to the DSO or TSO. Although this decision was made back in 2018 and it still holds, we see that

¹ Note that depending on the regulatory framework, some countries like Belgium prohibit the DSOs and/or TSO from owning any power generation units (incl. batteries).

some parts of our research can now be applied for residential users as well.² The thesis is organized in five chapters, where each chapter deals with a separate key question. All questions mentioned below came up in chronological order as the research work evolved:

Chapter 2: What are the opportunities for battery storage ?

- Which applications exist and how do they work in practice ?
- Which applications have the biggest potential; is there sufficient market liquidity or are these unique non-reproducible use cases ?

Chapter 3: What is the self-sufficiency of hybrid renewable energy installations ?

- How is the self-sufficiency affected under different system topologies and dimensioning criteria (e.g., only PV, PV and wind, PV and wind and battery) ?
- What is the impact of using different battery technologies in terms of utilization, efficiency and the overall added value to the system ?

Chapter 4: How does the time resolution of the data inputs impact the simulation result in self-sufficiency studies ?

- How big is the simulation error as we move closer to real time: 60 min > 15 min > 1 min > 1 sec ?
- Is it worth recording high resolution measurements for the load, PV or wind power source ?

Chapter 5: What is the value of peak shaving for enterprises in Belgium ?

- How do we simulate the peak shaving process and how do we optimize the battery size ?
- What is the battery utilization, degradation and economic profitability of the application ?

Chapter 6: How can we deploy a battery for day-ahead pricing arbitrage combined with peak shaving ?

- Do we need forecasting or not; if yes for which data inputs (e.g., load, PV yield, market prices) and what kind of models can we use ?
- What is a suitable optimization methodology ?

² Residential users are now charged for their peak demand and have access to dynamic pricing contracts, thus allowing them to take advantage of pricing arbitrage and peak shaving.

- How does the model perform in different scenarios of forecasting uncertainty ?

1.3 CONTRIBUTIONS

[Figure 3](#) summarizes the contributions delivered by each chapter of the thesis; we split the contributions in four segments: (a) Theory, (b) Data, (c) Methodology, and (d) Results. The present research work has delivered three journal publications, each one treated in a separate chapter (see Chapters 3 – 5); these chapters correspond to an extended version of the original published papers.

Chapter 2 is split into two parts. The first part is an introduction to the electricity market in Belgium. It gives a bird's eye overview how the market works. We start by presenting who are the market players and how the market is structured in general. Then we continue elaborating on the different market mechanisms: (a) forward/futures, (b) day-ahead, (c) intraday, (d) balancing market, (e) imbalance pricing and (f) retail market. In the second part of Chapter 2, we give an overview of the different battery storage applications describing how each application works, for whom it creates value and what is the current state of the application in Belgium. Finally, we close the chapter summarizing our conclusions and decisions for the next research objectives. Chapter 2 forms the basis of the research providing input to all next chapters but also being constantly updated following the latest market evolutions (see [Figure 2](#)).

Chapter 3 was published in the International Journal of Hydrogen Energy (see Ref. [\[1\]](#)). Here, we carried out a real case study on increasing the self-sufficiency of a renewable energy installation considering different scenarios for the power source (only PV, PV and wind, PV and wind and battery). The electric load is a 1 MW PEM electrolyzer powered by a 15 MW photovoltaic park. In this paper, we deploy battery storage to assist the PV and wind power sources during nighttime or time periods of low wind speeds in order to maximize the utilization (self-sufficiency) of the electrolyzer. The contributions of Chapter 3 are: (i) the datasheets & quotations that we have received from the involved business partners, (ii) the sensitivity analysis on the impact of wind and battery storage (VRB and Lithium-ion) in terms of increased self-sufficiency and battery utilization, (iii) the economic profitability analysis (payback period & accumulated profit) given real market data, quotations and offers received by the project developers from that time. Next, based on this study, we decided to focus on investigating the impact of the time resolution, therefore setting the path for Chapter 4.

Chapter 4 was published in Applied Energy (see Ref. [\[2\]](#)). In this paper, we carried out a comparative study investigating how the self-sufficiency of a wind powered industrial site changes considering different time resolutions (10 min vs 1 sec). For this study, we collected

high resolution measurements (1 sec) both for the power source (wind turbine) and the load (industrial site). The study delivered two major contributions: (i) the analytic power flow model of the battery storage system developed in Matlab Simulink, (ii) the sensitivity analysis on the self-sufficiency and battery utilization error. Next, the developed power flow model was used as input in Chapter 5, where we also applied some improvements by integrating non-linearity in the efficiency curve of the DC/AC converter.

Chapter 5 was published in *Energies* (see Ref. [3]). In this paper, the focus lies on peak shaving. We carry out a techno-economic analysis on 40 low voltage enterprise users. We consider that each user has a battery storage system which is (dis)charged to minimize the peak demand, therefore reducing the electricity costs imposed by the DSO. The contribution of this work are: (i) the dataset that was used as input for our analysis (40 enterprise power profiles, 3 years of 15 min resolution data), (ii) the optimization algorithm for the sizing of the battery capacity, (iii) the economic profitability analysis for all 40 use cases, taking into account the battery degradation, the DSO grid tariff tables/costs and electricity prices from that time. The conclusions from this paper led to the final part of our research work where peak shaving is combined with day-ahead pricing arbitrage.

Chapter 6 is the final part of our research work. Here, the battery application is day-ahead pricing arbitrage under peak power constraints. The end user has a dynamic pricing contract with an energy supplier. The goal is to define a (dis)charging policy for the battery controller in order to minimize the total electricity cost of the next day. Chapter 6 delivered two contributions: (i) the multi-objective optimization algorithm, which is a variant of the DQN architecture from Reinforcement Learning, (ii) the sensitivity analysis on the performance of the algorithm affected by the forecasting accuracy of the power profiles. Finally, we close the thesis summarizing important conclusions and making suggestions for future research ideas in Chapter 7.

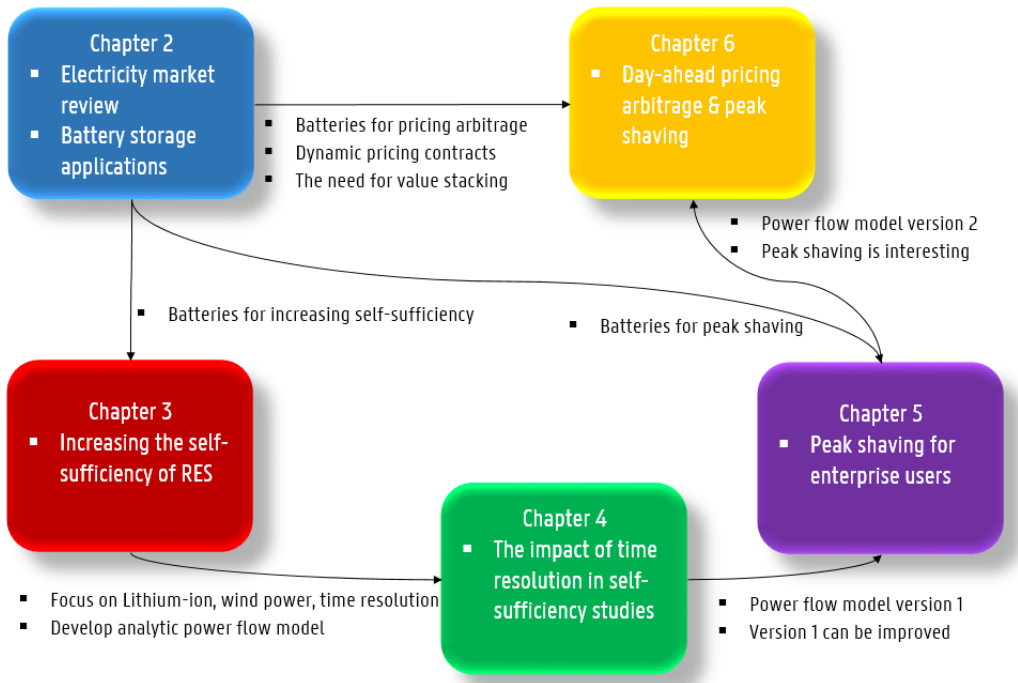


Figure 2: Flowchart - Relation between the different chapters

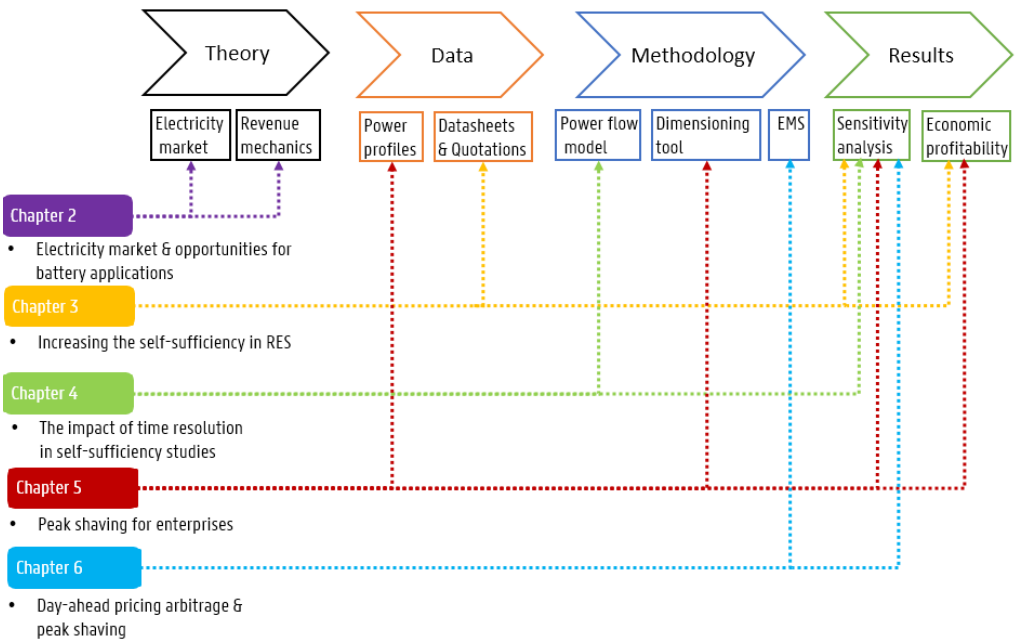


Figure 3: Thesis contributions by chapter

1.4 LIST OF PUBLICATIONS

Journal Article A1
V. Papadopoulos, J. Knockaert, C. Devellder, and J. Desmet, "Peak Shaving through Battery Storage for Low-Voltage Enterprises with Peak Demand Pricing," <i>Energies</i> , vol. 13, no. 5, 2020, doi: 10.3390/en13051183
Conference Paper P1
V. Papadopoulos, J. Knockaert, C. Devellder, and J. Desmet, "Techno-economic study of hydrogen production using PV, wind power and battery storage," <i>Proceedings of 2019 IEEE PES Innovative Smart Grid Technologies Europe (ISGT-Europe)</i> , 2019, doi: 10.1109/isgteurope.2019.8905629
Journal Article A1
V. Papadopoulos, J. Knockaert, C. Devellder, and J. Desmet, "Investigating the need for real time measurements in industrial wind power systems combined with battery storage," <i>Applied Energy</i> , vol. 247, pp. 559-571, Aug 1 2019, doi: 10.1016/j.apenergy.2019.04.051
Journal Article A1
V. Papadopoulos, J. Desmet, J. Knockaert, and C. Devellder, "Improving the utilization factor of a PEM electrolyzer powered by a 15 MW PV park by combining wind power and battery storage - Feasibility study," <i>International Journal of Hydrogen Energy</i> , vol. 43, no. 34, pp. 16468-16478, Aug 23 2018, doi: 10.1016/j.ijhydene.2018.07.069

2 Electricity market & opportunities for battery storage

2.1 ELECTRICITY MARKET IN BELGIUM

2.1.1 Introduction

This chapter was written having in mind the non-expert reader. The aim is to provide a bird's eye view of how the electricity market works in Belgium. We start by defining the market players, then provide a generic overview of the market structure and afterwards address each market segment separately. This chapter can be used as a backbone guide for those who want to understand the basic driving mechanisms of the market but also forms an introduction for later diving into the main scope of this thesis on battery storage applications.

The electric grid as we know it today has been shaped over time by different players, ranging from governments, public institutions, regulators, private enterprises and single individuals, each one with his own interests and responsibilities but all actions governed by the fundamental necessity of maintaining grid stability. Next, we present a list of the most important players describing their role.

- *Transmission System Operator (TSO)*: The TSO is responsible for the management of the high voltage electric grid. This includes the maintenance and upgrade of the high voltage transmission line infrastructure transferring electricity over long distances, from power plants to distribution networks and directly connected customers. Furthermore, he is the operator of the balancing reserve market, providing ancillary service products to BSPs and activating those products when required to ensure grid stability in real time (per second based controlling mechanisms). In Belgium, the TSO is Elia.
- *Distribution System Operator (DSO)*: The DSO is responsible for the management of the distribution electric grid, including the medium and low voltage distribution line infrastructure. He operates all energy metering installations (residential digital meters and enterprise AMR) based on which end users are invoiced by energy suppliers. In some countries, DSOs also offer secondary grid support services for managing congestion issues; such services are expected to become more popular with the increase of renewable energy systems. In Belgium, there are different DSOs for each region separately. These are Fluvius in Flanders, ORES and RESA in Wallonia and Sibelga in Brussels [4-6].
- *Producer*: These are owners of power sources that inject electricity directly into the electric grid without serious load consumption behind the meter. A producer can be a big nuclear power plant, an offshore wind farm, a CHP or even a small scale PV park. The producer usually requires an energy supplier to purchase his energy and sell it to the electricity

market; sometimes to maximize the profits, big producer companies may choose to sell their energy without the mediation of energy suppliers.

- *Prosumer*. The majority of users belong to this category ranging from homes, small residential communities, small and big industrial enterprises. In the past, prosumers were simply consumers since there was no or little decentral generation. However, with the advent of renewables, the once only passive end user now interacts with the grid through PV, wind and flexibility assets (batteries, EV, heat pumps).
- *Energy supplier*. The energy supplier is a company that buys electricity from producers and sells it to prosumers at a profit. They buy and sell electricity in energy exchange markets (forward, day-ahead, intraday). Producers and prosumers engage with energy suppliers through contracts defining the electricity price paid by (to) consumers (producers). In the past, electricity price tended to be fixed for long periods of time, in the range of years, whereas today users are more exposed to short-term variable and dynamic pricing formulas.
- *Balancing Service Provider (BSP)*. These are the parties that provide balancing services to the TSO for maintaining grid stability. There are three main balancing services available to BSPs: FCR, aFRR, mFRR (see section on balancing market). The BSP engages with the TSO through short term (4h block) capacity reservation agreements. In the past, providing balancing services to Elia was available only to big companies (e.g., MW scale, gas fired generators) whereas today the market has opened also to smaller units such as batteries [7, 8].
- *Balancing Responsibility Party (BRP)*. (Also called ARP – Accessible Responsible Party in Belgium) Each access point on the transmission grid must have a designated BRP, which can be a producer, major customer, energy supplier, or trader. The BRP is responsible for a portfolio of access points. The BRP takes care to maintain always a balanced portfolio including all injections, offtakes and commercial power trades. At each quarter of the hour (15 min resolution), the BRP's portfolio is checked against imbalances and if an imbalance occurs the BRP is subject to imbalance tariffs [7, 8].
- *Energy Service Company (ESCO)*. These are companies that offer energy services to other players (mostly prosumers). Examples of such services are energy audits, energy management systems, monitoring equipment, system integrators of renewable energy systems, data analytic platforms.
- *Regulators*. The electricity market in Belgium is supervised by four regulators, one on federal level (CREG) and one for each region separately: VREG (Flanders), CWaPE (Wallonia), BRUGEL (Brussels). Regulators can express opinions, examine and approve

official documents related to diverse aspects of the electricity market and grid infrastructure management (e.g., tariffs, infrastructure upgrades, design of new products).

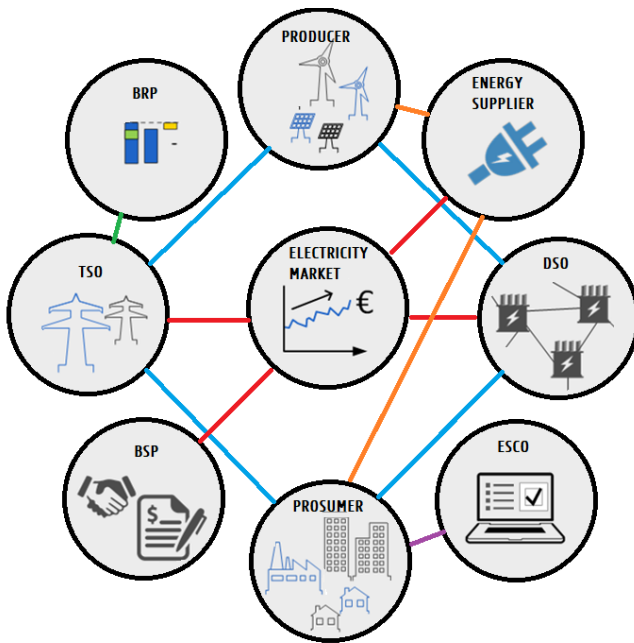


Figure 4: Market players

2.1.1.1 Market structure

One of the main characteristics of electricity is that it cannot be stored cost effectively. The electric grid must stay in equilibrium operating at constant voltage and frequency, which requires electricity generation adapting to the electricity consumption in real time. Large voltage or frequency deviations may cause malfunctions and damage the infrastructure or even result in complete system blackouts. Maintaining the equilibrium is a difficult task especially after the liberalization of the electricity market; electricity is purchased (sold) as a product over different time horizons and platforms. [Figure 5](#) gives an overview of the market structure in Belgium. The market can be viewed as a tree diagram evolving stepwise by asking the following questions:

What type of market is it?

At the bottom level, we distinguish two types of markets: a) wholesale market and b) retail market. The wholesale market is where electricity is purchased and sold in bulk. This market is

accessible to energy suppliers, traders, big power generators and large enterprise consumers. A large part of the electricity that is purchased in the wholesale market is then sold in the retail market by energy suppliers to end users. The price of electricity in the wholesale market is usually lower than the price in the retail market; in the latter case, additional costs are charged e.g., transmission and distribution costs, energy supply fees, levies and taxes.

What is the electricity unit traded?

The electricity market is basically an energy only market since generators (consumers) are remunerated (charged) based on the energy volume (MWh) generated (consumed) rather than the power capacity (MW). In Belgium, as of 2024, the only case where electricity is traded based on power capacity (MW) is the balancing market (FCR, aFRR, mFRR). Special cases are also the Strategic Reserve (SR) and Capacity Remuneration Mechanism (CRM). We elaborate on these in the next sections.

What is the time horizon from the contract trade to the electricity delivery?

All products are traded in advance before the actual delivery of the energy. Examples of notations such as Y-3, M-1, D-1, D correspond respectively to 3 years ahead, 1 month ahead, day-ahead and same-day delivery. Having different time horizons is essential to all involved players for maintaining grid stability under forecasting uncertainties and hedging against financial risks.

What are the traded products?

Each market segment has its own products depending on the type, unit and time horizon of the contract trade. In the next sections, we provide a bird's eye view how those products work, who are the primary players involved, recent market evolutions and statistics.

What are the trading platforms?

Depending on the product, electricity is traded, purchased and sold in different ways such as: a) power exchanges or multilateral trading platforms, b) bilateral over-the-counter (OTC), c) organized OTC trading, d) auction based platforms, e) energy supplier websites for retail contracts.

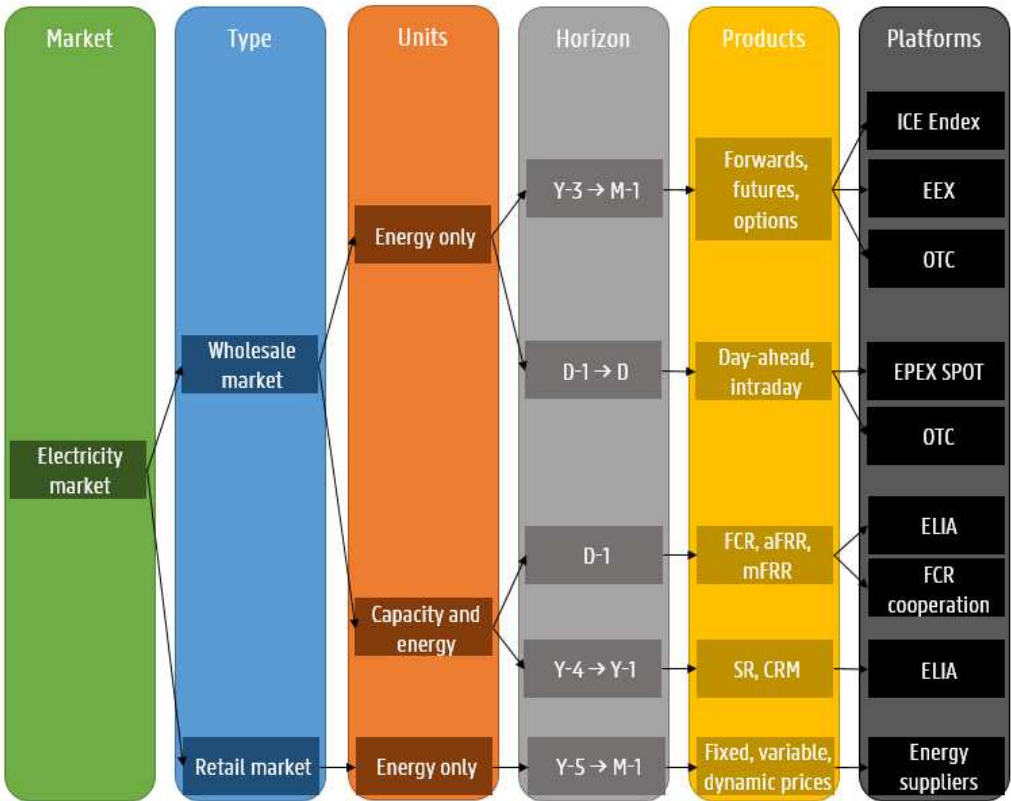


Figure 5: Electricity market structure in Belgium

2.1.2 Forward and future market

Forward and future markets are both derivative³ arrangements involving two parties who agree to buy or sell electricity at a set price by a certain date in the future. These markets run from years before up to the day before delivery [9]. The main difference between the two, is that future contracts are public whereas forwards are private. Trading electricity in these markets has the advantage that the involved parties can hedge against risks of price fluctuations by setting fixed prices over the entire delivery period, which enables them to forecast more accurately their revenues and costs .

In the future market, contracts are traded on power exchanges. They are settled on a daily basis and they are standardized in terms of quantity, quality, delivery and maturity date. Buyers and sellers submit bids (orders) to the power exchange platform. The trading algorithm checks all submitted bids; if a buyer and a seller agree on a price, the algorithm matches the two

³ In finance, derivative is a financial contract whose value depends on an underlying asset, group of assets or benchmark.

together and creates a contract. In Belgium, future contracts are traded on the ICE Exend and the European Energy Exchange (EEX).

In the forward market, contracts are traded bilaterally over-the-counter (OTC). OTC contracts are not standardized, thus allowing more flexibility in terms of trading volumes and pricing since agreements are reached bilaterally among the involved participants. However, unavoidably, the lack of standardisation exposes the participant to increased risks. In general, future contracts are less risky than forward contracts since they are traded on power exchanges that guarantee fixed maturity dates, uniform terms and payments on the agreed upon date [10].

ICE Exend publishes an index reflecting the price of electricity traded in Belgian Power Base Futures. The index indicates the price that the different market players are willing to pay (receive) for buying (selling) electricity at a specific date of delivery. It publishes prices for the next three years (CAL+1, CAL+2, CAL+3), next four quarters (Q+1, Q+2, Q+3, Q+4) and next three months (M+1, M+2, M+3). Figure 6 (Ref. [11]) shows an example of the price evolution in 2022 for electricity to be delivered in 2023, 2024 and 2025 [11].⁴

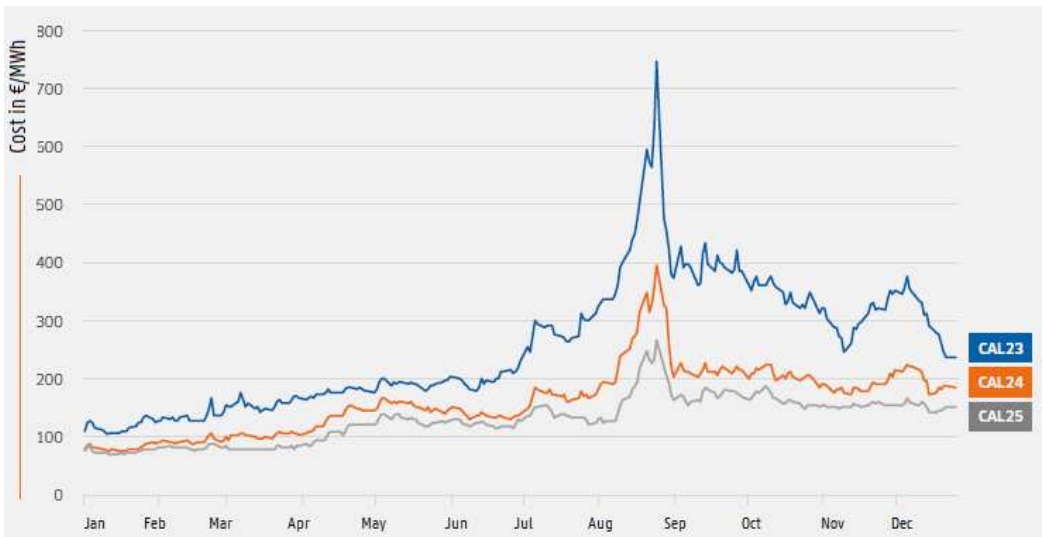


Figure 6: Evolution of prices in 2022 for a delivery in 2023, 2024 and 2025 [11]

⁴ In 2022, due to the adequacy uncertainty in natural gas supply caused by the war in Ukraine electricity prices skyrocketed to record levels.

2.1.3 Day-ahead

In the day ahead market, electricity is traded on the short-term, just one day before the actual delivery. Trading electricity in the day ahead market occurs either through a power exchange or bilaterally OTC [9, 12]. In Belgium, the leading day-ahead power exchange platform is EPEX SPOT. In the next paragraphs, we explain how the market works on a power exchange having as reference EPEX SPOT.

The Day-ahead market works as a blind auction that occurs once every day of the year. The Market participants submit their orders before the order book closes at 12:00 CET. Day-ahead contracts are traded either in single hours or in blocks of combined hours at the same time. Every day, 24 hourly contracts are available corresponding to the 24 hours of the next day. The minimum price and volume increment are 0.1 €/MWh and 0.1 MW respectively. The minimum and maximum price are -500 €/MWh and 4000 €/MWh respectively. For each hour of the next day, the trading algorithm calculates a clearing price, known as the Market Clearing Price (MCP). In Belgium, the index showing the evolution of the day-ahead prices is called Belpex (see Figure 7, Ref. [11]). This index is essentially the backbone of dynamic pricing formulas (see section 2.1.7). Another important index is the DAM (Day-Ahead Monthly), which is the monthly average of the Belpex. Next, we explain how the MCP is calculated.

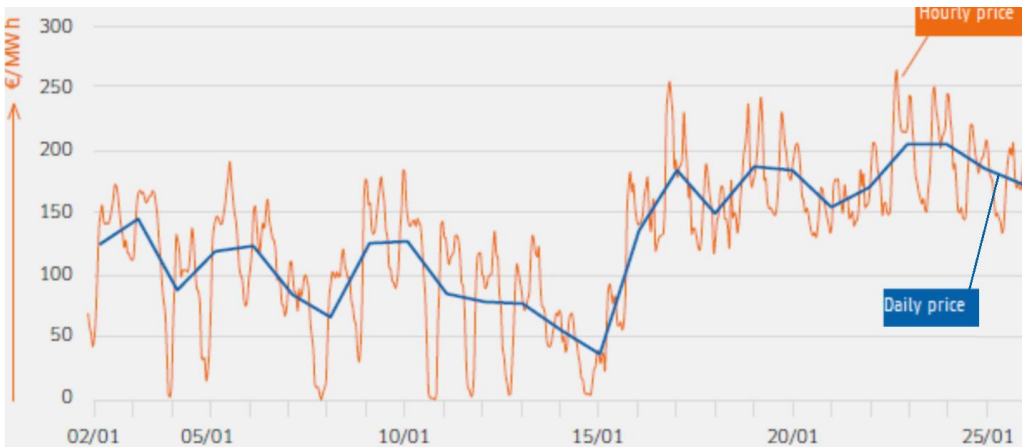


Figure 7: Evolution of Belpex for Jan 2023 [11]

Sell-orders correspond to power generation bids while buy-orders correspond to power consumption bids. At each hour, a supply curve is established by aggregating all generation bids from the lowest price to the highest [13]. Second, a demand curve is established by aggregating all consumption bids from the highest price to the lowest. The intersection of the two curves defines the Market Clearing Price (MCP) and volume (MCV) (See Figure 8, Ref. [13]).

All bids located at the left side of the intersection are considered as accepted and all bids at the right side are rejected. The MCP is always lower or equal to the price set by the buyer and always higher or equal to the price set by the seller. The MCP is a single price that applies to all accepted buyers and sellers; all accepted buyers will pay the MCP and all accepted sellers will be paid the MCP regardless of the price of the submitted bids.

In the auction, there is no one-to-one match between buyers and sellers. There is an aggregated executed sell volume that equals an aggregated executed buy volume for each delivery period (1 hour). The advantage of the auction is that it offers liquidity to the market in general and that it offers transparency regarding the clearing volume and price.

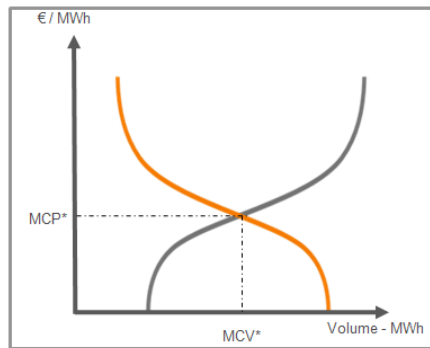


Figure 8: Market Clearing Price in Day-Ahead auction [13]

Spot markets such as day-ahead and intraday are beneficial in different ways but also come with their own risks. A major advantage when compared to forwards and futures is that the participant has a better understanding about the future (next day). Since the delivery day is closer to the trade, forecasts are more accurate e.g., weather prediction, loss of power due to defects in generators, unforeseen events that could cause load peaks. The spot market in essence is an extra lever for increasing the balance between nominations and actual measurements, consequently reducing exposure against real time electricity prices. An obvious disadvantage is that the electricity price on spot markets is difficult to predict, especially on the long term (weeks to years ahead), therefore costs and revenues of the involved assets (power generators and loads) are also difficult to assess on the long term.

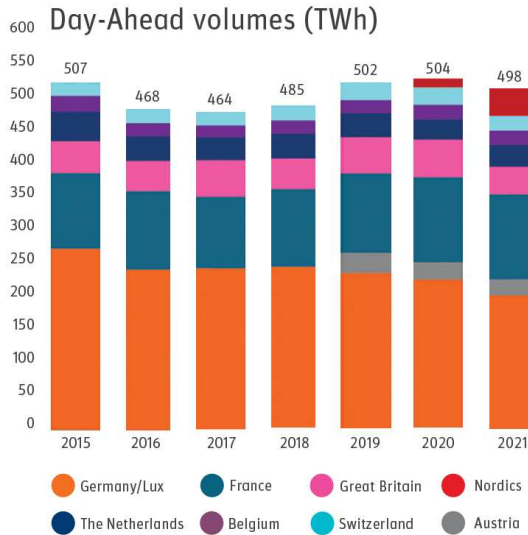


Figure 9: Evolution of Day-Ahead volumes traded in EPEX SPOT [14]

Single Day-Ahead Coupling (SDAC)

The EPEX SPOT Day-ahead auction is part of the Single Day-ahead Coupling (SDAC) which is a broader pan-European day-ahead auction covering 27 countries all over Europe (Figure 11, Ref. [15]), excluding Great Britain and Switzerland (see Figure 10, Ref. [14]). Having all different day-ahead markets integrated into a single auction system is beneficial for boosting competition, increasing liquidity and enabling a more efficient usage of the generation and consumption resources in Europe. SDAC operates a single algorithm called PCR EUPHEMIA that processes various inputs (i.e. bids, transmission capacities and constraints such as local market rules) from all involved countries (NEMOs and TSOs) to finally output matched trades, clearing prices, scheduled exchanges and the net position of bidding areas [15].

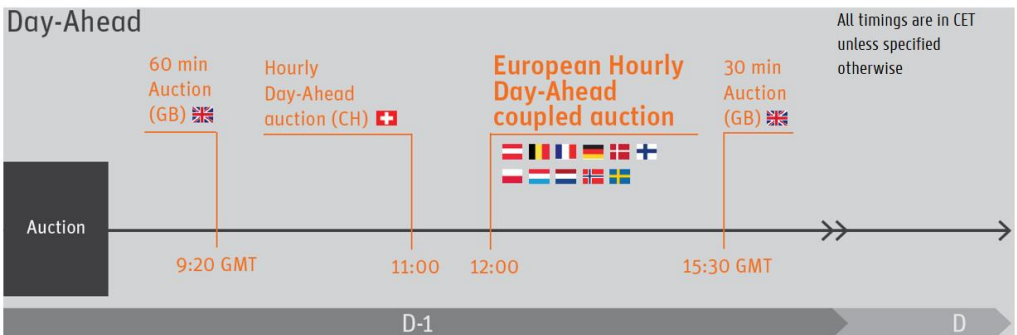


Figure 10: Time frame of Day-ahead auctions [14]



Figure 11: Countries participating in Single Day-Ahead Coupling [15]

2.1.4 Intraday

In the intraday spot market, electricity is traded for delivery in the same day, up to 5 minutes before delivery. Here also, trades occur either through a power exchange or OTC. The largest spot market exchanges in Europe are EPEX SPOT and Nord Pool. In Belgium, the intraday market is operated by EPEX SPOT. In EPEX SPOT the intraday market is divided into continuous and auction based trading.⁵ In the next paragraphs, we address specifically the continuous trading case which is the most popular and provides by far the most liquidity in Europe [14].

The continuous intraday market is running 24/7 (7 days a week, 24 hours a day). A major difference compared to the day-ahead market is that in intraday there is no single market clearing price (MCP) that applies for all accepted bids; prices are set in a “pay-as-bid” process where each trade has its own price. The trading platform checks continuously for any submitted supply and demand bids. If a supply bid has a price lower than a demand bid and they have the same volume then a trade is closed between the two. The intraday market is very often called an organized OTC market because trades are closed directly between two parties but still operated by the power exchange [16].

In Belgium, the market opens at 15:00 on the previous day (see [Figure 12](#), Ref. [14]). The minimum price and volume increment are 0.01 €/MWh and 0.1 MW respectively. The minimum

⁵ More information on auction based intraday trading can be found in the website of EPEX SPOT.

and maximum price are -9999 €/MWh and 9999 €/MWh respectively. With respect to the time resolution, depending on the country different contracts exist (e.g., 60 minutes, 30 minutes, 15 minutes). In Belgium, the market is organized in 15 minute contracts.

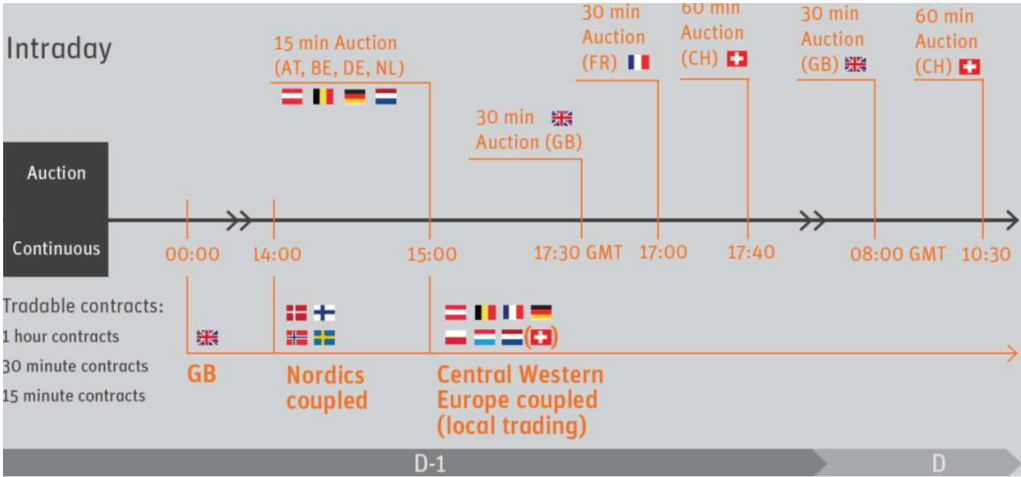


Figure 12: Timeframe of Intraday trading in EPEX SPOT [14]

Over the past decade, the energy volumes traded in the intraday market have increased considerably (see Figure 13, Ref. [14]). The main reason for this trend is due to the increase of the renewables share in the electric grid. The intraday market is a traders last chance to improve their purchases and sales based on the latest forecasts and unforeseen events. It is an additional flexibility mechanism that allows market participants to adjust their positions even closer to real time compared to the day-ahead market. Furthermore, similarly to SDAC, there is also a pan-European intraday market coupling (SIDC) where traders can take advantage of price arbitrage through cross border transactions.

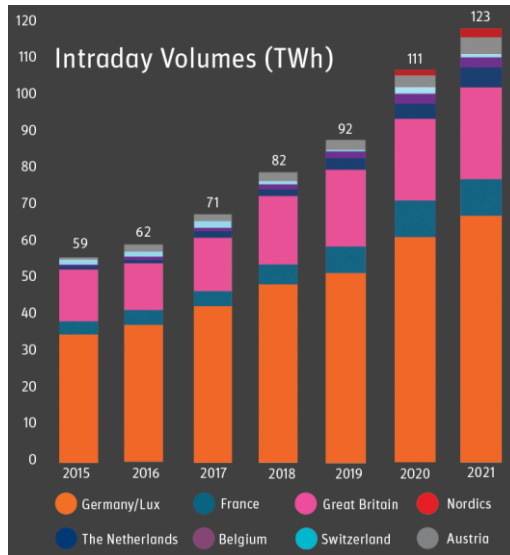


Figure 13: Evolution of Intraday volumes traded in EPEX SPOT [14]

Single Intraday Coupling (SIDC)

SIDC creates a single pan-European cross border intraday electricity market. SIDC makes intraday trading more efficient in Europe by promoting competition, increasing liquidity, allowing the share of generation resources across different market zones and generally helping market participants being in balance. SIDC has evolved to this date through four waves of country integrations (see [Figure 14](#), Ref. [17]). Next, we explain briefly how SIDC works.

SIDC works on a common IT system comprising three main components: a) a Shared Order Book (SOB), b) a Capacity Management Module (CMM) and c) a Shipping Module (SM). When market participants of each NEMO (e.g., EPEX SPOT, Nord Pool) submit orders, they are put in a Shared Order Book (SOB). Furthermore, the different TSOs enter the cross-border capacities in the Capacity Management Module (CMM). Orders from different countries can be matched together provided that the cross border capacity is available and that local market rules are in agreement.

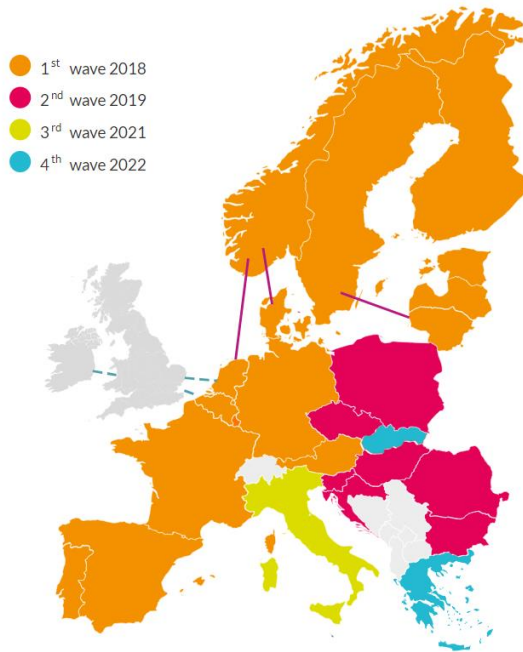


Figure 14: Evolution of SIDC in 4 major waves [17]

2.1.5 Balancing market

At the moment of the electricity delivery (real time) after completing all trades – nominations (purchases and sales in the forward/future, day-ahead and intraday markets), the total consumption (sum of loads) must be equal to the total generation (sum of power sources). Nevertheless, this equilibrium cannot be met by relying exclusively on the operation of the energy markets (forward/future, day-ahead and intraday) due to the inherent forecasting uncertainty. The System Imbalance (SI) reflects the deviations from this planned balance which are compensated by the activation of balancing reserves (mainly aFRR and mFRR, see next paragraph). When the system imbalance is negative there is generation shortage (consumption excess) and vice versa when the system imbalance is positive there is generation excess (consumption shortage).⁶

To maintain grid stability (satisfy the power equilibrium consumption = generation), the TSOs across Europe need to operate continuously in real time different balancing reserves. A balancing reserve can be simply viewed as a pool of flexible assets (e.g., power generators, hydro pumped station, batteries) that are activated in real time either upward (system

⁶ $SI = ACE - NRV$, the system imbalance is expressed as the difference between the Area Control Error (ACE) and the Net Regulation Volume (NRV), where NRV is roughly equal to the sum of aFRR and mFRR. Analytic explanations regarding the definitions of terms and mathematical notations can be found in the website of Elia.

imbalance is negative) or downward (system imbalance is positive) in function of an imbalance signal (e.g., frequency deviation, ACE). In Belgium (and most European countries), the balancing market consists of three main balancing products/services: a) Frequency Containment Reserve (FCR), b) automatic Frequency Restoration Reserve (aFRR), c) manual Frequency Restoration Reserve (mFRR).⁷

Activation sequence of balancing reserves

In this paragraph we give an example how the balancing process works (see [Figure 15](#)). Suppose, that at some moment, unexpectedly, a big power generator that is connected to the grid goes off (e.g., due to some malfunction). This event will result in a drop of the grid frequency below its reference value (50 Hz).⁸ To restore the frequency, the TSO activates the three balancing reserves in sequence FCR > aFRR > mFRR. Here, FCR is the fastest reserve. As the FCR is activated (in our case upward), the frequency is contained from further dropping until it reaches a stable point (but still below the 50 Hz reference). Next, aFRR is activated to restore the frequency and gradually take over from FCR. aFRR is slower than FCR; aFRR requires that the reserved capacity be provided within 7.5 minutes after receiving the command. Finally, in the event of a major disturbance, the TSO activates as a final support mechanism mFRR to relieve the burden from aFRR. mFRR will be activated as long as needed until the frequency is fully restored. Here, also note the presence of RR (Replacement Reserve) which is an extra measure taken in some countries but not in Belgium. The activation of balancing reserves is a non-stopping continuous process running 24/7. In the aforementioned example we took the extreme case of having a major power loss on the grid resulting in the activation of all three (or four) balancing reserves. Nevertheless, most of the time, the frequency deviation is relatively small and therefore only FCR and aFRR suffice.

⁷ In some countries, there is also a fourth product called Replacement Reserve (RR), but this is not applicable in Belgium.

⁸ At the very first moment after the generator goes off, there is an imbalance between mechanical and electrical power, and directly coupled synchronous machines will then decelerate and, thus, kinetic energy is converted into electrical energy. This explains how the electrical balance is kept at first instance (before FCR takes over)

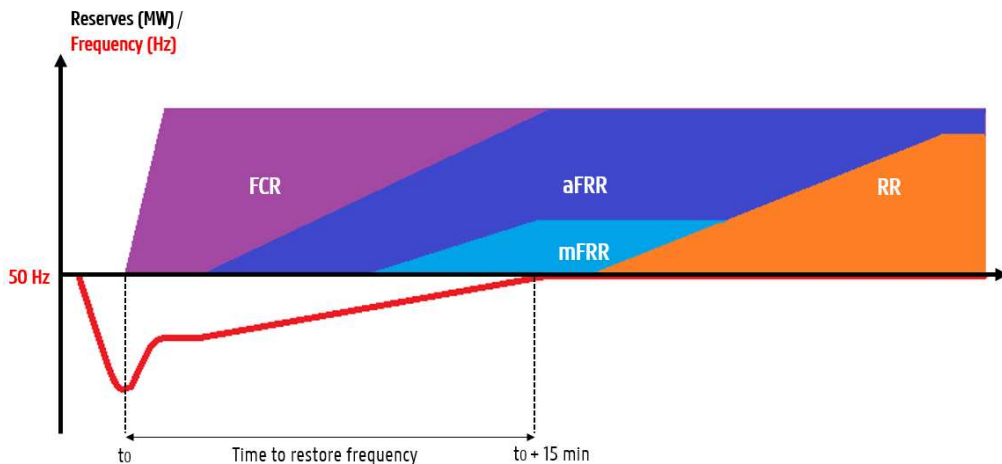


Figure 15: Activation sequence of balancing reserves in Europe

Auction system

The balancing market is an auction based system. For each product, there are six 4-hour capacity auctions every day (0–4, 4–8, 8–12, 12–16, 16–20, 20–24). Interested BSPs willing to sell their capacity submit bids (i.e. capacity volumes and prices); then based on the merit order principle, the TSO selects those bids minimizing the total operating cost of the system. The auctions take place in sequence FCR > aFRR > mFRR and end before the opening of the day-ahead market to allow participants to re-optimize their planning (Figure 16, Ref. [18]). Furthermore, only in aFRR and mFRR, apart from the capacity auctions, the winners of the capacity auction are required to participate in an energy auction. In the energy auction, the BSP submits energy bids (€/MWh) in 15 minutes resolution. The merit order curve is calculated 96 times per day for each quarter of the day and direction (see Figure 17: upward – from lowest to highest activation price, downward – from highest to lowest activation price).

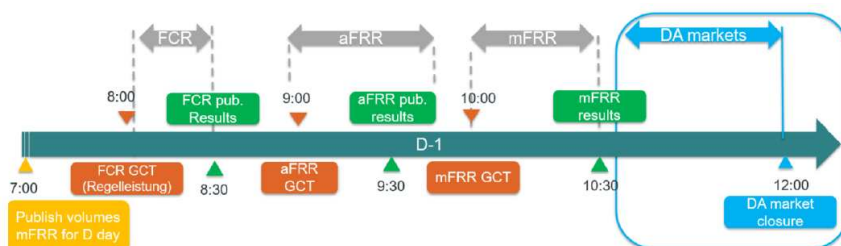


Figure 16: Sequence of capacity auctions in the balancing market [18]

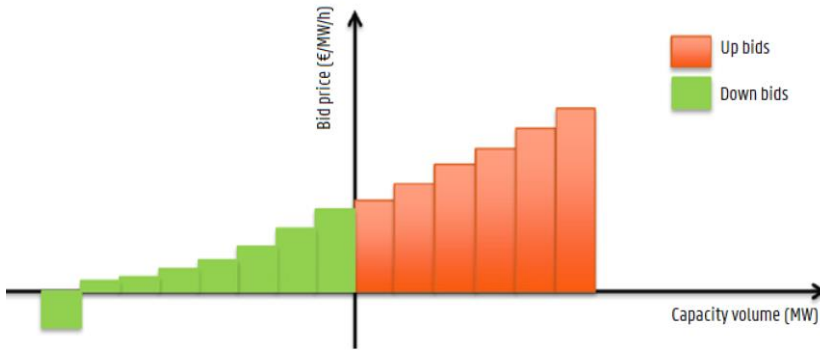


Figure 17: Merit order curve in aFRR and mFRR energy bids

Activation method

In FCR, the frequency droop control method is used (Figure 18). The activation of FCR is symmetric within a frequency range of 0.2 Hz (positive and negative). The power reference to be followed is inversely proportional to the frequency deviation from 50 Hz (Note here also the dead band within 49.99 – 50.01). In aFRR, the aFRR controller defines the global power reference based on the Area Control Error (ACE) (see Ref. [19] for analytic mathematical notations) and selects, according to the merit order principle, each 4 seconds the energy bids that need to be activated and the power reference per energy bid. In mFRR, a major difference is that the activation does not happen continuously as in the case of FCR and aFRR; this is why it is called “manual”. In general, Elia will analyze the need for possible activation of mFRR depending on the system imbalance of at least the last 10 minutes and the level of activated aFRR. When needed, mFRR is activated based on the merit order of energy bids but also taking into account technical properties of the BSPs assets.

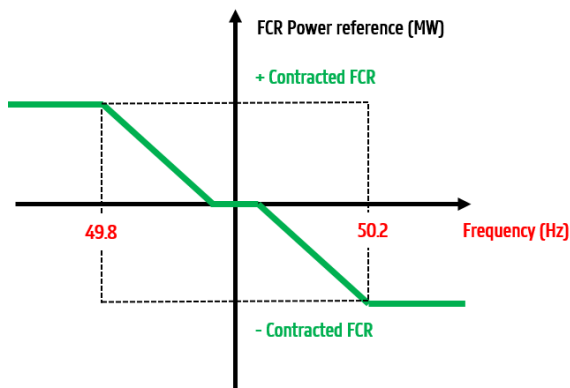


Figure 18: FCR activation method: Frequency droop control

Remuneration

With respect to the BSP remuneration, in FCR the remuneration is exclusively capacity based (see Equation 2-1). In aFRR and mFRR, apart from the capacity component, the remuneration includes also an energy based component (see Equation 2-2):

$$R_{\text{capacity}} = P_{\text{capacity bid}} \cdot Pr_{\text{capacity bid}} \cdot \Delta T \quad 2-1$$

where:

- R_{capacity} is the remuneration in € for the reserved power capacity
- $P_{\text{capacity bid}}$ is the power of the capacity bid in MW
- $Pr_{\text{capacity bid}}$ is the price of the of the capacity bid in €/MW/h
- ΔT is the time period of the reserved capacity in hours (e.g., 4 hours, 8 hours etc.)

$$R_{\text{energy}} = \sum_{q=1}^{q=N} E_{q \text{ activated}} \cdot Pr_{q \text{ energy bid}} \quad 2-2$$

where:

- R_{energy} is the remuneration in € for the total energy volume activated from quarter 1 to quarter N
- $E_{q \text{ activated}}$ is the activated energy volume in MWh for quarter q
- $Pr_{q \text{ energy bid}}$ is the price of the of the energy bid in €/MWh for quarter q

As of 2024, the balancing market in Europe is undergoing an important transition. In 2017, the European Commission established the Electricity Balancing Guideline (EBGL) aiming to develop a common and standardized framework that will finally integrate the different markets into a single cross-border pan-European balancing market. The FCR market is already running through the FCR cooperation; a common platform exists for the procurement and exchange of FCR between 12 TSOs in 9 countries [20]. With respect to aFRR and mFRR, two pilot projects are currently under development; these are the PICASSO project for aFRR and MARI project for mFRR [21, 22].

As already mentioned, FCR, aFRR and mFRR are in essence the backbone of the balancing market. However, TSOs need also other grid support services to guarantee grid stability. In Belgium, Elia has the Strategic Reserve (SR) which is a kind of reserve that is activated very rarely in special occasions (e.g., in winter to meet peak load consumption). Furthermore, Elia

implements the Capacity Remuneration Mechanism (CRM) to deal with the imminent phase-out of the nuclear power plants and secure energy supply in the long term. Big power generators participate in annual auctions starting from 2021 for deliveries planned from 2025 onwards, after the closure of the nuclear plants. Other less popular grid services worth mentioning are the provision of reactive power for voltage support and the deployment of start-up power generation units in the event of a black out.

2.1.6 Imbalance pricing

As mentioned in the previous section, the TSO is responsible for maintaining the instantaneous balance between generation and consumption. In Belgium (and many other European countries), Elia outsources this responsibility to the so-called Balance Responsibility Parties (BRPs). A BRP is private entity that oversees one or multiple access points on the transmission grid. Each BRP is holder of a balancing portfolio that comprises generations, consumptions and exchanges with other BRPs. The BRP has to make sure that the amount of electricity sold (generation) always equals the amount of electricity purchased (consumption) for each and every hourly quarter (15 minute) of the day. When the BRP fails to keep the balance, then any deficits or surpluses of power, which are measured at the moment of the electricity delivery, will be subject to imbalance pricing. The imbalance pricing settlement is a continuous process running in real time 24/7 every quarter of the day (96 quarters per day); it consists of two parts:

- a) Marginal Incremental Price (MIP): This is the highest price (€/MWh) paid by Elia to BSPs for the upward activation of balancing reserves for a given quarter.
- b) Marginal Decremental Price (MDP): This is the lowest price (€/MWh) received by Elia from BSPs for the downward activation of balancing reserves for a given quarter.

[Figure 19](#) illustrates how imbalance pricing is settled. In the event of a negative system imbalance (generation shortage) Elia activates the balancing reserves for upward regulation. The last activated balancing unit, which is the most expensive, defines the MIP.⁹ BRPs who are in negative position (generation shortage) will pay the MIP to Elia, whereas BRPs who are in positive position (generation excess) will be paid the MIP by Elia. Similarly, if a positive system imbalance (generation excess) occurs, Elia activates the balancing reserves for downward regulation. BRPs who are in negative position (generation shortage) will pay the MDP to Elia,

⁹ Note here the presence of IGCC (see imbalance netting in Terminology). TSOs check each other's imbalance and if they are in opposite sign they would first subtract them before the activation of aFRR. IGCC reduces the total system cost by avoiding the simultaneous activation of opposite reserves from different TSO control areas (without IGCC if TSO A is in positive imbalance and TSO B is in negative imbalance they would counteract each other).

whereas BRPs who are in positive position (generation excess) will be paid the MDP by Elia. Here, note also the presence of parameter α which is applied only in cases of big system imbalances (larger than 150 MW) as an incentive mechanism encouraging BRPs keeping their portfolio always in balance (more information regarding parameter α can be found in Ref. [23]).

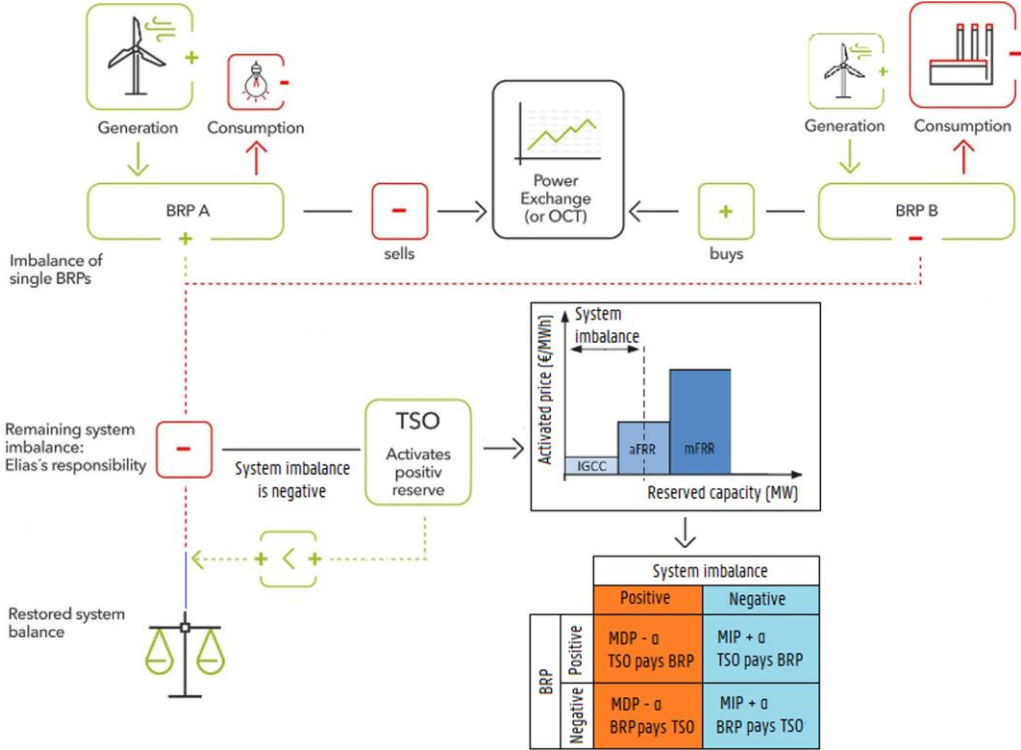


Figure 19: Imbalance pricing settlement

Trading example

Closing this section, we give an example of how the different market mechanisms (forward/future market, day-ahead, intraday, imbalance pricing) work together in a trading process. The owner of a wind farm has contracted an energy supplier to act as BRP for all the electricity generated by the wind farm. In a first trading step, the biggest part of this energy is sold through a PPA (Power Purchase Agreement) contract to a large consumer. The PPA is simply a long term (forward) OTC contract defining a power base profile (see Figure 20) at a fixed price. In reality, the wind power profile is fluctuating, resulting in energy surpluses or deficits that need to be sold or purchased at a later step as we approach the delivery date. In the second step, one day before the delivery, the trader makes a first rough estimation of the wind power profile for the next day and decides to sell the energy that is left (after subtracting

the base profile) to the day-ahead market (OTC or through power exchange). Finally, when the delivery date arrives, the trader has access to accurate weather forecasts and therefore is able to re-estimate the wind power profile; this results in surpluses and deficits that have to be traded intraday. Afterwards, by the end of the delivery date, any deviations between all aggregated (PPA, day-ahead, intraday) nominations and real time measured power profile will be subject to imbalance pricing.

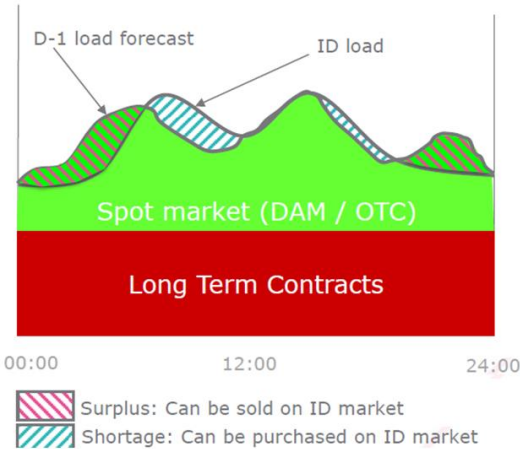


Figure 20: Trading example combining forwards/futures, day-ahead and intraday contracts

2.1.7 Retail market

In the retail market, electricity is purchased and sold through energy supply companies. Energy suppliers are the mediators between the wholesale market and end users (e.g., households, SMEs). Electricity invoices for end users typically consist of three main cost components:

- Energy supply cost: This is the amount of money you pay for the electricity you consume. This cost is paid to the energy supplier and is proportional to the consumed energy quantity (kWh). Users that inject energy to the grid (e.g., owner of PV or wind installations) receive a payment proportional to injected energy quantity (kWh). The energy cost or revenue is calculated differently depending on the energy supply contract.
- Cost for the distribution and transmission of electricity: These are the costs charged by the DSO and TSO for using the electric grid infrastructure (e.g., transport of electricity, maintenance, telemetering). Factors that influence these costs are the location of the end user's installation, type of connection (e.g., low voltage, medium voltage, connection capacity), the consumed energy quantity and the peak power of the load.

- Taxes and levies: These costs are imposed by the government for funding various programs and initiatives. They are very often expressed in function of the total consumed energy or as a percentage of the total electricity cost.

Over the past decade, we have seen some important evolutions in the retail market due to the renewable energy transition and technological advancements primarily in the field of Information Technology (IT). One of the main events currently in progress is the roll out of digital meters in Europe. Digital meters allow the measurement of power and energy consumption (and generation) in high resolution intervals (e.g., every day, 15 minutes). High resolution measurements open opportunities for new types of energy supply contracts that create benefits both for the end user and supplier company. In general, energy contracts can be divided into three categories depending on how often the electricity price changes.¹⁰ Here, “electricity price” refers exclusively to the energy supply component (see first bullet in previous list):

- a) Fixed pricing: In the past, fixed pricing was the norm; a fixed price was applied over a long time period (e.g., 1–5 years). In fixed pricing, the user knows what the price will be from the present until the next year(s).¹¹
- b) Variable pricing: In variable pricing, the electricity price changes on a monthly to yearly-quarter (e.g., a new fixed price is set every month or every 3 months) basis following a market index usually from the future market. Popular market indexes in variable pricing are the endex101¹² and endex103¹³ from the ICE Endex power exchange. In variable pricing, the user knows what the price will be from the present until the next month or 3 months.
- c) Dynamic pricing: In dynamic pricing, the electricity price follows the spot market. Here, there are mainly two market indexes: the day-ahead price (Belpex) and the DAM (Day-Ahead-Monthly). Belpex indexed contracts have a different price for each hour of the year (8760 hour per year); the user knows the prices for all 24 hours of the next day. In DAM indexed contracts, the price is calculated as the monthly average of the day-ahead prices and therefore the user only knows the price at the end of the month.

¹⁰ The contract duration on its own, is not a distinguishing factor. Most contracts have at least an annual duration, and they are automatically renewed when the contract ends. Users can change however their energy contract whenever they want as long as they notify their energy supplier at least 1 month in advance.

¹¹ Nowadays, having fixed prices longer than 1 year is a rare case.

¹² Endex101 is the arithmetic average of the closing prices in Belgian Power Base Load Futures for the month preceding the month of delivery.

¹³ Endex103 is the arithmetic average of the closing prices in Belgian Power Base Load Futures for the month preceding the quarter of delivery.

Below we present a generic pricing formula that can model all aforementioned types of energy contracts. Most energy supply contracts in Belgium are built based on this formula. We also include some examples in the next paragraph:

$$Pr_{\text{energy}} = A \cdot \text{Belpex} + B \cdot \text{DAM} + C \cdot \text{Endex101} + D \cdot \text{Endex103} + E \quad 2-3$$

where:

- Pr_{energy} is the energy price €cent / kWh paid to or remunerated by the energy supplier for the energy offtake or injection.
- A, B, C, D, E are the parameters of the respective market index.
- All market indexes are expressed in € / MWh

Table 1: Examples of pricing formulas in energy supply contracts

Pricing examples	Offtake (€cent / kWh)	Injection (€cent / kWh)
Fixed price, with injection	$Pr_{\text{off}} = 8.5$	$Pr_{\text{inj}} = 5$
Variable price, only offtake	$Pr_{\text{off}} = 0.1 \cdot \text{Endex101} + 2$	N/A
Dynamic price, with injection	$Pr_{\text{off}} = 0.1 \cdot \text{Belpex} + 1.5$	$Pr_{\text{inj}} = 0.1 \cdot \text{Belpex}$
Hybrid variable and dynamic, only offtake	$Pr_{\text{off}} = 0.05 \cdot \text{Belpex} + 0.05 \cdot \text{Endex101} + 1$	N/A

Having different types of contracts gives flexibility to end users and suppliers. Energy suppliers design their contracts based on their client portfolio and trading strategy. Energy suppliers that buy bulk quantities of electricity from the future or forward market can estimate their costs in advance, years before the delivery and therefore can offer fixed pricing contracts. Nevertheless, as renewable energy sources grow, trading electricity takes place closer to real time through short term futures/forwards and spot markets. Consequently, pricing needs also to be adapted on the short term to hedge against financial risks. For end users, especially dynamic pricing has the benefit that the user can reduce the energy supply costs by adapting consumption or generation based on the spot market price; users with flexible assets (e.g., heat pumps, electric vehicles) can take advantage of price arbitrage.

2.2 BATTERY STORAGE APPLICATIONS

2.2.1 Introduction

As mentioned in Chapter 1, battery storage systems have different applications depending on the involved market players. As mentioned before, we focus on behind-the-meter systems. This means that the primary end user of the system is a prosumer and that the battery is installed as part of his energy infrastructure (e.g., house, apartment, office, industrial site) in order to reduce the total electricity bill. Nevertheless, in this section, we keep a global scope, addressing all different applications that are currently present in the electric grid. Finally, we summarize important notes and key conclusions which influenced the further evolution of our research work.

2.2.2 RES self-sufficiency

PV and wind turbines are very often installed behind-the-meter in households and businesses in order to reduce the electricity bill. Since the cost of energy produced by the renewable energy source (pv or wind) is much cheaper than the cost of energy consumed from the electric grid, the goal here is to help the user become as much as possible self-sufficient (independent from the electric grid). However, becoming fully independent from the grid (100 % self-sufficiency) is not possible e.g., due to the inevitable presence of night time, low wind speeds. To maximize his self-sufficiency the user can deploy a battery. In the case of a PV power source, the battery is charged for example during the day when there is excess of power ($P_{pv} > P_{load}$) and then discharges the energy back to the load in the evening when there is shortage of power ($P_{pv} < P_{load}$).

This type of application has been more popular in residential systems rather than enterprises since in the first case the electricity bill is usually much higher due to the increased costs for distribution, taxes and levies. In the past, designing an energy management system for this type of application was not a complex task. Fixed pricing contracts were the norm; the end user would be charged (paid) at a fixed price proportionally to his energy offtake (injection). Since the cost for the energy offtake was always higher than the revenue for the energy injection from PV, a naïve threshold controller could do the job; the battery was (dis)charged in function of the power difference ($P_{pv} - P_{load}$). However, nowadays, due to the rise of short-term trading in spot markets (day-ahead, intraday), the energy supplier might expose the end user to dynamic pricing formulas. In such case the electricity price is changing every hour. For example, during the day it is possible that the electricity price goes below zero and consequently, it might be beneficial to charge the battery even if the PV power is higher than the load. An energy management system must be able to deal with such occasions.

2.2.3 Peak shaving

Peak shaving has been existing as an application in enterprise users for a long time before the advent of batteries. DSOs usually split the cost for the electricity distribution into two components: (i) power (kW), (ii) energy (kWh). For (ii), the cost is usually proportional to the total energy offtake from the grid. For (i), different approaches exist among the DSOs in Europe; for instance, it can be a function of the connection capacity of the installation, the highest measured peak over the past 12 months, the average annual of the monthly peaks or a combination of the above. An installation with high peak demand would result in increased electricity costs and therefore the end user would “shave” his peak to save some money.

In the past, peak shaving was possible through different mechanisms. For example, an assistant power generator would be activated during periods of peak demand or the user would change the production plan to shift the operation of an energy intensive process to off-peak periods. Nowadays, as battery prices continue to fall, peak shaving is becoming more appealing for battery storage. The profitability of an investment in such application varies a lot, but mainly affected by three things that usually change over time: the electricity tariff structure, the load profile and the capital & operating expenditures for the battery storage system.

With respect to the battery controller, it depends on different factors. Here, the predictability of the load plays a crucial role. A user with a very deterministic load profile allows the design of time-based controllers where the battery is scheduled hours in advance to be (dis)charged during certain time periods. Conversely, a user with a very stochastic load profile imposes the design of power threshold-based controllers where the battery is (dis)charged on demand based on the current real time measurement. Furthermore, if the user considers additional revenue streams (value stacking) the controller gets more complex (e.g., predictive analytics, advanced optimization algorithms, battery capacity segmentation).

2.2.4 Pricing arbitrage

In this type of applications, the main idea is that we have a market mechanism that exposes the end user to fluctuating electricity prices. The end user wants to charge the battery (buy energy) when the electricity price is low and discharge the battery (sell energy) when the electricity price is high. There are mainly three arbitrage mechanisms in the electricity market for battery storage: (i) day-ahead, (ii) intraday, (iii) imbalance. We address each mechanism separately in the next paragraphs.

In day-ahead pricing arbitrage, we distinguish two types of end users: (i) the user who buys or sells electricity directly through the wholesale day-ahead auction, (ii) the user who buys or sells electricity through the retail market having a dynamic pricing contract based on the Belpex index. In (i), the end user acts like an energy trading company e.g., large industrial consumer or power plant or an energy supply company. The battery can generate profit by buying energy from the day-ahead auction when the price is low and selling it back when the price is high. The main difficulty with this practice is that the user needs a way to predict the clearing prices of the auction for each one of the 24 hours of the next day; therefore the profitability is influenced considerably by the accuracy of the forecasting model. Conversely, in (ii), the user buys (sells) electricity from (to) the energy supply company based on the dynamic pricing formula of his contract. Here, the main difference with (i) is that the prices are known in advance; the day-ahead prices are published the day before the energy delivery at the end of the auction. Consequently, in case (ii), there is no need to forecast the prices and the optimization is easier; we still though need a forecasting model for the load and power source profile (e.g., PV, wind).

In intraday pricing arbitrage, the arbitrage mechanism is the intraday market. Here, the end user acts like an energy trading company. Similarly to the day-ahead arbitrage case (i), the user needs a way to forecast the intraday prices. Nevertheless, forecasting the intraday prices several hours in advance is a very difficult task. First of all, the intraday market evolves as a result of the very short term weather forecast data and latest unforeseen events. Secondly, the intraday prices are calculated in bilateral agreements and there is no single clearing price reference like in the day-ahead market.

In imbalance pricing arbitrage, the end user is exposed to imbalance fees (e.g., BRP, large consumers or power plants). We distinguish two control strategies: (i) the user wants to minimize the imbalance fees by keeping his portfolio as much as possible in balance, (ii) the user wants to take advantage of imbalance fees by going on purpose in imbalance; when the system imbalance is positive (generation excess) the user's portfolio is negative (generation shortage) and vice versa. In case (i), the battery is (dis)charged mainly in function of the user's portfolio imbalance. While the battery helps reducing the portfolio's imbalance, we still need to make sure that the battery State-of-Charge (SoC) stays within the limits (e.g., SoC recovery through purchases or sales in the intraday market). In case (ii), the control strategy is more complex since the user needs to forecast accurately the overall system imbalance hours in advance which is very difficult. Also in this case, similarly to (i), a secondary mechanism is required for SoC management.

2.2.5 Power Quality

Enterprise users very often suffer from Power Quality issues. Batteries have been well established in this field a long time ago. Uninterruptible Power Supplies (UPS) are an example of such applications. In the event of a voltage dip or power outage UPS ensures the smooth operation of the business process, by bridging the power loss through an energy buffer component (e.g., battery, capacitor). Another popular application related to Power Quality is the reactive power compensation, known also as power factor correction. DSOs very often apply additional costs to enterprise users based on their reactive power footprint; the higher the reactive power (inductive or capacitive) with respect to the active power the higher the electricity distribution costs. As a result, enterprises are incentivized to maximize their power factor to reduce the electricity bill. Batteries have been proven very efficient in such applications. A major advantage here, when compared to other technologies (e.g., capacitor banks) is that battery can provide additional services to the end user. For instance the controller decouples the power in two parts: (i) reactive component for power factor correction, (ii) active component for increasing the self-sufficiency of a PV installation.

2.2.6 Balancing market

The balancing market forms another opportunity for battery storage to create value for enterprise users. In the past, participating in FCR, aFRR, mFRR was only available to big players (power generators in the MW scale). However, nowadays, TSOs in Europe are redesigning the market to allow broader participation and increase competition. Small decentralized assets such as batteries, EVs and heat pumps can offer their flexibility to aggregators. In general, the basic idea is that market is becoming gradually more consumer centric – Consumer Centric Market Design (CCMD) where end users i.e., prosumers are put at the forefront of the renewable energy transition [8].

Batteries have been proven very efficient especially for the provision of FCR. FCR is the fastest from all three balancing reserves requiring the full activation of the BSP asset within 30 sec. Batteries can deliver almost instantly their power (ms – sec) either in charging or discharging mode. In essence, the main issue is that the battery storage system be appropriately dimensioned. Elia requires that the minimum reserved power capacity of an asset providing FCR be at least 1 MW. Furthermore, for assets with limited energy (e.g., batteries), the energy capacity must suffice to foresee a worst case of 40 minutes of continuous activation (either upwards or downwards) [24]. These specifications need to be considered when designing a battery storage system for FCR.

Regarding aFRR and mFRR, the requirements are more strict. The participant asset in aFRR or mFRR must be capable of providing power for as long as needed. Each balancing reserve is organized as daily auction comprising six 4h blocks. In the simplest case, having no consecutive blocks, the BSP must foresee a worst case of 4 hour continuous activation (upwards or downwards). One way to make sure that there is always enough energy is to segment the battery power in two parts; 50 % for the provision of the balancing service (aFRR or mFRR) and 50 % for managing the SoC [25]. For instance, 2 MWh a LiFePO₄ battery at 1 C rate can provide 1 MW for upward or downward aFRR (or mFRR) and use the remaining 1 MW for SoC management.

To summarize, battery storage is an appropriate technology for all three balancing reserves. Nevertheless, the profitability of an investment in such applications is still questionable. First of all, as already mentioned, the balancing market is undergoing a transition; the PICASSO and MARI projects are in progress and there is not yet a well-established regulatory framework to be based on. Furthermore, another issue is that the balancing market is an auction based system with limited procurement demand; in Belgium, the FCR and aFRR procurement demands for 2024 were merely 93 MW and 117 MW respectively [8].

2.2.7 Other grid services

To guarantee the smooth operation of the electric grid infrastructure, apart from the balancing market, TSOs and DSOs very often need other services. For example, in the event of a black out, TSOs have to manually restore the grid by activating black start services. In Belgium, Elia first activates black start services from the neighboring TSOs and if these are not available, it will look for providers within its zone to power up the grid. Another example of grid services is the provision of reactive power control. While grid frequency mainly depends on the active power flows, grid voltage depends on the reactive power flows. To maintain the voltage level within the specified limits, Elia makes contracts with Voltage Service Providers (VSP). If an incident occurs destabilizing the grid voltage, Elia activates automatically or manually VSPs to generate or absorb reactive power and restore the voltage level.

Batteries storage has been proven a suitable technology candidate for providing black start and voltage control services. Finally, another example worth mentioning here is the use of battery storage in grid infrastructure upgrades. TSOs and DSOs usually foresee large hosting capacities in their grid plans. However, some parts of the grid might become vulnerable to congestions with time as the load increases. In such occasions, investing in new infrastructure (e.g., bigger cables, transformers) can be very expensive. Instead, deploying a battery storage can be much cheaper. The battery supports the grid during congestion moments by delivering

part of the power to the load; this is similar to peak shaving but at grid level (usually low or medium voltage grid).

2.2.8 Conclusions and discussion

In this section, we summarize some important conclusions that shaped in a way the further evolution of this thesis. We note once more, in this research work we want to valorize battery storage from a prosumer's perspective.

From those applications mentioned above, we decided to focus on the following three: (i) increasing the self-sufficiency of RES, (ii) peak shaving, (iii) pricing arbitrage in retail contracts. In our opinion, these are currently the most interesting for enterprises as they have the biggest potential for widespread adoption. All next chapters of the thesis are dedicated to these applications.

Regarding Power Quality applications, we believe that these are already well established in the industry world and there is not much need to make a contribution towards this direction. Most companies are well aware and have taken action to install UPS or power factor correction units.

With respect to the other categories of pricing arbitrage (i.e. day-ahead, intraday, imbalance) we note two issues. One issue is that the profitability of such applications depends substantially on the accuracy of the electricity price forecasting model; building such models is a very complex or in some cases even impossible task. Another issue is that these applications are very limited since they concern only the big players and not the typical enterprise end user who buys his energy from the retail market; big power generators or industrial consumers can act on their own as traders without energy supply mediators.

Regarding the balancing market, there are certainly opportunities here but there are still challenges to overcome. From our literature review and based on discussions with experts in the field, we note the following challenges especially from a prosumer's perspective:

- Unstable regulatory framework: As noted, the balancing market is in a transition phase through pan-European integration initiatives; the MARI and PICASSO projects are still in progress and consequently important parts of the existing regulatory framework are under revision.
- Difficult access for prosumers: A lot of work needs to be done to encourage participation from small prosumers (kW scale). At this moment, the minimum capacity bid is 1 MW. Small user groups can participate only through aggregators.

- Unpredictable revenues: Furthermore, other factors that would make it unattractive to investors is the fact that it is an auction based system having its ups and downs and the fact that the total procurement demands are not large enough for having reproducible use cases.

Finally, we leave all other grid support services (i.e. black start, voltage control or infrastructure upgrade) out of scope also. These are very special use cases for battery storage especially from a prosumer's centric perspective.

3 Increasing the self-sufficiency in renewable energy systems

3.1 INTRODUCTION

In this chapter, we present a case study of a hybrid renewable energy installation combining PV, wind power, batteries and a PEM electrolyzer device. This work reflects a real use case that was conducted as part of a feasibility study on the 15 MW photovoltaic park of Terranova Solar located in Zelzate, Belgium. For the rest of this introduction section, we elaborate on hydrogen as a technology and address previous works on hydrogen projects. Afterwards, we give a detailed description of our study, mentioning the differences with previous projects and the main contributions delivered.

In general, energy storage systems can be classified into three categories: i) short-term storage (sec-min), ii) medium term storage (min-hours-days), iii) long-term storage (days-months) [26, 27]. Among these categories, especially, long-term storage systems can make a crucial contribution by absorbing renewable energy over extended periods of time without exceeding capacity limits. Long-term storage can be implemented by units with high energy densities and very low rates of self-discharge. Hydrogen is considered to be one of the most appropriate energy carriers for long-term storage [27-29]. In addition, hydrogen can provide several services in different sectors such as: i) backup power generators (fuel cells or internal combustion engines (ICEs)) ii) transportation sector iii) chemical industrial processes iv) gas boilers v) combustion turbines [30-33].

Among those sectors mentioned above, hydrogen has been used until now mostly for chemical industrial processes. For the rest, it has not yet reached commercial success. An explanation for this lies in the fact that electromechanical power generators (i.e. fuel cells and ICEs) making use of hydrogen are still under development [34]. Other explanations can be attributed to the need for demonstration projects, limited political incentives and the current public acceptance [34]. A major factor impeding the commercialization of hydrogen applications is the absence of a well-established infrastructure; by this meaning production, transport and distribution of the fuel [35, 36]. In order to accelerate the progress of a hydrogen economy, all these challenges need to be resolved.

Depending on the primary energy source (e.g., electrical, thermal, photonic etc.) different hydrogen production methods exist; each one having its own environmental footprint [37, 38]. A recent study has shown that hydrogen production through electrolysis driven by photovoltaics and/or wind power exhibits by far the lowest environmental impact, compared to conventional methods based on fossil fuels [39]. So far, hydrogen production through

electrolysis has been too expensive to compete against fossil fuel production methods such as steam methane reforming (SMR) [40]. However, as the price of photovoltaics and wind turbines decreases in combination with more austere regulations towards environmentally friendly solutions, renewable energy electrolysis becomes more attractive.

In the next two paragraphs, a short review of previous studies is given addressing the feasibility of Power to Hydrogen projects from a techno-economic point of view. These studies can be divided into two categories: i) Grid to Hydrogen [41-45], ii) PV/Wind to Hydrogen [46-50]. The difference is that in the first category the electric grid is used as the main power supply to drive the electrolytic process, whereas in the second category the power supply is exclusively a renewable energy source (PV and/or Wind power) without any contribution from the electric grid. Grid to Hydrogen studies: Kopp et al. [42] analyzed the performance of a 6 MW PEM electrolysis Grid to Hydrogen plant. Different market mechanisms were explored in order to generate revenue. It was concluded that through participation in the secondary reserve market the profitability of the plant can be improved. However, as stated by the authors, the study was carried out without considering the required capital expenditures of the electrolyzer. In Ref. [45], an economic study of a Grid to Hydrogen system is presented. Here, one of the objectives is to identify the optimal wholesale electricity price at which the levelized cost of the system is minimized. The study considered both PEM and alkaline electrolysis. Other factors included in the analysis are the size of the electrolyzer and its degradation. One of the conclusions was that the utilization factor of systems making use of PEM electrolysis must be higher compared to systems with alkaline electrolysis in order to minimize the levelized cost. Another Grid to Hydrogen project is presented by Felgenhauer and Hamacher in Ref. [43]. In this project, hydrogen is intended to be used for fuel cell logistic vehicles in an automobile factory. The study shows clearly that the production cost of hydrogen is influenced considerably by the cost of electricity and the utilization factor of the electrolyzer. In addition, the authors suggest that research scientists should focus on renewable energy in order to reduce the production cost of the fuel. In Ref. [44], an economic study was conducted regarding a hydrogen refueling station, located in Halle, Belgium. The station is powered partially by the electric grid. The other part of the power supply is provided by wind and PV power. As stated by the author, no information was provided to assess the contribution of renewables to the total power supply and therefore the study was done considering as electricity price the average grid price of Belgian medium-sized enterprises. A complete overview regarding the cost of each component (e.g., electrolyzer, compressors, storage, civil works etc.) is presented in the paper. The results show that the production cost of hydrogen can be reduced at 10.4 €/kg as long as the utilization of the system is maximized and provided that the electricity price is 0.04 €/kWh. Walker et al. [41] simulated the economic performance

of a Grid to Hydrogen plant considering different sizes of the electrolyzer (2 MW, 5 MW and 30 MW). Given an input value/threshold (e.g., 40 US \$/MWh) a comparison was made with the hourly wholesale electricity price. When the wholesale price is higher (lower) than the input threshold, the electrolyzer operates at minimum (maximum) power. It is mentioned that the profitability of the plant is strongly dependent on the utilization factor of the electrolyzer. Moreover, it was concluded that with big-sized systems the investment can achieve internal rates of return in the range of 15–21 %.

PV/Wind to Hydrogen studies: A Wind to Hydrogen project is presented in Ref. [46]. In this study, the objective is to generate hydrogen that will be used in refueling stations for fuel cell vehicles, in Sweden. The researchers used HOMER (software tool developed by NREL) to calculate the levelized cost of hydrogen production. Two types of wind turbines were considered: i) type V112, ii) type V82. The results delivered a levelized cost in the range of 5.18–7.25 US \$/kg and 6.52–9.62 US \$/kg respectively for the type V112 and V82. In Ref. [49], different scenarios of hybrid renewable energy systems were investigated to optimize the design of off-grid systems in Saudi Arabia. The simulation was done considering input data (PV, wind) at hourly resolution. Although this research work does not focus explicitly on the production of hydrogen, its proposed methodologies and results are interesting to take into account. An important conclusion is that in an optimized configuration where hydrogen production makes part of the system topology, wind power co-exists with PV power instead of using single sources (only PV or Wind). In Ref. [50], the objective is to design a hydrogen fueling station using only renewable energy sources. Given a specified demand to supply on daily basis 25 fuel cell vehicles, the researchers used HOMER to define an optimal combination of PV with wind power and battery storage. The resolution of the input data (i.e. wind speed, solar irradiance) used in this study is hourly. The results delivered a configuration at which the levelized cost of hydrogen production was in the range of 7.5–7.8 US \$/kg. Hou et al. in Ref. [48] carried out a techno-economic study of a Wind to Hydrogen system. The system was simulated using hourly resolutions of electricity price and wind speed data. One of the conclusions was that generating hydrogen from the wind farm in order to re-inject it afterwards back to the grid (re-electrification) using fuel cells is not profitable. Nevertheless, if instead of re-electrification hydrogen is sold to the industry at prices above 5 €/kg high returns of investment can be achieved. In Ref. [47], the research goal is to design optimally a renewable energy source system in order to maximize the amount of hydrogen produced by alkaline water electrolysis. It is mentioned that optimization is achieved by combining PV with wind power. Furthermore, it was concluded that wind power delivered a greater contribution to the total production of hydrogen compared to PV.

Conclusions and relation to present work

In this paragraph we summarize important conclusions drawn from the literature review and explain how these are related to the present research work:

- **Research should focus on the utilization of the system:** In general, the economic profitability of the installation increases with the utilization of the electrolyzer. Nevertheless, increasing the utilization is not a straightforward process as the utilization depends on several factors such as: (i) system topology (e.g., Grid and/or PV/Wind), (ii) electrolyzer technology (e.g., PEM or alkaline), (iii) control strategy [41], [45].
 - Present study: We consider different system topologies (PV, Wind, Batteries) to investigate how their impact on increasing the utilization of the system, taking into account the existing geographical conditions and topological limitations of the site under consideration.
- **The need for hybrid power sources:** Research suggests that projects targeting renewable energy electrolysis should investigate synergies on the power source i.e., combining PV with wind power. A hybrid power source, where PV co-exists with wind, typically exhibits better stability (lower intermittency) on the long term (i.e., months – years) [47], [49].
 - Present study: The analysis starts from the basic scenario where only PV exists as the power source. Wind power is considered in all subsequent scenarios coexisting with PV. Wind power was sized (i.e., total wind power capacity) based on the provided datasheets from the involved wind turbine manufacturer and considering the topological input data of the site.
- **PEM technology is preferred for renewable energy electrolysis.** Regarding the electrolyzer technology, there are in essence two major technologies: (i) PEM and (ii) alkaline. PEM has the advantage that the electrolyzer device can operate at full load range. On the other hand, alkaline electrolyzers are cheaper but they require a minimum partial load and therefore they are less flexible in the context of intermittent power sources such as wind and pv [38, 42, 51].
 - Present study: In this study, we received quotations for both PEM and alkaline electrolyzers. Finally, it was decided to go forward with PEM. We explain in more detail why this decision was made in the relevant section presenting the electrolyzer specifications.
- **Battery storage has not been addressed.** Previous research works have investigated different control strategies for operating the electrolyzer (e.g., in function of renewable power yield, wholesale electricity price). However, there is very limited knowledge about the potential added value of a battery storage system.

- Present study: A sensitivity analysis was carried out quantifying the impact of battery storage in increasing the utilization of the system in function of the battery energy capacity. Two popular battery technologies were considered (Vanadium Redox Flow, Lithium NMC). Furthermore, results include the annual battery utilization (cycles per year) and an economic profitability analysis considering real market prices and quotations received by the involved partners.
- **The need for real case studies**: In general, the great majority of research works are purely theoretical investigations built upon key assumptions very often not curated by industry experts and practitioners in the field.
 - Present study: This research work forms the deliverable of a real feasibility study – producing hydrogen from the biggest photovoltaic park (15 MW, as of 2018) in Belgium. The research was conducted under the supervision and in strong collaboration with industry experts comprising (i) a PV park owner, (ii) energy supply company, (iii) electrolyzer manufacturer, (iv) wind turbine manufacturer, (v) battery storage system developer, (vi) natural gas pipeline company and (vii) Ghent university.
- **The business case is selling hydrogen to the industry**: Although hydrogen technically has a broad scope of applications, there are not many options when considering the profitability of the system. Research has shown that compression and storage in high pressure tanks can add up significantly to the total capital expenditures [44]. The cost of hydrogen sold through refueling stations (e.g., fuel cell cars or trucks) is too high to compete with today's conventional fuels in mobile applications (e.g., diesel, gasoline) and re-electrification is not an option due to the large efficiency losses power-to-gas-to-power [48]. Other ideas such as grid support services (e.g., provision of aFRR) are doubtful for providing stable revenue streams on the long term [42].
 - Present study: We present a techno-economic feasibility study for 'hydrogen blending'. By injecting hydrogen directly into the natural gas pipeline, there is no need to install compressors and high pressure storage tanks, therefore significant cost reductions can be achieved.

Research core, key questions & contributions

An overview of the system topology is given in [Figure 21](#). A 15 MW PV park provides power to the electrolyzer device generating hydrogen that is later sold to the industry. The business owner wants to keep the electrolyzer powered as long as possible during the year in order to maximize the hydrogen quantity generated. The hydrogen must be 100 % green meaning that the electric grid cannot be used as a power source; it is only used as a sink to absorb the power

surplus of the PV (and/or Wind) when it exceeds the power of the load. The electrolyzer uses renewable energy derived either directly from the sources (i.e. photovoltaic park, wind turbines) or indirectly from the battery that has been charged by the sources. Next, we present the key research questions addressed in this work including the delivered contributions.

- Which electrolyzer technology and what size should I choose ?
In Section [3.2.3](#), we provide explanation which technology was chosen and how the size of the electrolyzer was selected. The electrolyzer datasheets and quotations can be used as references in future research works.
- How do I calculate the utilization of the electrolyzer ?
To calculate all performance metrics (e.g., battery cycles, hydrogen quantity, utilization) a power flow model was developed (see Section [3.2.5](#)). This is a basic power flow model ignoring non-linearities in the efficiency of the electrolyzer device and the battery storage system (see Chapter 5 for the analytic model in Matlab/Simulink).
- What is the utilization of the electrolyzer under different system topologies ?
We analyzed and compared the utilization of the system in four separate scenarios (Section [3.3.1](#)). All simulations had a yearly time period (1 Jan 2016–31 Dec 2016) at 10 min resolution. [Table 5](#) summarizes the techno-energetic results from all four scenarios including the renewable energy yield, utilization factor, hydrogen quantity and battery cycles.
- What is the added value of battery storage and which technology to choose ?
A sensitivity analysis was carried out in Section [3.3.1](#) and [3.3.2](#) investigating the impact of battery storage in increasing the utilization of the system. Results are given separately for the VRB and Lithium NMC technology.
- How do I store, distribute and sell hydrogen ?
This question is treated in Section [3.3.2](#). We explain which options were available for the PV park owner given the topological conditions of the site and input/constraints from the involved partners.
- What is the cost of hydrogen (€/kg) within an investment payback period of 5 – 10 years ?
In Section [3.3.2](#), we present the results from the economic profitability study focusing on two (out of four) scenarios.

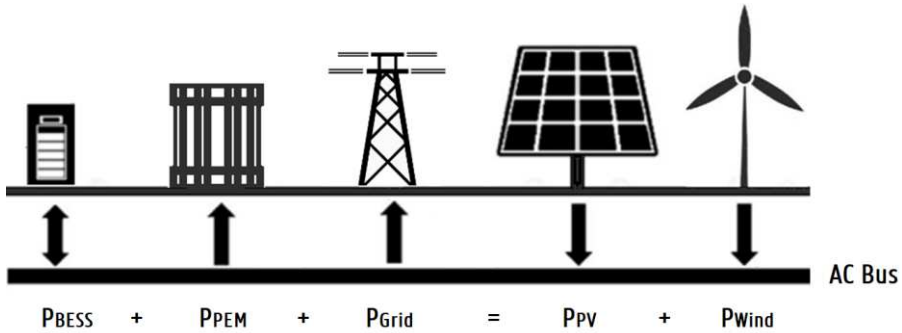


Figure 21. System topology

Section [3.2](#) presents the methodology of the study. It explains the input data (i.e. wind speed, PV power profile), the technical specifications of all participant components (PV, wind, electrolyzer and battery) and the power flow model. At this point, it is worth mentioning that this methodology is not exclusively applicable to the present case study. It is a data driven approach that can be generalized to other locations as well, as long as the appropriate input data is available. Section [3.3](#) is dedicated to results, comprising two parts. Part 1 deals with generic energetic assessments. The aim of Part 1 is to investigate how the utilization factor of the electrolyzer changes for each scenario (A, B, C and D) depending on the type and size of the source and storage component. Part 2 concerns economic evaluations (i.e. payback period, accumulated profit) only for scenarios B and C which seemed to be the most realistic to implement taking into account the constraints of the existing installation. Finally, all relevant conclusions, remarks and ideas for further research are given in Section [3.4](#).

3.2 METHODOLOGY

3.2.1 Photovoltaic park

The photovoltaic park is located in Zelzate, East Flanders, Belgium. To give an indication of its size, the total surface covered by photovoltaic panels is estimated at 240000 m². With respect to the electric peak power, 15 MW is the highest ever measured value during sunny days. So far, the photovoltaic park has been injecting all its energy into the electric distribution grid ¹⁴. Since its commissioning, the active power generation is measured and monitored per timeslots of 5 min. ¹⁵ In all scenarios presented in section [3.3](#), the photovoltaic power profile was simulated using the measurements of the period: 1 January 2016–31 December 2016.

¹⁴ The voltage level of the distribution grid at which the photovoltaic park is connected is 12000 V.

¹⁵ This means 1 average active power registration every 5 min.

3.2.2 Wind turbines

The simulation of the wind power profile was more complicated since no measurements were available for the location and type of wind turbines that were meant to be installed. The methodology followed in this study consists of three steps: Initially wind speed data was received and processed for the concerned location and period of simulation. Afterwards, the processed wind speed data was converted into electric power data using the datasheets of the chosen wind turbine manufacturer. Finally, the power data of the single wind turbine was multiplied by a constant to calculate the total wind power profile according to the desired wind power capacity. The methodology is further explained in the following paragraphs.

Wind speed data was received from a weather station located nearby the site. The wind speed measurements were carried out at 10 m height above the ground at 1 registration every 10 min, concerning the period: 1 January 2016–31 December 2016. However, the actual hub height of the wind turbines studied in this project was 55 m. In order to calculate the respective wind speed values at 55 m the following equation was used [52]:

$$\frac{v}{v_{10}} = \left(\frac{h}{h_{10}} \right)^a$$

where,

- v is the wind speed (m/s) at height h
- v_{10} is the wind speed (m/s) at 10 m height
- a is the Hellman exponent

In this study, the Hellman exponent was set at 0.5 regarding the geographical topology of the site. This choice resulted in multiplying all speed values at 10 m by 2.35. The probability density function of the final calculated wind speed at 55 m is given in [Figure 22](#). The average wind speed is 6.7 (m/s).

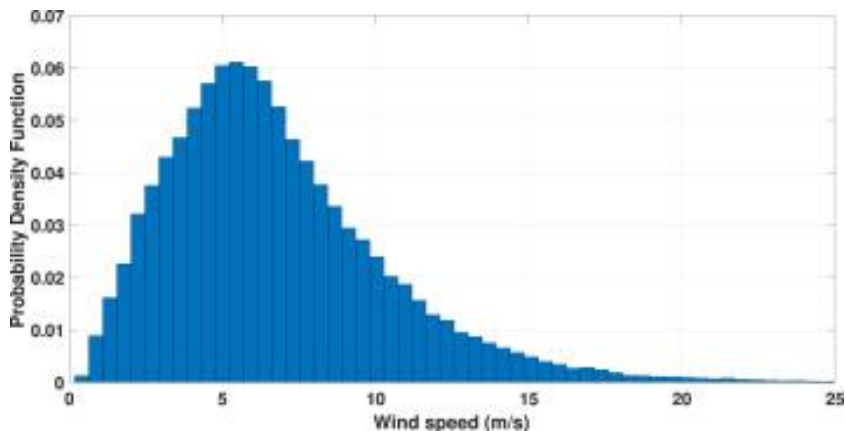


Figure 22: Wind speed distribution

After having defined the wind speed profile, the active power profile of a single wind turbine can be calculated, based on the datasheets provided by the manufacturer. The technical specifications and the power-to-speed curve of the chosen type of wind turbine are given in [Table 2](#) and [Figure 23](#) respectively. The wind turbine can deliver up to 330 kW electric power. It has an automatic yaw control mechanism, meaning that it always follows the optimal wind speed direction. If the wind speed is very high (above 20 m/s) the wind turbine is shut down for protection. It is also important to note that, during periods of speeds below 3 m/s the wind turbine does not generate electricity. The probability of having wind speeds below that value is 12 % (See [Figure 22](#)). Finally, the total wind power profile is formed by multiplying the wind profile of a single wind turbine with a constant depending on the desired power capacity. For example: A 2 MW wind farm is almost equivalent to six medium-sized wind turbines of the type XANT L-33: $330 \times 6 = 1980$ MW.

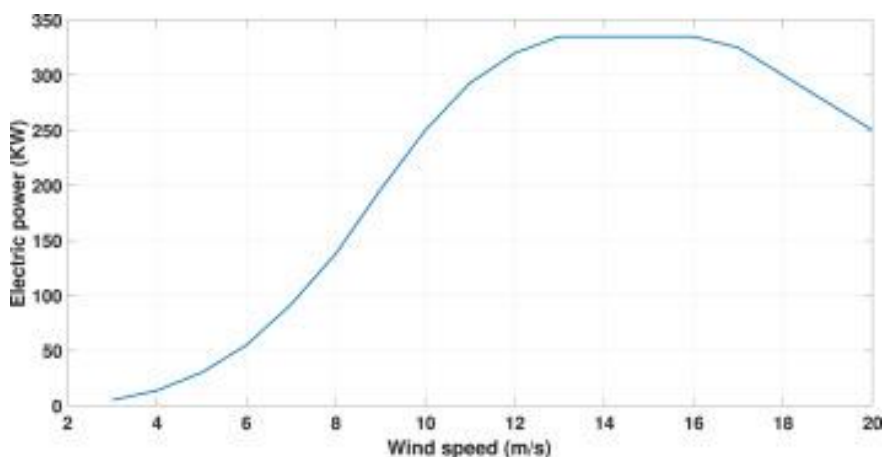


Figure 23: XANT L-33: Power-to-speed curve

Table 2: Wind turbine: Technical specifications

Characteristics	Specifications
Type	XANT-L33
Number of blades	3
Rotor diameter	33 m
Hub height	55 m
Rated electrical power (see also ¹⁶)	330 kW
Cut-in wind speed	3 m/s
Cut-out wind speed	20 m/s
Orientation	Downwind
Yaw control	Auto-yaw

3.2.3 Electrolyzer

The technical specifications of the electrolyzer used in this study are presented in [Table 3](#). The technology chosen is Polymer Electrolyte Membrane (PEM) electrolysis instead of alkaline electrolysis. As mentioned before, in contrast to alkaline electrolyzers that require a minimum partial load, PEM electrolyzers can operate at full load range [[38](#), [42](#), [51](#)]. Based on our literature review and discussions with the involved electrolyzer manufacturer it was concluded that PEM electrolyzers are more suitable for applications where the power supply is intermittent (e.g., PV, wind turbines). This conclusion is doubtful in the scenario where battery storage makes part of the system topology to support the power source (similarly to UPS applications). If the battery storage is appropriately sized (in terms of power and energy capacity) the combined power source (i.e., PV/Wind and battery) can provide continuous power to the alkaline electrolyzer; loss of power is less frequent. Nevertheless, the disadvantage of this approach is that the battery design is unavoidably coupled to the electrolyzer device specifications; for instance a 1 MW alkaline electrolyzer at 40 % minimum load would require a 400 kW battery. Based on the received quotations and discussions with the battery storage developers, it was concluded that neither the battery costs were sufficiently low nor the

¹⁶ At standard conditions (air density 1.225 kg/m³)

necessary expertise existed in building such large scale UPS for alkaline electrolyzers. Finally, the decision was made to proceed with the PEM technology.

Regarding the size of the electrolyzer device we received quotations for a modular system: 250 kW, 500 kW, 1 MW, 2 MW and 4 MW. [Figure 24](#) illustrates the capital expenditures (normalized in €/kW) of the system comprising (i) electrolyzer stack, (ii) software and (iii) installation. On the one hand, as can be seen, the cost of smaller installations becomes higher due to the impact of fixed costs (i.e. manufacturing, project development, installation & maintenance). On the other hand, smaller systems have higher utilization; the smaller the system the higher the utilization (and therefore the normalized revenue). Based on a preliminary study, maximizing profits within a 10 year payback period, we concluded that 1 MW is the optimal size to proceed with.

Table 3: Electrolyzer: Technical specifications

Characteristics	Specifications
Type	PEM
Rated stack power	1 MW
Lifetime	70000–80000 h
Efficiency	60 %
Load range	0–100 %
Hydrogen production at rated power (see also ¹⁷)	200 Nm ³ /h or 18 kg/h
Purity	99.99 %
Output pressure	30 bar
Water consumption	0.019 m ³ /kg H ₂

¹⁷ Considering the lower heating value of hydrogen: LHV = 119.9 (MJ/kg)

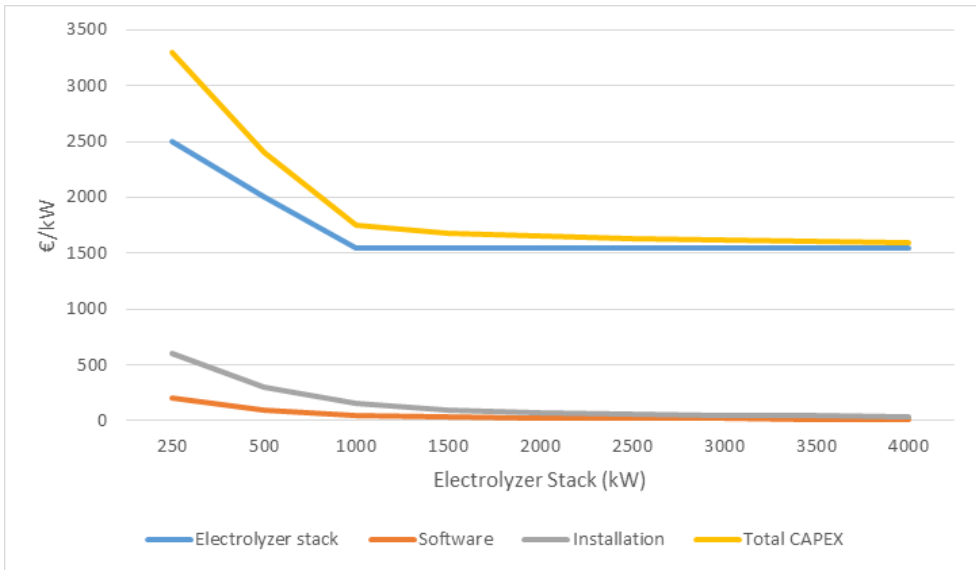


Figure 24: Electrolyzer capital expenditures

Monetization

Four monetization options were investigated and presented to the PV park owner: (i) provision of grid support services to the TSO, (ii) hydrogen re-fueling station for mobility, (iii) re-electrification, (iv) hydrogen blending. Regarding (i), the idea was to use the electrolyzer for the provision of aFRR (downward regulation). The owner acts as a BSP participating in aFRR auctions; winners of the auction get remunerated for their reserved capacity and activated energy volume. The aFRR market serves as mechanism for reducing the electricity price (i.e., electrolyzer operating cost). However, the disadvantage is that control is taken over by the TSO and therefore this impacts negatively the utilization of the system. Option (i) was finally rejected; our analysis showed that the added value of aFRR is very stochastic and therefore difficult to establish a predictable revenue stream on the long term. With respect to (ii), the idea was to build a local re-fueling station for fuel cell vehicles e.g., early adopters of hydrogen buses, trucks and cars. In such case, once hydrogen is produced after the electrolysis process, the next step would be to store hydrogen in high pressure tanks before it can be distributed through hydrogen dispensing systems. Our analysis showed that investing in additional components (mainly compressors and storage tanks) would result in significant capital expenditure increase, 40–50 % above the basic case having only the electrolyzer device (see Section 3.3.2 for quotations). Finally, option (ii) was abandoned because the hydrogen cost proved to be unacceptably high for mobility end users (above 9 €/kg). In (iii), the idea is

building a complete power-to-gas-to-power plant. Similarly to (ii), compressors and high pressure storage tanks are needed. What is more, a fuel cell system would be installed to convert hydrogen back to electricity and inject power to the grid. By combining hydrogen storage with fuel cells we decouple the weather conditions from electricity generation and similarly to conventional power plants we can inject power at any moment we want. The plant would be in essence a 'green' alternative of fossil fuel based generators (e.g., natural gas, diesel) setting the price in the merit order of electricity generation and providing flexibility to the system (i.e. ancillary services to the TSO). Nevertheless, this option (iii) was also abandoned; a preliminary study showed that the capital expenditures were too high to compete against today's natural gas driven generators. Option (iv) was the most promising to proceed with. The availability of a natural gas pipeline passing nearby the PV site allowed us to consider 'hydrogen blending'. In such cases, hydrogen can be injected directly into the pipeline without the need of local on-site storage. Discussions started with the company/owner of the pipeline to investigate the feasibility of the idea. The company verified that there would be no issues regarding the potential risks in mixing hydrogen with natural gas. Furthermore, they stated they were willing to purchase the fuel at a reasonable price (see Section [3.3.2](#) for sensitivity analysis on the fuel price).

As already mentioned, in order to evaluate the performance of the system, in all scenarios presented in the following section, the term utilization is used. The definition of the term is given as the ratio of the actual hydrogen quantity generated within a certain time period to the ideal hydrogen quantity generated if the electrolyzer was operating continuously at its rated power. In this study, where the simulation period was always one year the utilization was calculated as follows:

$$U_{PEM} = \frac{\text{Actual H}_2 \text{ quantity}}{\text{Ideal H}_2 \text{ quantity}} = \frac{\text{Actual H}_2 \text{ quantity}}{18 \frac{\text{kg}}{\text{h}} \cdot 8760 \frac{\text{h}}{\text{year}}}$$

3.2.4 Battery storage system

Inevitably, there are always periods when the sun does not shine and the wind speeds are very low irrespective of the size of the renewable energy sources. The idea was to use a battery storage system to support the electrolyzer during those periods of poor renewable energy yields. With respect to the type of battery, it was difficult to identify a battery technology that best suited the intended application of this project. Based on literature reviews, It was decided to focus on two technologies: Redox Flow and Lithium-ion batteries. Although both technologies exhibit interesting characteristics especially for stationary grid-scale applications, there are many differences between them as explained in the following paragraph.

One of the most important advantages of redox flow compared to Lithium-ion is that the energy capacity component is independent from the power component, thus allowing a more flexible design. Redox flow batteries can endure many more cycles than Lithium-ion with almost zero capacity fade. New generations of Lithium-ion batteries can undergo high depths of discharge (DoD) comparable to those of redox flow batteries. However, this comes at the expense of accelerated capacity fade. The major advantages of Lithium-ion is that their efficiency is higher and that they are much cheaper per unit of power capacity (expressed in €/kW) [28, 53, 54].

Among all scenarios investigated in this study, only scenario C includes a battery storage system. The analysis in scenario C was done twice. The first simulation was done with a Vanadium Redox Flow battery whereas the second simulation was done with a Lithium NMC battery. Table 4 presents the technical specifications of both batteries. This information was derived from commercial datasheets. It is also worth mentioning that the presented batteries belong to the same price range,¹⁸ therefore maintaining a fair comparison.

Table 4: Battery: Technical specifications

Characteristics	Specifications	
	Vanadium Redox Flow	Lithium NMC
Type	Vanadium Redox Flow	Lithium NMC
Cycles	>> 12000	6000 ¹⁹
Efficiency	75 %	95 %
Capacity fade	Insignificant	70 % EoL
DoD	100 %	100 %
Self-discharge	Insignificant	Insignificant
C-Rate	0.2 C	1 C
Cost	400–600 €/kWh	400–600 €/kWh

¹⁸ The price indications are based on offers received from different battery storage developers. Due to confidentiality agreements, the participant industrial partners preferred that the origin of these offers is not mentioned in the publication.

¹⁹ Under a (dis)charging rate of 1C, at 100 % DoD after 6000 cycles the battery capacity will have decreased at 70 % of its initial value. At that moment the battery has reached its End-of-Life (EoL).

3.2.5 Power flow model

Figure 25 illustrates the pseudocode of the power flow algorithm that was used to calculate the results for all four scenarios presented in Section 3.3.1:

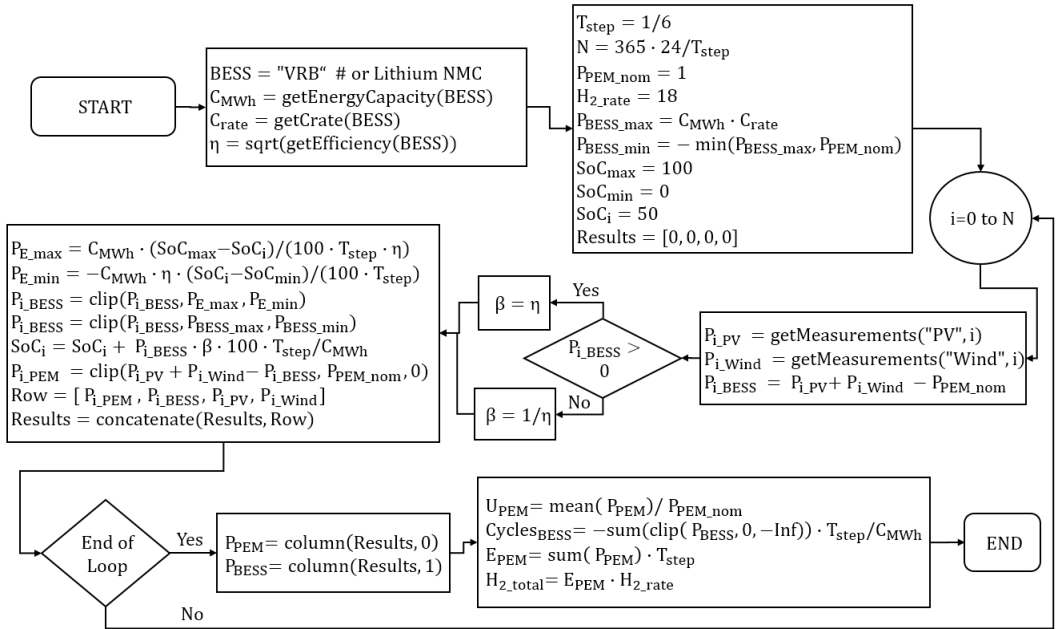


Figure 25: Power flow model (pseudocode)

where:

- C_{MWh} is the energy capacity of the battery (MWh)
- T_{step} is the time step of the yearly simulation (h^{-1}).
- P_{PEM_nom} is the nominal power of the PEM electrolyzer (MW)
- i is the index of the current simulation step
- P_i is the power of the component (i.e., PV, Wind, battery or electrolyzer) during the time slot $[i, i + 1]$
- SoC is the State-of-Charge of the battery (%)
- H_{2_rate} is the rate of hydrogen production (kg/MWh) when the electrolyzer operates at nominal power.
- E_{PEM} is the total energy consumption of the electrolyzer (MWh) over the year.
- H_{2_total} is the total hydrogen quantity (kg) produced over the year.

The time step of the simulation is set at 10 min (1 / 6 h); the time step was defined by the dataset with the lowest time resolution which was the wind speed measurements.

Consequently, the power profile of the PV park, recorded at 5 min resolution, was scaled-down to 1 average measurement every 10 min. At this point, it is important to note that PEM electrolyzers can respond very fast to command signals. The rate of hydrogen production can change from 0 to 100 % within a few seconds [55]. Therefore, since the yield data changes much slower, it can be considered that the available for hydrogen production energy is always captured by the PEM electrolyzer at any time. The time period in all power flow simulations is set fixed 1 Jan 2016–31 Dec 2016.

Regarding the operation of the battery, we considered a simple rule based control strategy. When the power of the renewable energy power source (PV and Wind) is higher (lower) than the rated power of the electrolyzer, the battery is charged (discharged) with the power surplus (deficit). The (dis)charging power is always constrained by the battery C rate. Furthermore, in discharging mode the battery is never allowed to discharge more power than the electrolyzer rated power; in other words, the battery is exclusively used to power the electrolyzer in no case is it allowed to discharge (inject) power back to the grid.

3.3 RESULTS

3.3.1 Energetic assessments

[Table 5](#) summarizes the results from all four scenarios investigated in this study:

Table 5: Energetic results

		Scenario A	Scenario B	Scenario C		Scenario D
				Lithium NMC 0.05–10 MWh	VRB 0.05–10 MWh	
PV energy yield (MWh)		16150	16150	16150	16150	16150
Wind energy yield (MWh)		N/A	5594	5594	5594	41960
Battery cycles		N/A	N/A	424–179	242–159	N/A
Electrolyzer	Energy consumed (MWh)	3365	5740	5792–7554	5784–7361	7183
	H ₂ quantity produced (kg)	65495	103000	103950–135550	103780–132090	128900
	Utilization (%)	41.5	65.5	66.1–86.2	66.0–84.0	82.0

Scenario A: electrolyzer, 15 MW PV

The participant components are the photovoltaic park and the electrolyzer. This is the basic scenario where PV is the only source of electric energy; no contribution is made by wind power or by a battery storage system. The total annual energy yield delivered by the photovoltaic installation is 16150 MWh. Comparing the power capacity of the PV park (15 MW) to the power capacity of the electrolyzer (1 MW), one could state that the photovoltaic installation is overdimensioned. Nevertheless, despite the abundance of solar energy, the amount of energy consumed by the electrolyzer was found to be merely 3635 MWh or 22.5 % of the total solar energy yield. The utilization of the electrolyzer is 41.5 %.

The fact that no energy is generated during the night and the frequent presence of cloudy days are the most important factors affecting the utilization. Due to the low utilization factor, an investment in such system would not be very competitive. Consequently, the results of scenario A lead to the development of scenario B where PV co-exists with wind power.

Scenario B: electrolyzer, 15 MW PV, 2 MW wind

The system comprises the photovoltaic park, six XANT L-33 wind turbines and the electrolyzer. The owner of the photovoltaic park was considering, before the start of this study, to upgrade his renewable energy installation by adding wind power; we also noted that previous research works suggested the co-existence of wind with PV in renewable energy electrolysis projects. Due to space limitations and geographical constraints, it was not possible to install more than six medium-sized wind turbines. This explains the choice in scenario B (and C) to consider precisely six medium-sized wind turbines and no more than that.

The additional amount of renewable energy produced by the wind turbines is 5594 MWh. The energy consumed by the electrolyzer is 5740 MWh or 26.5 % of the total energy produced (PV and wind). The utilization of the electrolyzer is 65.5 %. This is an increase by 24.0 % compared to scenario A. It can be concluded that the contribution made by wind power is bigger, proportionally to its size, than the contribution of photovoltaic power. A way to explain this fact is that the capacity factor of wind power in this project is almost three times bigger than the capacity factor of the photovoltaic installation. The capacity factor is defined as the ratio of the actual energy yield produced within a certain period to the ideal energy yield if the unit operated continuously at its maximum power. In this project the capacity factors for PV and wind are:

$$CP_{PV} = \frac{16150 \text{ MWh}}{15 \text{ MW} \times 8760 \frac{\text{h}}{\text{year}}} = 12 \%, \quad CP_{Wind} = \frac{5740 \text{ MWh}}{2 \text{ MW} \times 8760 \frac{\text{h}}{\text{year}}} = 33 \%$$

With the utilization factor at 65.5 % scenario B proves to be more competitive than scenario A. However, this percentage is the maximum that can be achieved using only power source components. To increase the utilization beyond this limit it is necessary to include also an energy storage component in order to allocate more efficiently the already available renewable energy yield. Such hybrid topology comprising PV, wind and battery storage has been studied in scenario C.

Scenario C: electrolyzer, 15 MW PV, 2 MW wind, battery

The components participating in this scenario are the photovoltaic park, the electrolyzer, six XANT L-33 wind turbines and a battery storage system. As already mentioned, two cases were considered, one with Lithium-ion NMC and the other with Vanadium Redox Battery (VRB). For each case, the simulation was done repeatedly by changing the battery capacity within the range 0.05–10 MWh.

The utilization for the Lithium-ion NMC case is 66.1–86.2 %, which is slightly better compared to the 66.0–84.0 % of the VRB case. Thanks to its higher efficiency and C rate, the Lithium NMC battery can transfer more energy to the electrolyzer than the VRB, given the same time period and battery capacity. Finally, it is noticeable in both cases that as the battery capacity increases the number of battery cycles per year declines. In other words, although bigger batteries make larger contributions to the increase of hydrogen production, their investment potential is lower compared to smaller batteries.

As expected, scenario C outperforms scenario B, where the percentage of improvement is obviously dependent on the size of the battery. What is important to note here is how wind power outperforms battery storage in increasing the utilization (and generally speaking as an investment choice in the context of renewable energy electrolysis). 2 MW of wind power resulted in increasing the utilization by 24 % compared to a 10 MWh Lithium battery resulting in 22 % increase. Although we cannot reveal the quotations that we received from the wind turbine manufacturer, we can confidently state that the cost of a 10 MWh Lithium NMC battery is clearly higher than the cost of an equivalent 2 MW wind power installation. What is more, another important advantage of wind power is that the owner still generates a considerable revenue stream by injecting power to the grid, which is of course something that the battery cannot do standalone.

In both scenarios B and C, it was assumed that the wind power capacity is maximized at 2 MW. What has not been mentioned yet and it is interesting to address is a system that consists of both infinite PV and infinite wind power (scenario D).

Scenario D: electrolyzer, 15 MW PV, 15 MW wind

The system consists of the photovoltaic park, forty five XANT L-33 wind turbines and the electrolyzer. One of the ideas proposed by the industrial partners, was to purchase electric energy from an external already existing wind farm, instead of installing new turbines inside the site. The wind farm was located at less than 300 m outside the photovoltaic park. It was therefore possible with a cable connection to transfer energy directly from the wind farm to the electrolyzer. The power capacity of the wind farm was estimated around 15 MW. Since no data was available, the power profile of the wind farm was simulated by multiplying the power profile of a single XANT L-33 by forty five: $330 \times 45 = 14.85 \approx 15 \text{ MW}$

The energy yield produced by wind in this scenario is 41960 MWh. The energy consumed by the electrolyzer is 7183 MWh or 12.5 % of the total energy produced (PV and wind). The utilization of the electrolyzer is 82.0 %. This is an increase by 40.5 % compared to scenario A. Proportionally to its size, scenario D performs worse than scenario B. The amount of additional hydrogen quantity produced by wind in scenario D is almost 1.7 times greater compared to scenario B. However, the total wind energy yield in scenario D is 7.5 higher than the wind energy yield in scenario B. It was therefore concluded that by oversizing the renewable energy sources only, it is not possible to reach 100 % utilization. Even with abundant solar and wind energy, the utilization is saturated due to the inevitable presence of unfavorable weather conditions (i.e. night-time, cloudy days, low wind speeds). In order to increase hydrogen production beyond the saturation point a battery storage system is needed.

3.3.2 Economic evaluations

The economic evaluations presented in this section concern specifically scenario B and C. Scenario A was left out of scope due its limited utilization (merely 41.5 %). Furthermore, scenario D was not considered despite its high utilization, since it required additional studies to clarify some technical and legal issues. It is important to note, that the entire economic study was based on the assumption that the renewable energy sources, both PV and wind, already exist. This means that hydrogen production comes only as a solution to increase the value proposition of the renewable energy installation that was initially designed to produce and provide electric energy to the grid. As a result, the capital investments needed to realize the photovoltaic and wind power installation were ignored.

The economic analysis was done considering the parameters and variables that are given in [Table 6](#). The most important parameters are the costs of the electrolyzer and electricity consumption. Regarding the electrolyzer, the investment was split into two components: i) capital expenditures and ii) operating expenditures. The cost of each component was the

average value calculated on three separate offers received from well-known manufacturers in the European region (Once more, it is mentioned that is not possible to disclose the origin of these offers. Readers who want to draw a comparison with price indications presented in other papers can refer to [44, 56, 57]). Furthermore, the electricity cost was set at 0.04 €/kWh, which is representative of the average price for the Belgian wholesale electricity market in 2017 [58]. Lastly, the study included also the cost of water consumption [59] and a moderate rate of inflation.

Table 6: Economic evaluations: Parameters & Variables

		Value
Parameters	Electrolyzer CAPEX	1750 €/kW
	Electrolyzer OPEX	4 % of the CAPEX per year
	H ₂ O cost	4 €/m ³
	Electricity cost	0.04 €/kWh
	Inflation	2 %
Variables	H ₂ price (revenue)	4–7 €/kg
	Battery capacity	500–5000 kWh
	Battery CAPEX	150–600 €/kWh

With respect to the price of hydrogen purchased by the gas supplier, there were no exact indications. Nevertheless, it was estimated that a realistic value would be within 4–7 €/kg. The battery capacity was also regarded as variable, as already presented in the energetic assessments of scenario C. However, the analysis was done this time considering only the type Lithium NMC which proved to be more efficient compared to the VRB. Finally, the capital expenditure of the battery was selected to be the third variable. Although the available price indications suggested to set the variable within 400–600 €/kWh (See Table 4), it was decided to extend the range at 150–600 €/kWh, thus taking into account scenarios of significant cost reductions as expected in the near future [38].

The economic performance of each scenario was evaluated by two indicators: i) the payback period (years) of the investment and ii) the accumulated profit (€) realized 10 years after the system was commissioned. The payback period is simply the time in years needed to pass until the revenue equals the total capital and operating costs of the system. The accumulated profit

is the difference between the revenue and the total capital and operating costs of the system precisely 10 years after the start of the project.

The results of scenario B are given in [Table 7](#). Since no battery storage system exists in this scenario, the price of hydrogen is the only variable influencing the two indicators. In order to reach a payback period in less than 10 years, hydrogen must be sold at least 5 €/kg. If hydrogen is sold above 6 €/kg the return of investment is quite higher delivering a payback period less than 6 years.

Table 7: Economic evaluations: Scenario B

Hydrogen price (€/kg)	Payback period (Years)	Accumulated profit after 10 years (€)
4	15	-582000
4.5	11	-13800
5	8	554000
5.5	7	1120000
6	6	1690000
6.5	5	2260000
7	5	2830000

The results of scenario C cannot be presented effectively using tables, since the outcome is always a function of three variables. The performance of scenario C can be illustrated in the form of a 4D space, where three dimensions correspond to the variable coordinates and the fourth dimension is colorized representing the result of the function (payback period or accumulated profit).

The payback period is given in [Figure 26](#). The price of hydrogen remains the most important factor affecting the payback period. Another conclusion to note is that the payback period becomes higher as the battery capacity increases. This can be explained by the fact that the battery is getting more underutilized (lower number of cycles) as its size increases. It is worth mentioning that compared to scenario B, the payback period in scenario C is always higher (or slower). The accumulated profit of scenario C, illustrated in [Figure 27](#), is expressed as the additional accumulated profit (%) having as reference scenario B. All values in [Figure 27](#) equal to 0 % represent cases where the accumulated profit is equal or worse to that of scenario B.

As it can be seen, there are cases where scenario C outperforms scenario B in terms of accumulation of profit. Such cases require that the maximum capital investment of the battery does not exceed 250 €/kWh. Furthermore, as it can be seen in some cases, for a given hydrogen price and battery cost, the profit becomes higher as the battery capacity becomes bigger. In other words, given a certain period of comparison (in this experiment 10 years) there are cases where scenario C is more profitable than scenario B although the return of investment is always faster in scenario B.

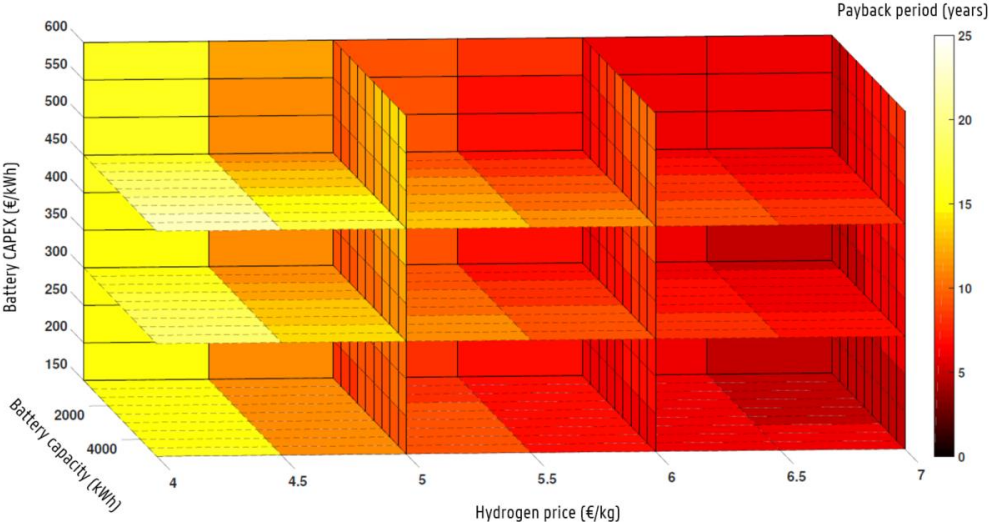


Figure 26: Economic evaluations: Payback period of scenario C with Lithium NMC

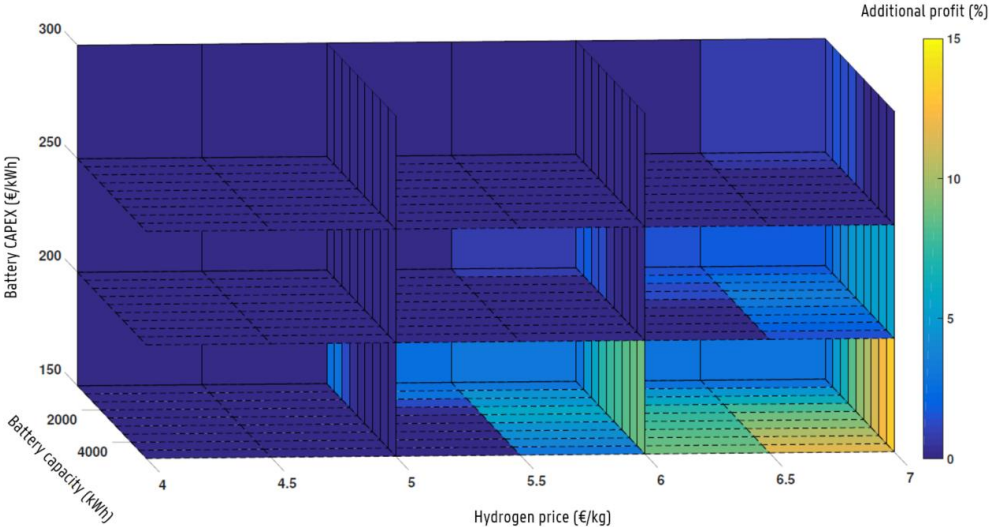


Figure 27: Economic evaluations: Additional accumulated profit of scenario C with Lithium NMC, having as reference of comparison scenario B

3.4 CONCLUSIONS

An overview of the most interesting conclusions/notes drawn out of this feasibility study is presented below:

- **Renewable energy electrolysis can be a profitable business case.** Hydrogen production through electrolysis powered by photovoltaics and/or wind turbines can add value to an already existing renewable energy installation as long as the electrolyzer is not underutilized. In this study, we showed that a payback period below 8 years is achieved provided that hydrogen is sold at least 5 €/kg. In this project, the business case is selling hydrogen to the industry; after production the fuel is injected directly into the natural gas pipeline eliminating the need for additional components (i.e., compressors, storage tanks) that would lead to an overall capital expenditure increase of 40–50 %.
- **For new system topologies, we suggest the priority order Wind → PV → Battery.** In this study, our analysis started from PV since the installation already existed. As has been proven (also concluded from the literature review), wind power contributes more than PV in generating hydrogen in terms of power capacities. We also note that the availability of space for placing PV panels is always a major concern for new installations. In the context of renewable energy electrolysis, we suggest that wind power be considered as the basic scenario; PV comes as a second choice. Regarding the battery, given the currently high prices, a battery may be considered as a last auxiliary component for maximizing the utilization of the system (e.g., refueling stations requiring non-stop continuous production).
- **Lithium-ion NMC outperforms VRB.** The techno-energetic results show that Lithium-ion performs better than the VRB. Thanks to its higher C rate and efficiency, Lithium-ion can transfer more energy to the electrolyzer given a period of one year. The VRB could outperform Lithium-ion if the comparison was extended up to the moment that Lithium-ion reaches its end of life. By that time, the VRB would still have lots of cycles to provide. However, such scenario would require many years to pass (at least 15) exceeding the payback period of investment. Consequently, the Lithium-ion battery is preferred.
- **Battery storage is still very expensive in the context of renewable energy electrolysis.** Under the current price indications received from battery developers (400–600 €/kWh) and considering the targets when setting the price of hydrogen that is sold to the industry, it is concluded that battery storage is for the time being too expensive to provide added value.

It must be emphasized once more that the time resolution of all datasets used to carry out this techno-economic analysis was set at timeslots of 10 min. In comparison to many other studies

where the time resolution is lower (e.g., 15 min, 30 min, 1 h or even lower), a 10 min resolution leads to more accurate estimations. However, in reality, the characteristic frequency spectrum of both the photovoltaic and wind power profile lies in the range of seconds. Depending on the intensity of those second occurring variations, the validity of all studies conducted at lower resolutions is influenced. Consequently, the next goal of our research is to focus on high time resolution datasets (e.g., 1 min, 30 s, 10 s) in order to evaluate the performance of the system under real-time conditions. Having datasets at such high resolution will enable us to estimate the simulation error when lower resolutions are considered.

Moreover, in the next chapter, we will shift our focus on the lithium-ion technology. From our literature review and discussions with industry partners, we conclude that this is currently the most promising technology primarily due to its high energy efficiency and high C rate capabilities. What is more, lithium-ion is the technology preferred in the automobile sector and we see a big potential in reusing batteries from EVs in second life stationary applications. Finally, a next milestone to be reached in the next chapter is the development of a power flow model that is suitable for high resolution simulations (simulation step > 1 sec).

4 The impact of time resolution in self-sufficiency studies

4.1 INTRODUCTION

In general, regarding the application of the renewable energy source (e.g., PV, wind turbine), there are two basic services: (i) either the source is deployed as a standalone production unit where no load exists; here the objective is to sell the entire energy yield to an electricity supplier (ii) or the source is installed behind the consumption meter of a user; in this case the objective is to consume the energy yield locally to increase the self-sufficiency rate of the installation and thus reducing the electricity invoice [60-62]. As already mentioned, in this thesis we address the second service (case ii).

When the source is located behind the consumption meter, a battery storage system can act as an asset to better exploit the customer's renewable energy installation to become more independent from the grid. When analyzing the performance of such topology, most scientists follow a data driven approach. Historic load and yield power data are imported into a model generating a number of key performance metrics based on which conclusions are drawn. In an attempt to obtain better results, the scientists typically concentrate extensively on improving the model by adding new features or even introducing completely different methodologies. Nevertheless, they very often omit to consider that no matter how advanced their methodology is, the accuracy of the results will always be dependent on the quality of the data inputs and more specifically the time resolution.

Even though the variability of the output, both of PV and wind power sources, can have high frequency components in the range of seconds [63-66], the yield measurements are usually registered as average values at lower resolutions (e.g., 10, 30, 60 min) aiming to reduce the size of data. Similar conclusions apply also for the load consumption [67, 68]. Depending on the origin of the dataset, the resolution can be different. When the data comes from weather stations in the form of solar irradiance or wind speed measurements, then the resolution in most cases does not exceed the 10 min. If the data is derived from the AMR (Automatic Meter Reading) infrastructure delivered by the system operator of the electric grid then the resolution is typically 15 min, for both load and yield measurements. The main conclusion to note out of this paragraph is that, given the resolution scale of the existing datasets it is not possible to know how the power profiles behave in real time (in seconds) and therefore the presence of errors in our simulation results is always inevitable.

The impact of time resolution on the performance of renewable energy storage systems has been investigated by previous research works. Wright and Firth [69] conducted simulations at

different resolutions (1, 5, 15 and 30 min) for residential consumers with on-site generation (e.g., micro-CHP,²⁰ PV). The results showed that when the resolution is lower than 1 min (bigger time slots e.g., 5, 10 min), the total energy quantities imported by the grid and exported to the grid are underestimated. Cao and Siren [70] carried out a comparative study for residential consumers with PV installation at 1, 5, 15, 30 and 60 min resolution. Using the self-sufficiency error (See definition in Subsection 4.2.3), as a performance metric, they found that in some scenarios, when the simulation is done at 60 min resolution, the error can be bigger than 60 %. In [67], an optimization algorithm was applied to design a residential PV battery system. Real-time measurements at 10 s resolution were used, derived from 25 different households in Germany. One major conclusion was that the time resolution must be higher than 5 min for sizing the battery inverter effectively. In [68], the researchers also studied a residential PV battery system. The study, focusing on the performance of the battery, showed that the battery utilization is always underestimated at lower resolutions. At 60 min resolution the battery delivered on average 10.70 % less energy compared to the results at 1 min resolution. Hoevenaars and Crawford [71] studied different hybrid systems including wind, PV, CHP, battery storage and residential loads. The results were compared at 1 s, 10 s, 1 min, 10 min and 60 min resolution. It was concluded that the errors were higher when the CHP was used as the back-up generator compared to the scenarios having the battery as the back-up generator. Kools and Phillipson [72] investigated the impact of time resolution (1 min, 15 min and 60 min) on the optimal planning of a residential district with distributed generation (DG). Here, the objective is to determine the capacities of DG (i.e. PV and micro-CHP) in order to minimize the energy losses of the grid. They concluded that for optimization purposes, the 60 min resolution is sufficient. In [73], the researchers simulate a LV grid that has PV sources and residential consumers. One of the objectives was to study how the time resolution (10 min and 60 min) influences the statistical distribution of the voltage. The results were not considerably different for the two resolutions. Consequently, it was suggested that higher than 60 min resolution measurements are not needed. Hawkes and Leach [74] developed a simulation model for grid-connected households with micro-CHP using load profiles at 5 min, 10 min, 30 min and 60 min resolution. They concluded that at 60 min resolution the results can be very inaccurate. In particular, the total CO₂ emission reduction was overestimated up to 40 %. In [75], the researchers developed a PV battery optimization model using both PV and load profiles at 30 s, 1 min, 2 min, 5 min, 15 min, 30 min and 60 min resolution. The results showed that at 60 min resolution the optimized costs and savings for a battery owner with flat tariff are underestimated by 2.9 % and 12.6 % respectively. It was suggested that 5 min resolution measurements deliver sufficiently accurate results. In [56], a residential PV battery system is

²⁰ CHP stands for "Combined Heat and Power"

considered. Here, the objective is to show how the battery cost-savings are affected by the time resolution (1 min, 2 min, 5 min, 10 min, 30 min) of the PV and load profile. The results revealed that at 30 min resolution the cost-savings delivered by a 5 kWh battery are underestimated by 17 % compared to the same scenario at 1 min resolution.

Conclusions and relation to present work

In the paragraphs above, we summarized studies from a broader scope on the impact of time resolution. In this study, however, we investigate in particular the impact on the self-sufficiency and battery utilization. Next, we summarize important conclusions drawn from the literature review and explain how these are related to the present research work:

- **Wind power has not been addressed:** All previous works have addressed PV systems, mainly for households. Generally speaking, compared to PV, wind power is less popular in prosumer applications; the number of wind power installations is significantly lower than PV and therefore obtaining high resolution datasets is an issue.
 - Present study: This study focuses on wind power. We investigate the simulation errors (i.e., self-sufficiency, battery utilization) having as input 2 months of high resolution power measurements (1 sec) recorded from an industrial site and a medium sized wind turbine.
- **60 min resolution is unacceptable for PV systems:** Previous research works suggest that simulations at 60 min resolution can lead to significant errors [70] [74]; the self-sufficiency error may exceed 60 % in some cases [70].
 - Present study: We strongly suggest for self-sufficiency studies to avoid simulations lower than 10 – 15 min resolutions (e.g., 30 min, 60 min). We confirm from our own experience that this statement applies not only for PV but also for wind power systems. When estimating errors, as a general recommendation, future research should focus on the critical zone 10 – 15 min; the great majority of today's digital metering infrastructure sooner or later (depending on the roll-out of digital meters) will be working in this time resolution. In this study, we examine the errors between 10 min and 1 sec.
- **15 min resolution is a good choice for PV systems:** The self-sufficiency is always overestimated at lower resolutions [69], [70]. Furthermore, it has been shown that at 15 min resolution, the self-sufficiency error is relatively low (a few percentage points, around 0–5 %) [70]. Regarding the battery utilization error, we know that it is always underestimated at lower resolutions [56, 68, 75]. In [68] where a residential PV battery system is considered, the error is in the range of 2.57–11.52 % at 1C. In other words, previous

studies on PV systems suggest that both the self-sufficiency and battery utilization errors are not significant and therefore a 15 min resolution is a good choice.

- Present study: In our work, it has been proven that the self-sufficiency error ranges merely between 0.06 – 3.6 % at 10 min resolution; this is in agreement with previous studies on PV indicating that 15 min is a good choice for estimating the self-sufficiency. Conversely, regarding the battery utilization, our study shows that the error can be significant ranging within 18.1 – 33.1 % at 1C or even higher when we increase the battery C rate to 3C.

Research core, key questions & contributions

The system topology under consideration is given in [Figure 28](#). The system comprises an on-shore medium sized wind turbine,²¹ a high power LiFePO₄ battery, an industrial consumer and the electric grid. We focus specifically on the performance error generated at 10 min resolution having as reference of truth real time measurements at 1 s resolution. The reason for this decision is that the majority of studies dealing with wind power modeling techniques adopt the 10 min resolution. The classic method followed by many scientists is using wind speed data, mostly available at 10 min resolution from weather stations, as input to the wind turbine power curve provided by the manufacturer and thus converting wind speed into wind power. Yet, this technique is only applicable to calculate the average per 10 min wind power output and it does not reveal any information about the dynamic behavior of the wind turbine [76]; [Figure 29](#) shows in comparison the scatter plots of the wind speed and wind power for the same time period at 1 s and 10 min resolution. To simulate the load consumption and wind power output, real time measurements were recorded at 1 s resolution over a total period of 2 months (June–August 2017), derived from two different locations in Belgium.²² The battery storage system, including the DC/AC converter, was modeled in Matlab®. In order to evaluate the errors of the simulation, three key performance metrics were used: (i) total self-sufficiency, (ii) battery utilization, (iii) instantaneous self-sufficiency. Moreover, each metric was calculated for different variable settings by changing the battery capacity, battery C rate limit and the load ratio of the installation. Next, we present the key research questions addressed in this work including the delivered contributions.

- What is a suitable model to carry out the power flow simulation ?

²¹ Here, "medium sized" means that the electric power output of the wind turbine lies in the range of 100–1000 kW.

²² Since it was not possible to find a single installation offering both measurements together. Furthermore, we assume that the wind and load power profiles are not correlated to each other.

One of the concerns when conducting simulations at high time resolutions (msec – sec) is the method used to calculate the power flow equations; do we need a full dynamic model solving the equations in the time domain or can we simply proceed with a steady state model without sacrificing accuracy when calculating energy losses ? In Section [4.2.2](#), we present the methodology used to develop the power flow model.

- What is the self-sufficiency and battery utilization error at 10 min resolution ?
In Section [4.3](#) we present the results of a sensitivity analysis showing the self-sufficiency, battery utilization and the respective errors in function of three variable settings: (i) the load ratio, (ii) battery capacity (kWh) and (iii) battery C rate.
- How does the relation between the power source and load profiles impact the self-sufficiency ?
In Section [4.3.5](#), we also examine how the self-sufficiency error behaves instantaneously instead of exclusively looking at the average error over the entire simulation period. This enables us to link the instantaneous self-sufficiency error with the instantaneous ratio of the averaged powers P_{load}/P_{wind} .
- Is 10 min resolution a good choice for studies considering wind power ?
This question is partly addressed in Section [4.3](#) (see results from the sensitivity analysis). We also elaborate on this in Section [4.4](#) and [4.5](#).
- How to interpret results and make suggestions for project developers and practitioners?
This question is addressed in Section [4.5](#).

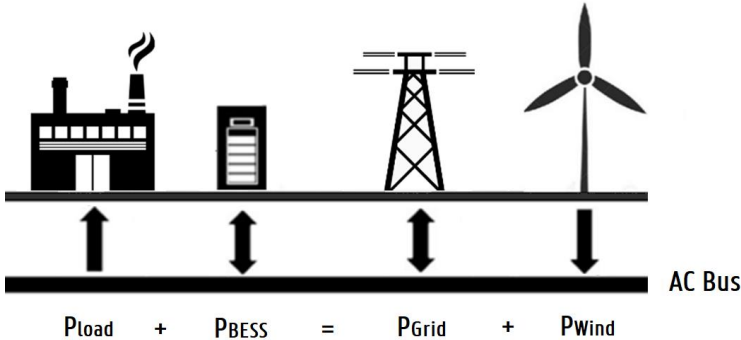


Figure 28: System topology

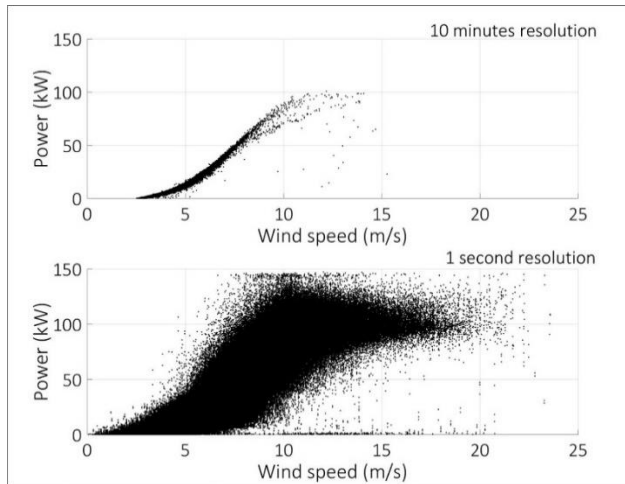


Figure 29: Scatter plot of wind speed and wind power at 1 s and 10 min resolution for the 2 months period: 1 June 2017 12:00:00–1 August 2017 11:59:59.

The rest of this chapter is structured as follows. Section [4.2](#) provides a short description of the data inputs (load and wind power data). It describes the dynamic model of the battery which was initially used to specify the characteristics of the battery and evaluate its dynamic response. Afterwards, an analytic description of the power flow model is given which was used to conduct all final simulations needed. The last part of Section [4.2](#) defines the three performance metrics mentioned in the previous paragraph including also the definition of the respective errors. Section [4.3](#) presents the results, discussing the error deviations between the two resolution scales. Finally, Section [4.4](#) and [4.5](#) summarize the most important conclusions, recommendations and ideas for future work.

4.2 METHODOLOGY

4.2.1 Data inputs – wind power and load power

The entire study was conducted using two data inputs: (i) wind power and (ii) load power. The resolution scale and the time period of the measurements is the same for both data sets. The measurements were recorded at 1 s resolution with a total duration of two months, starting from 1 June 2017 12:00:00 until 1 August 2017 11:59:59. The wind data was derived from a wind turbine located in Zwijndrecht, Belgium. The specifications of the wind turbine are presented in [Table 8](#). The load data was provided by an industrial consumer located in Ronse, Belgium. As explained further, multiple simulations were executed by scaling down the load profile with a factor of 1/2, 1/6, 1/10 and 1/20. The reason for doing so was that the actual load profile was quite bigger than the wind profile.

Table 8: Wind turbine: Technical specifications

Characteristics	Specifications
Type	XANT-M21
Rotor diameter	21 m
Hub height	31 m
Rated electrical power (see also ²³)	100 kW
Cut-in wind speed	3 m/s
Cut-out wind speed	20 m/s
Yaw control	Auto-yaw

4.2.2 Battery model

The battery model forms the core of the simulations carried out in this research work. The first step, towards the development of the model, was the definition and evaluation of a fundamental equivalent capable of simulating the behavior of the battery under dynamic conditions. Our choice to follow a fundamental approach instead of considering a simplified model can be justified by the high resolution scale of the measurements. However, as explained in the following paragraphs, the dynamic equivalent was finally replaced by the power flow model after concluding that this simplification would not influence the accuracy of the simulation even at such high resolutions. Hence, all simulations leading to the final results (section 4.3) were done using the power flow model. The dynamic equivalent was only used to calculate the internal parameters of the battery (e.g., open circuit voltage, resistance) which were used for the development of the power flow model.

4.2.2.1 Dynamic model

The battery technology is LiFePO₄ (LFP). The specifications of the LFP cell are presented in [Table 9](#). The dynamic response of the battery cell was analyzed using the second order RC equivalent model ([Figure 30](#)). Our decision to choose this type of model was based on previous studies that validated its performance as very accurate [[77](#), [78](#)]. The open circuit voltage (OCV) to the state of charge (SOC) characteristic of the battery was derived in [[79](#)]. In general, the OCV to SOC characteristic of the battery is defined with hysteresis, since the OCV depends not only on the SOC of the battery but also on the (dis)charging process [[80](#)]. However, in this study the hysteresis effect was ignored given our research goal and also knowing that such

²³ At standard conditions (air density 1.225 kg/m³)

simplification does not influence dramatically the model accuracy. The OCV to SoC characteristic was made based on the [79], taking as equivalent the voltage discharge curve at C/25 (Figure 31).

Table 9: LFP cell characteristics [79]

Characteristics	Specifications
Chemistry	LiFePO ₄
Nominal capacity	2.28 Ah (7.52 W h)
Nominal voltage	3.3 V
Recommended voltage range	2 to 3.6 V
Operating temperature range	-30 °C to +60 °C
Cell weight	70 g

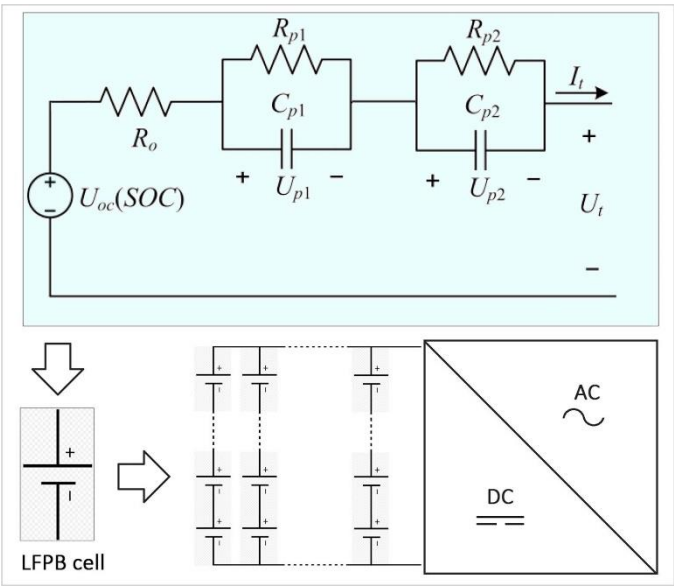


Figure 30: 2nd order RC equivalent for LFP cell

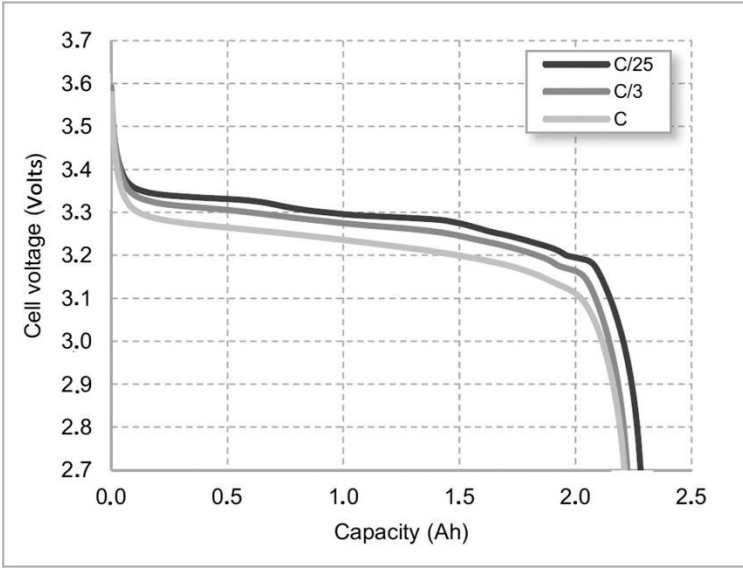


Figure 31: Voltage discharge curves for C/25, C/3 and 1C according to Ref. [79]

To estimate the parameters R_0 , R_{p1} , R_{p2} , C_{p1} , C_{p2} , the response of the model was optimized to match the voltage discharge curve at 1C (Figure 31). As shown in Figure 31 each voltage discharge curve corresponds to a constant C rate. Knowing that the current is always constant during the discharging process and that the accumulated charge (expressed as capacity in Ah) can be found at any given point on the curve, it is possible to construct the time axis of the process. In other words, each static voltage-to-capacity curve can be transformed into a dynamic voltage-to-time curve. The dynamic current-to-time curve can be easily defined by calculating the total duration of the discharging process. As can be seen with a discharge rate at 1C the battery will have delivered almost 2.2 Ah. Therefore the total duration is calculated as follows:

$$T_{\text{total}} = \frac{2.2}{C_{\text{rate}} \times C_{\text{Ah}}} \times 3600 = \frac{2.2}{1 \times 2.28} = 3474 \text{ s}$$

Now that both the voltage-to-time and the current-to-time curves are known, the response of the model can be optimized. The current-to-time curve was used as the input of the model whereas the voltage-to-time curve was selected to be the output. We assumed that the LFP cell is connected at its output with a current source. Furthermore, we considered as initial conditions that the SoC is 100 % and that no current flows towards or from the battery (open circuit condition). Next, the current source is commanded to discharge the battery at 1C over a period of 3474 s. The experiment ends at 3474 s and the voltage response of the battery is compared to the desired response.

Table 10 presents the values for the parameters R_0 , R_{p1} , R_{p2} , C_{p1} , C_{p2} . These values were calculated using Matlab's optimization toolbox. The two voltage-to-time curves, the reference to follow and the result of the simulation, are illustrated in Figure 32. The small deviation towards the end close to 3500 s is possibly due to the change of the battery's internal resistance when the SoC becomes almost 0 %. In reality the internal resistance of the battery can slightly change when the SoC is close to the upper (100 %) or lower (0 %) boundary [77]. Nevertheless, all final simulations (section 4.3) were done with the battery operating in the range of 10–90 % SoC and therefore the internal resistance was considered constant. Our decision to set the SoC within 10–90 % is explained in a separate paragraph (See Process 2 - Limitation imposed by power capability).

Table 10: Parameters of the 2nd order RC model using Matlab's optimization toolbox. The values refer to a single LFP cell.

Parameters	Values
R_0	0.02 Ω
R_{p1}	0.005 Ω
R_{p2}	0.004 Ω
C_{p1}	600 F
C_{p2}	1500 F

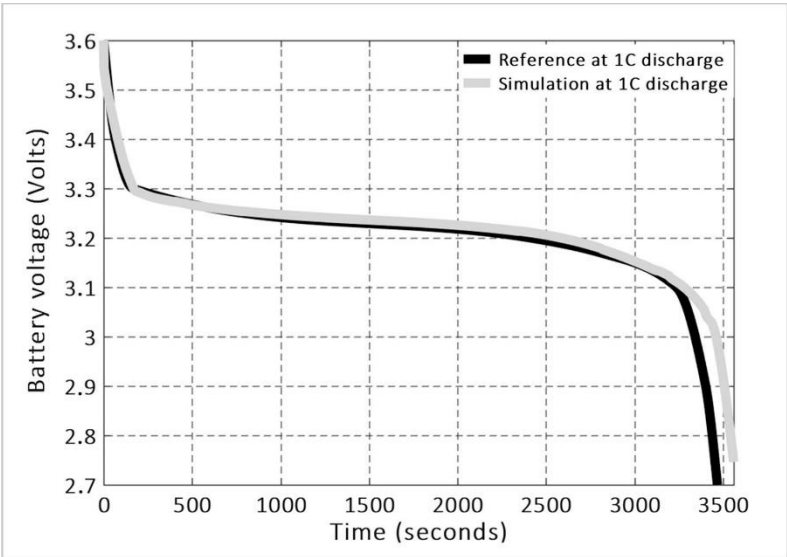


Figure 32: Comparison of voltage to time curves between simulation and reference with optimized parameters

4.2.2.2 Evaluation of the dynamic response

As can be seen from [Figure 30](#), the model of the battery consists of an ideal voltage source, resistors and capacitors. Since the model does not include any inductances, when the battery is discharged (charged) the maximum voltage drop (increase) at its output (compared to the OCV) is affected only by the amplitude of the current and the size of the ohmic elements (R_o , R_{p1} , R_{p2}). We note also that the presence of the capacitive elements does not influence the maximum voltage drop (increase) because both capacitors are connected in parallel with a resistor. In other words, the derivative (rate of change) of the (dis) charging current cannot impose limitations to the reaction time of the battery. As a result, the battery is expected to respond instantaneously to any power commands specified by the control system of the DC/AC converter. This is in agreement with previous studies that state that the reaction time of lithium-ion batteries is very fast, in the range of ms according to [\[81\]](#) and below 5 ms according to [\[82\]](#).

In fact, if any delays occur between the power command and the actual power delivered by (to) the battery, these are probably due to extended software execution time and bandwidth limitations of the communication protocol. In the present study, we considered that the communication protocol operates at 20 Hz, which is much faster compared to the resolution scale of the simulations carried out at time slots of 10 min and 1 s. The resolution scale of the simulation defines how often a power command can be sent to the DC/AC converter. Since the resolution scale of the communication protocol is much higher, it can be concluded that the actual power delivered by (to) the battery during a single time slot (10 min, 1 s) will always be approximately constant and equal to the power command. Based on this fundamental assumption, it makes sense to ignore the dynamics of the system (including the battery and the DC/AC converter) and proceed with a more simplistic modeling method.

4.2.2.3 Power flow model

Following the conclusions of the previous paragraphs, it was decided to develop a new model for the battery storage system. Here, the modeling approach starts from the equation of power flows:

$$P_{\text{wind}}(t) + P_{\text{grid}}(t) = P_{\text{battery(ACoutput)}}(t) + P_{\text{load}}(t)$$

The power flow model is illustrated in [Figure 33](#). Data inputs are the load power and the wind power profile. The main objective-output of the model is the calculation of the battery's power profile. Obviously, after the battery power has been defined, the power of the grid can be defined as well, simply by satisfying the Equation [4-2](#).

The model has four variables: (i) simulation time step, (ii) battery capacity, (iii) battery C rate limit (iv) load ratio. During a single simulation the values of all variables remain constant. Each simulation is executed with a fixed discrete time step (1 s or 10 min). At each step the model calculates the battery power $P_{\text{battery}}(t)$ given the current values of the wind power, load power and state of charge ($P_{\text{wind}}(t)$, $P_{\text{load}}(t)$ and $\text{SoC}(t)$ respectively). Knowing the battery power $P_{\text{battery}}(t)$ allows to calculate the next value of the state of charge $\text{SoC}(t + 1)$ and therefore the simulation can proceed to the next step. The program runs repetitively until all values of the data inputs have been scanned. The rest of this section describes how the power flow model works given a single simulation step. The program is split into three major processes.

Process 1: Initially, the battery power equals the difference between the wind power and load power $P_{\text{wind}}(t) - P_{\text{load}}(t)$. The charging (discharging) process cannot start unless the available power surplus (deficit) is higher than a minimum power threshold (Condition 1). This threshold is imposed by the efficiency of the DC/AC converter, which is unacceptably low when the converter operates at power levels much lower than its rated specifications. After the power difference $P_{\text{wind}}(t) - P_{\text{load}}(t)$ has been checked to be higher (in absolute value) than the power threshold of the DC/AC converter the program executes a second control. If the battery is charged (discharged) then its power must be slightly lower (higher) than the available surplus (deficit) of energy due to DC/AC conversion losses (Condition 2). Here, charging (discharging) results in multiplication (division) by the DC/AC efficiency.

Process 2: This process works as a saturation block. It checks whether the power value calculated at the output of process 1 lies within an allowable range; If this is true then the value can pass through, otherwise the power is saturated by an upper and lower boundary. The saturation is applied in order to avoid operating the battery beyond its power capability. The factors affecting the value of the power limit are the battery capacity, the C rate limit and the SoC. Both the upper and lower limit are constantly updated at each simulation step since they are function of the SoC.

Process 3: This process acts also as a saturation block. Here, the intention is to take into account the resolution scale of the simulation as well. Such limitation becomes particularly noticeable when the resolution is low (i.e. 10 min) and especially when a high C rate limit has been selected. The SoC must always remain within its specified upper and lower limits. If for instance the SoC is quite close to the upper limit and the resolution scale is 10 min, then the maximum amount of energy that can be delivered to the battery between the current and next simulation step is possibly lower than the energy allowed by the power capability criterion (process 2).

4.2.2.3.1 Process 1 – DC/AC efficiency and minimum power threshold

To define the minimum power threshold $P_{DC/AC \min}$, it is important to analyze the total efficiency of the energy storage system. The total efficiency can be calculated as follows:

$$\eta_{\text{total}} = \eta_{\text{battery}} \cdot \eta_{DC/AC}$$

where η_{battery} is the round trip efficiency of the battery, $\eta_{DC/AC}$ is the efficiency of the DC/AC converter and η_{total} is the total efficiency of the system. The round trip efficiency of the LFP battery presented in this study lies approximately in the range of 90–97 % depending on its internal resistance and the square of the current. The efficiency of the converter $\eta_{DC/AC}$, however, depends on two components: i) the conduction losses which are proportional to the square of current and ii) the switching losses which are fixed, independent from the current [83]. The presence of switching losses becomes noticeable especially when the power of the converter is much lower than its nominal value. In this case, the efficiency of the converter can be quite low. Consequently, operating the battery at such relatively low powers leads to higher energy losses compared to the amount of renewable energy yield that we attempt to save. Based on information received from Ref. [84] we decided to set the efficiency of the DC/AC converter $\eta_{DC/AC}$ constant at 95 %. This is a good approximation considering that the load of the converter stays within 5–100 % of its nominal power. Below 5 %, the efficiency of the converter starts declining dramatically due to switching losses until it becomes zero. Therefore, the minimum power command of the battery $P_{DC/AC \min}$ was set at 5 % of its maximum power $P_{\text{battery_max}}$ under the assumption that the nominal power of the converter is always equal to the power capability of the battery:

$$|P_{DC/AC \min}| = 0.05 \cdot P_{\text{battery_max}}$$

4.2.2.3.2 Process 2 – Limitation imposed by power capability

The power capability of the battery depends on voltage and current limitations. As recommended by manufacturers and based on literature reviews [80, 85], the voltage of LiFePO₄ cells must not lie outside the range of 2.0–3.6 V in order to avoid accelerated degradation as well as safety issues. Furthermore, the (dis) charging current should preferably not exceed a maximum limit, also here in an attempt to extend as much as possible the lifetime of the battery. In general, higher C rates usually lead to accelerated capacity fade. However, depending on the application, the user can choose to operate the battery at high C rates if such option can increase the utilization of the energy storage system and as a result the return of investment.

In this research work, we considered four different current limitations: (i) 0.2 C, (ii) 0.5 C, (iii) 1 C, (iv) 3 C in order to investigate to what extent the power capability of the battery can affect the simulation error. For a given C-rate, the power capability can be calculated by the following two equations:

$$P_{\text{battery max}} = (\text{OCV} + I_{\text{C rate}} \cdot R) \cdot I_{\text{C rate}}$$

$$P_{\text{battery min}} = -(\text{OCV} - I_{\text{C rate}} \cdot R) \cdot I_{\text{C rate}}$$

Where OCV is the open circuit voltage, $I_{\text{C rate}}$ is the current limit, R is the total internal resistance ($R_0 + R_{p1} + R_{p2}$) of the battery cell according to the optimized values of the RC equivalent model, $P_{\text{battery max}}$ and $P_{\text{battery min}}$ are the upper (charging) and lower (discharging) power limits respectively. It is worth mentioning that these equations refer to the steady state power capability of the cell. Temporarily, during the transient state the power capability is always a bit higher. Therefore, the use of the steady state value leads always to more conservative calculations, meaning that the capability of the cell is not overestimated.

As can be seen from Equations 4-5, 4-6, the power capability of the battery cell is function of the SoC because it depends on the OCV. This function is illustrated in Figure 34 for the four different C rate limitations.²⁴ As expected all functions are almost constant for any given (dis) charging C-rate because the OCV specifically of a LiFePO4 cell does not deviate considerably from its nominal value within the range of 10–90 % SoC.

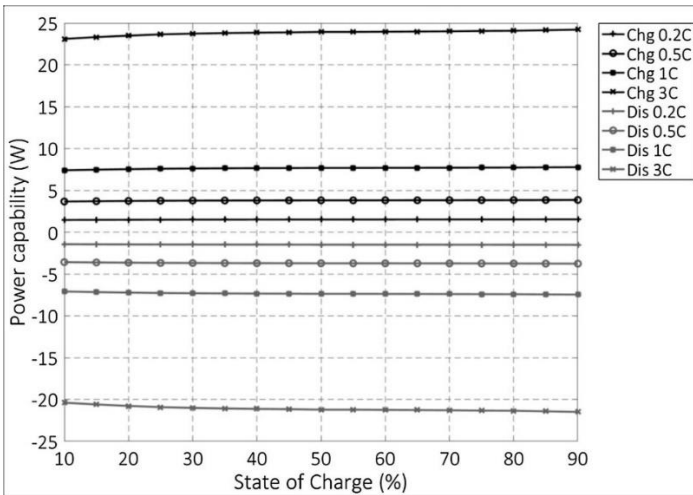


Figure 34: Power capability curves of a single LiFePO₄ cell, considering different C rate limitations. The indexes for the charging and discharging curves are “Chg” and “Dis” respectively.

²⁴ The power capability of a battery with a higher capacity is calculated easily by multiplying the power curves of a single cell with the equivalent number of cells needed in connection to reach the given capacity.

The choice to focus on the SoC interval 10–90 % is because we carried out the entire analysis considering a Depth of Discharge (DoD) 80 %. Compared to deep charging cycles of 100 % DoD, operating the battery at lower DoDs has been proven to be more appropriate for extending its lifetime [86]. Besides this, if instead the SoC was within the interval 0–10 % or 90–100 % then its power capability would possibly be subject to voltage limitations; the lower limit of 2 V within 0–10 % SoC during the discharging process and the upper limit of 3.6 V within 90–100 % SoC during the charging process [87]. The presence of voltage limitations results in power capability reduction since the current cannot be kept constant at its maximum value in those regions. In summary, setting the DoD at 80 % is not only beneficial for the lifetime of the battery but it also allows faster (dis)charging cycles.

4.2.2.3.3 Process 3 - Limitation imposed by resolution scale

The upper and lower power limit in process 3 are constantly updated at each simulation step since they are function of the SoC. The following two equations were used to calculate the power limits, considering that the SoC lies in the range of 10–90 %:

$$P_{\text{battery max}} = \frac{90 - \text{SoC}(t)}{100} \cdot C_{\text{kWh}} \cdot \frac{3600}{T_{\text{step}}}$$

$$P_{\text{battery min}} = \frac{10 - \text{SoC}(t)}{100} \cdot C_{\text{kWh}} \cdot \frac{3600}{T_{\text{step}}}$$

where C_{kWh} is the battery capacity in kWh and T_{step} is the time step (resolution scale) in seconds (1 s or 10 min).

To give an indication of how process 3 can influence the simulation, we present as an example two cases in comparison. In both cases we assume identical conditions for the battery capacity, C rate limit, SoC, wind power and load power but a different time step.²⁵ The objective is to calculate and compare the battery power at the output of process 3:

- C_{kWh} : 10 kWh
- C_{rate} : 3C
- SoC(t): 80 %
- $P_{\text{wind}}(t) \gg P_{\text{load}}(t), P_{\text{battery max (Process 2)}}$
- T_{step} : 1 s in case 1, 10 min in case 2
- Find $P_{\text{battery}}(t)$

In this example, the wind power $P_{\text{wind}}(t)$ is much higher than the load power $P_{\text{load}}(t)$ and the charging power capability of the battery $P_{\text{battery max (Process 2)}}$. Furthermore, the SoC(t) has not yet

²⁵ The efficiency of the battery and the DC/AC converter is not important in this example.

reached the upper limit (90 %). As a result, process 1 sends a command to charge the battery with the available surplus of powers $P_{\text{wind}}(t) - P_{\text{load}}(t)$ (slightly lower due to DC/AC losses). Process 2 is saturated at the upper limit since the surplus of powers is higher than the charging power capability of the battery. At this point (output of process 2) the battery power is the same for both cases (1, 2) and it equals 31.9 kW according to the values of C_{kWh} , C rate limit and $\text{SoC}(t)$. The maximum battery power $P_{\text{battery max}}$ calculated by process 3 (Equation 4-7) is 3600 kW and 6 kW in case 1 and case 2 respectively. Consequently, the final battery power $P_{\text{battery}}(t)$ (output of process 3) is 31.9 kW in case 1 and only 6 kW in case 2.

Certainly, although process 3 influences the simulation in case 2, it has no effect in case 1. The deviation between the final averaged power (6 kW) and the instantaneous power (31.9 kW) is undoubtedly significant. The aforementioned example shows that simulating the behavior of a high C rate battery at a resolution scale as low as 10 min can be difficult. As explained in the following section, the loss of information (absence of real-time measurements) during the averaging period can lead to inaccuracies that need to be further investigated.

4.2.3 Definition of performance metrics

The error between the low (10 min) and high (1 s) resolution simulation was evaluated using three key performance metrics: (i) total self-sufficiency, (ii) battery utilization and (iii) instantaneous self-sufficiency. Below follow the definitions of those metrics and the respective error measures.

The total self-sufficiency shows to what extent the consumer is independent from the electric grid. It is the ratio of the total renewable energy consumed by the load, either directly from the wind turbine or indirectly from the battery, to the total load demand over the entire simulation period. The total self-sufficiency forms a key performance index for every renewable energy installation since it can be used to estimate the periodic (per month/year) revenue stream generated by the system. If additionally the capital and operating expenditures are given, then it is possible to calculate the return of investment (ROI) as well. We define total self-sufficiency as:

$$S_{\text{tot}} = \frac{E_{\text{load tot}} - E_{\text{grid tot}}}{E_{\text{load tot}}} \cdot 100$$

where S_{tot} is the total self-sufficiency, $E_{\text{load tot}}$ is the total load demand and $E_{\text{grid tot}}$ is the total energy delivered to the load by the grid.

The battery utilization can be measured using different metrics. Here, the number of equivalent cycles is used. This can be expressed as the ratio of the total energy discharged by the battery

storage system (over the entire simulation period) to the battery's energy capacity. In contrast to the total self-sufficiency which is associated with the total revenue stream of the installation, this metric concerns specifically the profitability of the energy storage system. In general, it is desirable that the utilization be as high as possible. Given a certain time period, the ROI of the energy storage system becomes faster as the utilization increases. We define battery utilization as:

$$U_{\text{bat}} = \frac{E_{\text{dis tot}}}{C_{\text{kWh}}}$$

where U_{bat} is the battery utilization, $E_{\text{dis tot}}$ is the total energy discharged and C_{kWh} is the battery capacity.

The instantaneous self-sufficiency shows, as the total self-sufficiency does, to what extent the consumer is independent from the grid. However, in this case, the self-sufficiency is function of the time; it changes constantly as the simulation progresses because the time slot under consideration is temporary. Regarding the time slot duration, it was set at 10 min for both resolution scales. Choosing for a fixed duration enables us to draw the comparison we need by calculating the instantaneous self-sufficiency error. We define it such that, integrating the metric over the simulation period and dividing by the number of time slots returns the total self-sufficiency (Equation 4-9). The equation of the metric is as follows:

$$S_{\text{inst}}(t) = \frac{E_{\text{load inst}}(t) - E_{\text{grid inst}}(t)}{E_{\text{load tot}}} \cdot N \cdot 100$$

where $S_{\text{inst}}(t)$ is the instantaneous self-sufficiency, $E_{\text{load inst}}(t)$ is the instantaneous load consumption, $E_{\text{grid inst}}(t)$ is the instantaneous energy delivered to the load by the grid, $E_{\text{load tot}}$ is the total load consumption and N is the total number of time slots. In this study, N is equal to 8784.²⁶

Knowing how each performance metric is defined it is now possible to proceed with the calculation of the errors. We note once more that, in this study, the focus lies particularly on the error of the metrics rather than the metric itself. To generate a case study, the simulation is executed twice, at 1 s and 10 min resolution and by keeping the other three variables (battery capacity, C rate limit, load ratio) constant. The real time measurements form the data inputs at 1 s resolution. The data inputs at 10 min resolution are constructed simply by averaging the real time measurements over the time slot duration (10 min). The equations of the errors are given below:

²⁶ Dividing the simulation period (2 months or 61 days) by the time slot duration (600 s) we get the value of N .

$$ER_{tot} = S_{tot\ 10\ min} - S_{tot\ 1\ sec}$$

$$ER_{bat} = \frac{U_{bat\ 10\ min} - U_{bat\ 1\ sec}}{U_{bat\ 1\ sec}} \cdot 100$$

$$ER_{inst}(t) = S_{isnt\ 10\ min}(t) - S_{inst\ 1\ sec}(t)$$

where ER_{tot} is the total self-sufficiency error, ER_{bat} is the battery utilization error and $ER_{inst}(t)$ is the instantaneous self-sufficiency error.

4.3 RESULTS

The performance of the simulation was evaluated in function of the four variables ([Figure 33](#)). The power flow model was executed multiple times using all possible combinations that can result from the following set of values:

- Simulation step (resolution scale): 1, 600 s.
- Battery capacity: 0, 10, 25, 50, 75 kWh.
- C rate limit: 0.2 C, 0.5 C, 1 C, 3 C.
- Load ratio: 1/20, 1/10, 1/6, 1/2.

The value range of the battery capacity and the load ratio were chosen to make sense from a techno-economic point of view. Under the given data inputs, it is not worth exploring the simulation result at higher battery capacities and/or higher (lower) load ratios because the installation is badly dimensioned in those scenarios. With respect to the C rate limit, the maximum value was set at 3 C; charging the battery above this level would negatively affect its lifetime and therefore it is not recommended.

4.3.1 Total self-sufficiency

The total self-sufficiency error and the total self-sufficiency at 1 s resolution are illustrated in [Figure 35](#). As expected, the most important factor affecting the self-sufficiency is the load ratio. The self-sufficiency lies in the range of 9.7–10.6 %, 23–28.4 %, 31.9–41.7 % and 44.5–63 % when the load ratio takes the values 1/2, 1/6, 1/10 and 1/20 respectively. For a given load ratio and C rate limit, the self-sufficiency always increases as the battery capacity becomes higher. Needless to say, the contribution of the battery in increasing the self-sufficiency becomes less significant as the load ratio increases; note the small improvement from 9.7 to 10.6 % when the load ratio is 1/2 (underdimensioned wind turbine) compared to the improvement from 44.5 to 63 % when the load ratio is 1/20 (overdimensioned wind turbine). For a given load ratio and battery capacity, the self-sufficiency does not always increase with the C rate limit. Although the maximum self-sufficiency, indeed, is found always at 3 C when the battery capacity is 10 or 25 kWh (irrespective of the load ratio), the maximum value is found at 1 C when the battery

capacity is 50 or 75 kWh. The explanation of this lies in the minimum power threshold of the DC/AC converter. As an example we note that at 3C and 75 kWh the minimum power threshold equals approximately 11.5 kW. As long as the renewable power surplus does not suffice to overcome this value, the charging process will never start, thus affecting the total self-sufficiency negatively.

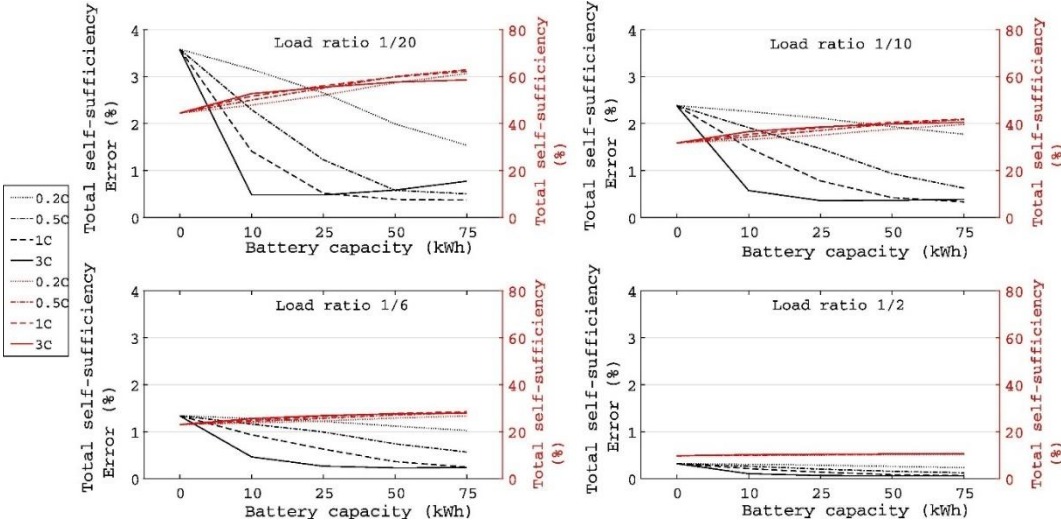


Figure 35: Total self-sufficiency at 1 s resolution (red), total self-sufficiency error (black).

4.3.2 Total self-sufficiency error

The total self-sufficiency error ranges between 0.06 and 3.6 %. The error is always positive meaning that all simulations conducted at 10 min resolution lead to overestimations of the real self-sufficiency. As can be seen, the maximum value is reached when the load ratio is 1/20 and the battery capacity is zero (C rate irrelevant). In most cases, the error declines with the increase of the load ratio. With respect to the battery capacity, similar conclusions as those discussed in the previous paragraph can be made, however, here the dependence follows the opposite direction. For a given load ratio and C rate limit, the self-sufficiency error always decreases as the battery capacity becomes higher. Regarding the C rate limit, in almost all cases, increasing the limit results in error reduction. Exception to the rule are the cases where the battery capacity is 50 or 75 kWh; an increase from 1C to 3C leads to a higher self-sufficiency error.

The most important conclusion to note is that, the estimation of the total self-sufficiency becomes more accurate as the size (capacity) and power capability (C rate limit) of the battery storage system increases. Considering two cases in comparison, presented in [Table 11](#) we see that although the self-sufficiency has increased from 44.5 to 58 %, the error has declined from

3.6 to 0.6 %. Apparently, the energy storage system acts in a similar way like a filter by absorbing the fast surplus (and deficit) variations. In other words, the loss of information due to the absence of real time measurements is compensated to some extent by the battery and therefore conducting the simulation at 10 min resolution cannot cause remarkable inaccuracies.

Table 11: Comparison of performance metrics for two cases derived from Figure 35

Variables/metrics	Case A	Case B
Battery capacity (kWh)	0	50
C rate limit	N/A	3 C
Load ratio	1/20	1/20
Total self-sufficiency at 1s resolution	44.5 %	58 %
Total self-sufficiency error	3.6 %	0.6 %

4.3.3 Battery utilization

The battery utilization at 1 s resolution and the battery utilization error are illustrated in [Figure 36](#). The utilization ranges between 17 and 190 cycles. For a given battery capacity and C rate limit, the battery utilization does not depend monotonically on the load ratio. In most cases, the maximum is found when the load ratio is 1/20 or 1/10. As expected, the higher the battery capacity is, the lower the total number of cycles delivered. Furthermore, the utilization increases with the C rate limit except for the cases where the battery capacity is 50 or 75 kWh; at 3C the utilization is lower than its value at 1C. The maximum number of cycles (190) is located at the point [x,y,z]: 10, 3C, 1/10, whereas the minimum number of cycles (17) is located at [x,y,z]: 75, 0.2C, 1/2, where [x,y,z] are the battery capacity, C rate limit and load ratio respectively.

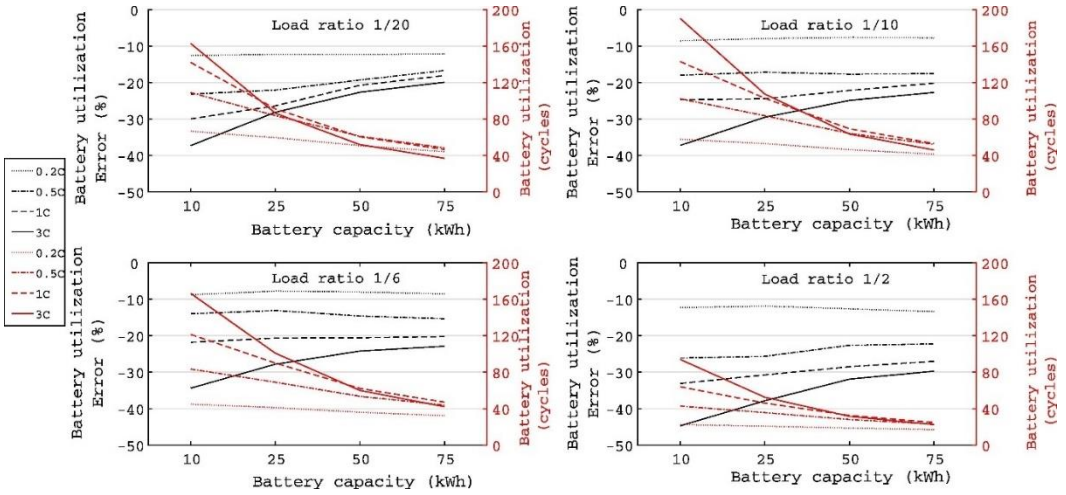


Figure 36: Battery utilization at 1 s resolution (red), battery utilization error (black).

4.3.4 Battery utilization error

Regarding the battery utilization error, this lies in the range of 7.5–44.7 %. The error is always negative meaning that all simulations conducted at 10 min resolution lead to underestimations of the real battery utilization. For a given battery capacity and C rate limit, the error is always maximized (in absolute value) when the load ratio is 1/2, despite the fact that the function is not monotonically increasing. The impact of the battery capacity is clear; the higher the battery capacity, the lower the error while keeping the other two variables constant. What is more, it is interesting to note that the C rate limit is by far the most decisive factor. The error increases always as the C rate becomes higher. Especially at high C rates (1 C, 3 C) the deviation from the true value can be significant; note that the maximum error (44.7 %) is located at the point [x,y,z]: 10, 3 C, 1/2.

To better explain how the errors are caused note that, at 3 C a fully charged battery can go from 90 % SoC to 10 % SoC approximately in less than 20 min when the battery delivers its maximum power. When the average load (wind) power is much higher than the average wind (load) power over the 10 min period, the two profiles do not cross each other very often in real time, therefore the error is negligible. However, when the two average powers are closer to each other, it is highly probable that the wind and load profiles cross each other very often in real time, thus resulting in relatively larger errors. The battery can complete several (dis)charging micro-cycles during the 10 min period that cannot be 'detected' through the low resolution data set. As the C rate increases, the size of those micro-cycles increases, or in other words the total not 'detected' energy, allocated by the battery between the source and the load, increases. The major conclusion in this section is that, simulating the performance of fast

charging (high C rate) batteries in wind power systems using data sets with a resolution as low as 10 min can lead to significant inaccuracies, in particular with regard to the battery utilization.

4.3.5 Instantaneous self-sufficiency error

As already mentioned, the total self-sufficiency error varies between a mere 0.06–3.6 %. Nevertheless, the results reveal that the instantaneous error can be much higher. [Figure 37](#) presents the instantaneous self-sufficiency error on 8 June 2017, considering that the battery capacity is zero (C rate not applicable) and the load ratio is 1/6. Additionally, the figure illustrates the wind and load power profile on the same day. As can be seen, the instantaneous error varies between 0 and 52.5 %; this is considerably higher than the total (or average) error. It is also interesting to notice how the error changes depending on the instantaneous relation between the wind power and load power. It seems that the error is minimized when the load power is clearly bigger than the wind power or vice versa. Moreover, the error seems to increase when the two powers are comparable to each other. In order to express this dependence more effectively [Figure 38](#) was created, explained in the following paragraph.

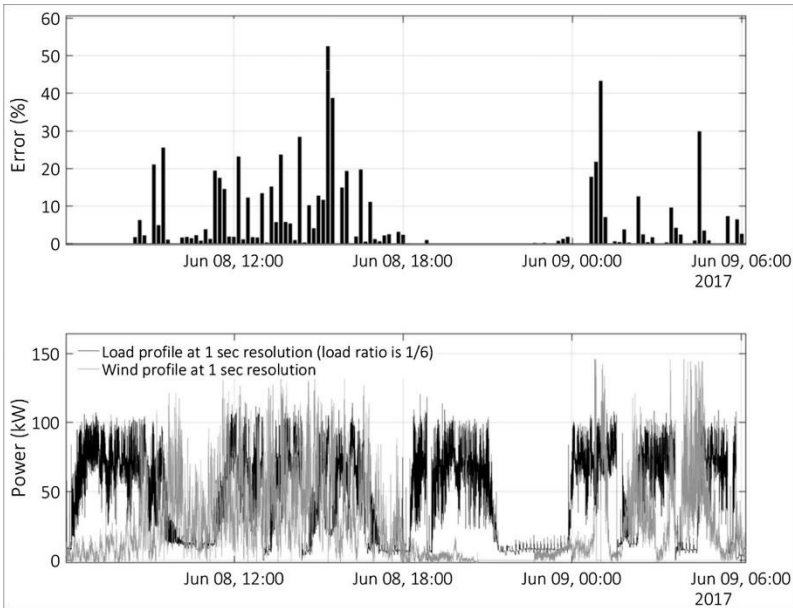


Figure 37: Instantaneous self-sufficiency error on 8 June 2017 without battery storage (Capacity is zero, C rate irrelevant) and load ratio 1/6.

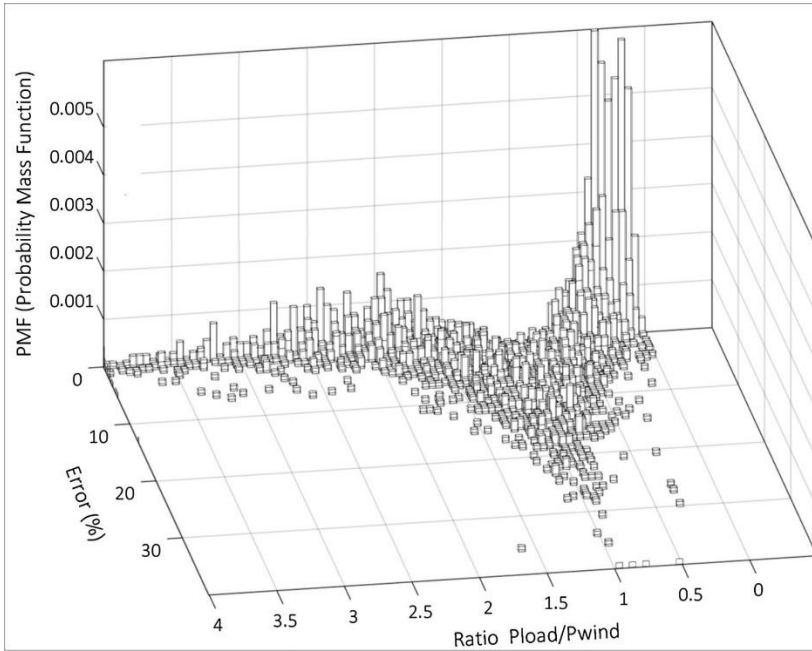


Figure 38: Bivariate probability mass function at 10 min resolution considering: (i) variable X: instantaneous ratio P_{load}/P_{wind} , (ii) variable Y: instantaneous self-sufficiency error, (iii) battery capacity is zero (C rate irrelevant), load ratio is 1/20.

Figure 38 refers to the case study where the battery capacity is zero (C rate not applicable) and the load ratio is 1/20. Here, the relation between the load power and wind power is expressed as the ratio of the average (per 10 min) powers P_{load}/P_{wind} . The figure shows the bivariate probability mass distribution of the instantaneous self-sufficiency error against the instantaneous ratio P_{load}/P_{wind} . It can be concluded that there is a clear correlation between the two variables. The error increases as the ratio of the powers approaches the value 1. For most of the time during the simulation, the error is higher than 10 % when the ratio ranges between 0.5 and 2. The reason why the error increases specifically in this range is that, the chance that the real time profiles will cross over each other becomes higher when the average powers are at the same level. In other words, the more equal the two average powers are, the worse the impact of not having real time information. In this case study, the maximum instantaneous self-sufficiency error is 140 % (not included in the figure) whereas the final total self-sufficiency error is only 3.6 %.

The fact that the total error is so low implies that the ratio P_{load}/P_{wind} is found usually outside the critical zone 0.5–2 where the instantaneous error increases considerably. **Figure 39** shows the univariate probability mass distribution of the instantaneous ratio P_{load}/P_{wind} for the same case study addressed above (capacity is zero, load ratio is 1/20). The peak value (21 %) at the

right side of the figure represents the probability of the ratio being equal to or higher than 10. The results reveal that the probability of the ratio being within 0.5–2 is 29 %. The remaining 71 % of the time the ratio lies outside the critical zone, thus positively affecting the total self-sufficiency error. Needless to say, all results presented so far are strongly dependent on the given data inputs. In the present study, as can be seen in [Figure 39](#), the load profile is quite consistent meaning that it maintains its pattern over the entire simulation period independent from the weather conditions. Possibly in another scenario, if the load consumption was influenced by the weather, the correlation between the load and wind power profile would be stronger and as a result the total self-sufficiency error could be higher.

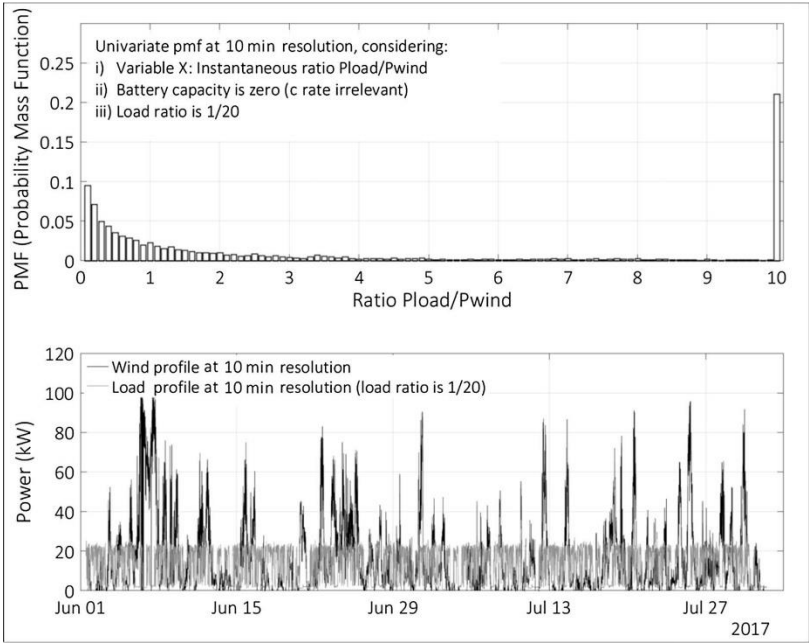


Figure 39: Univariate probability mass function at 10 min resolution considering: (i) variable X: instantaneous ratio P_{load}/P_{wind} , (ii) battery capacity is zero (C rate irrelevant), (iii) load ratio is 1/20.

4.4 CONCLUSIONS

In this section, we summarize the most important conclusions and interpretations following the results presented above. The study is finally closed making suggestions on how the research work can be further continued as well as discussing other ideas relevant to the topic.

- The total self-sufficiency error was found positive in all cases, meaning that conducting the analysis at 10 min resolution leads always to overestimation of the true self-sufficiency. The error ranges between 0.06 and 3.6 %. For a given load ratio, the error is always maximized when the battery capacity is zero, or in other words when the storage

system does not exist. Increasing the battery capacity results always in lower self-sufficiency error. The reason why this happens has to do with the battery's behavior acting like a filter. In reality, during the 10 min time slot, the battery absorbs the fast surplus and deficit variations that cannot be detected due to the loss of information. These variations are the primary cause of the error. Consequently, as the battery capacity increases and the real time (in seconds) varying component gradually disappears, the self-sufficiency calculated at 10 min becomes more accurate.

- The battery utilization was found negative in all cases, meaning that the utilization is underestimated when the simulation is done at 10 min resolution. The error ranges between 7.5 and 44.7 %. It was concluded that the C rate limit is the most decisive factor influencing the error. For a given load ratio and battery capacity, the error always increases with the C rate limit. Especially at high C rates, the deviation from the truth can be significant; the utilization error lies in the range of 18.1–33.1 % and 20–44.7 % at 1C and 3C respectively. The results reveal that simulating the performance of a fast charging battery in wind power systems can lead to remarkable inaccuracies when the resolution of the data inputs is as low as 10 min.
- Even though the total self-sufficiency error in the worst case scenario is only 3.6 %, the instantaneous error can be much higher, sometimes even beyond 100 %. What is more, it was concluded that there is a clear correlation between the instantaneous self-sufficiency error and the instantaneous ratio $P_{\text{load}}/P_{\text{wind}}$. The error can rise dramatically especially when the ratio $P_{\text{load}}/P_{\text{wind}}$ enters the critical zone of 0.5–2. The more equal the two powers are (averaged over 10 min), the higher the probability that the power profiles will cross over each other in real time and thus the higher the error. Nevertheless, in this research work, the ratio is usually outside the critical zone, therefore affecting positively the total (or average) self-sufficiency error. In another scenario, if for example the load was less consistent and dependent on the weather conditions, possibly the correlation between the load and the wind power profile would be stronger resulting in a higher total self-sufficiency error.
- The results of the present work can be interpreted also from an economic perspective. We note that, the total self-sufficiency is a measure for the total energy savings, where both the contributions of the wind turbine and the battery are taken into account. The battery utilization refers to the energy savings specifically made by the battery. If the user has not yet installed the wind turbine, the analysis will be done based on the total energy savings. In this case, the total self-sufficiency is used (error always positive), resulting in an overestimation of the revenue or a faster ROI. If however, the wind turbine is already present and the user considers to install the battery as an additional asset, the analysis will be done based on the energy savings delivered by the battery. In this case, the battery

utilization is used (error always negative), resulting in an underestimation of the revenue or a slower ROI.

4.5 DISCUSSION

This study forms one of the few attempts realized so far to emphasize the need for real time measurements in industrial wind power installations combined with battery storage systems. We showed that even at 10 min resolution (not exceeded by the great majority of published works), the results can be misleading. Researchers working with similar system topologies are recommended to check initially, even for a short time period, the real time performance of the load and the energy source before choosing the resolution scale of the dataset. At this point, it is worth mentioning that a number of recent works applied advanced algorithms to optimization problems in renewable energy storage systems, where the data resolution is hourly [88-92]. It would be interesting, for those studies, to investigate how the results would be affected when considering datasets of higher resolution.

Regarding the more practical applications, this research work adds certainly value to project developers of RES, especially in the design phase of wind power systems combined with battery storage. The results show that the total self-sufficiency is slightly overestimated at 10 min resolution. This means that, when the developer starts with a completely new design, where neither the wind turbine nor the battery preexist, he overestimates the total cost savings (or the revenue) of the system when using 10 min resolution; however the error is not significant (here, 3.6 % in worst case scenario). When the developer is only interested in the battery storage system, consider a preexisting wind turbine, he underestimates the total cost savings considerably. Even when the battery has a moderate C rate at 1C, which is very common for most new installations, the real revenue is 18.1–33.1 % more for this case study.²⁷ Moreover, besides the revenue miscalculation, the utilization error reflects also to the expected lifetime of the battery, which is of utmost importance if the developer bears a warranty obligation. In general, the battery lifetime varies depending on the lithium-ion technology. In case of a battery with a poor lifetime (e.g., 70 % capacity fade after 1000–2000 cycles), if the battery is overutilized, the developer, being unaware of the battery utilization error, could falsely believe that the battery can survive the payback period of the investment whereas in reality it would have to be replaced sooner. Finally, another practical contribution of this study is the methodology itself. An analytic power flow model was developed in Matlab®. The power flow model can be generalized for other applications as well, regardless of the battery technology,

²⁷ Here, we assume that the consumption energy tariff is fixed to translate energy savings into cost savings.

the DC/AC converter specifications and the resolution of the data inputs. All Simulink blocks and major mathematical formulas are presented in order to be easily reproduced.

A next step to continue the present work can be to carry out the same analysis (same system and variables), but changing the data inputs. Needless to say, the primary obstacle we are faced with here, is the acquisition of high resolution data. Recording real-time data particularly in industrial sites for long time periods is not an easy task due to several technical issues (e.g., storage capacity of the measurement device, permissions to enter the factory, time availability, etc.). It is still however necessary to investigate a variety of case studies before constructing empirical theories with regard to error expectations when low resolution data is used. One of the goals of the present work was to focus on the instantaneous error and see how it is affected by the ratio of the instantaneous (10 min averaged) load and wind power. Due to the low correlation between the two power profiles, it was concluded that the total self-sufficiency error is low. A next step for future research can be to dive deeper into this aspect. A very strong milestone to reach is to establish a mathematical link between the load profile, local wind speed measurements and the error expectation. It is worth noting that so far all studies agree that the self-sufficiency and battery utilization are always overestimated and underestimated respectively, which means that we know in which direction to correct the error. Consequently, the main issue left to resolve is determining the error magnitude in function of the system topology and time resolution.

In the next chapter, we will move our research scope to “peak shaving” which is another popular revenue stream for battery storage systems. The developed power flow model of this chapter will be used as input. Nevertheless, we will introduce some changes on the modelling technique of the DC/AC converter by integrating non-linearities in the efficiency curve which is very important for calculating accurately the energy losses of the battery storage system.

5 Peak shaving

5.1 INTRODUCTION

The increase of renewables goes hand in hand with technical challenges. The stochasticity of both PV and wind power systems causes the maintenance of grid stability to become more difficult [93, 94]. A major stakeholder impacted by the renewable energy transition is the distribution network operator. While end users are becoming increasingly more independent from the grid, the revenue constraint for the grid operator still remains [95]. Under the current tariff structure, which is primarily based on the energy-volume component, a 'death spiral' phenomenon is imminent [95, 96]. Nevertheless, the grid infrastructure costs are mainly dependent on the power capacity of the system. Yet, PV users have reportedly slightly lower peak power than non-PV users [97]. In other words, PV-users pay less than non-PV users even though both of them use the grid almost to the same extent [97]. To counteract such unfairness between different user groups and correctly attribute the costs to their origin, new tariff structures are being introduced that increase the weight factor for the peak demand component. This (peak demand pricing) will also apply for small user groups such as residential consumers who have been so far excluded from peak power measurements [98, 99].

Given these increased peak power costs, peak demand reduction ('peak shaving') has gained much attention in recent years. Peak shaving is not a new concept; industrial users with high peak demand already have been using diesel and gas generators to reduce electricity costs for a long time. Still, those conventional generation methods are expected to be replaced by 'green' technologies, among which energy storage and in particular batteries are the primary candidate.

Battery storage systems have been deployed in the past to provide different types of services, such as (i) increasing the self-sufficiency of PV/wind power installations [100-102], (ii) providing ancillary services to the grid operator [103-105], (iii) peak shaving [106-108], (iv) back-up generators and UPS [109, 110]. A common issue, arising particularly in (i), (ii) and (iii), is that due to the high cost of the storage system, battery storage investments are not yet economically feasible. However, we note that in the majority of those studies, the battery is deployed exclusively for one service. Therefore, to accelerate the return of investment, many suggest as a possible solution 'hybridizing' multiple services into a single application instead of providing each one separately [105, 111, 112]. Before studying how such a hybrid strategy can be applied, we should first identify the technical constraints of the services under consideration. In this study, we focus specifically on peak shaving and present some insights

that reflect its potential for hybridization. In the next paragraph, we review previous research works on peak shaving through battery storage.

In [107], the authors present a sizing methodology for defining the optimal energy and power capacity of battery storage systems used for peak shaving. An economic feasibility study was conducted for two different technologies, lead acid and vanadium redox flow (VRF). A control strategy was proposed, but it assumed that the load profile is perfectly predictable in advance. In [106], the researchers applied peak shaving for residential end users. One of the main conclusions was that the utilization of the lithium-ion battery stays very low, lower than 165 cycles per year. At such a low rate (here, the cycle lifetime is 3000 cycles) the system could be used for more than 20 years unless it exceeded its calendar lifetime. Finally, considering also its calendar lifetime, the battery would have to be replaced approximately after 10–15 years. Furthermore, the researchers suggested adding grid support services next to peak shaving in order to increase the utilization of the system. In [113], the researchers developed a model in Matlab/Simulink where a VRF battery is used to simultaneously provide frequency regulation and peak shaving. It was concluded that the battery storage system can successfully perform both services. However, the experiment was conducted only for a limited time period (30–140 s), thus, in essence, without affecting the battery state of charge (SoC) and as a consequence, it was not possible to evaluate the reliability of the control system under unfavorable conditions. In [114], a fuzzy control algorithm was developed for peak shaving in university buildings. The algorithm was tested and compared to two different peak shaving techniques, namely the fixed-threshold and adaptive-threshold controller. The results showed that the proposed algorithm was the best of all. Although the researchers conducted several case studies (with 8 different load profiles), they did not provide sufficient information about the load forecasting method. In [108], a control algorithm is proposed for peak shaving in low-voltage distribution networks based on day ahead aggregated load forecasts. The main novelty of that study is that the algorithm, considering also the inherent forecasting errors, relies solely on historic data; hence there is no need to intervene in real-time and readapt the discharging process of the battery. Results from a case study show that peak reduction is achieved for 97 % of the time and that for 55 % of the time, the peak reduction is at least 10 %. In [109, 110, 115, 116], peak shaving is addressed as a secondary application. Here, the primary service of the battery is to provide uninterruptible power supply (UPS) in data centers. The researchers argue that because of the significantly low probability of the peak occurrence (e.g., a Google data center exceeds 90 % of its power capacity only for 1 % of the time), it is possible to achieve peak reduction without impacting the reliability of the primary service. In [117], a battery sizing methodology and an optimal control algorithm is proposed for peak shaving in industrial and commercial customers. One of the main objectives was to determine an appropriate peak

shaving threshold. Three case studies were carried out, each one considering a different daily load profile. The results showed that adapting the peak shaving threshold in real-time leads to higher peak reduction than keeping a fixed threshold based only on a historic data analysis. A drawback of the study might be that when calculating the battery utilization, it is assumed that the battery is equally utilized every weekday of the year, thus omitting possible idle periods on days with low power consumption. In [118], a peak shaving algorithm was proposed for microgrid applications. In contrast to conventional approaches considering only the load consumption, here, the peak threshold applies also for the PV generation. The battery capacity is equally reserved for both positive (injection to the grid) and negative (absorption from the grid) peaks by setting the SoC during normal operation at 50 %. The algorithm was tested on a real-time microgrid, implemented in the lab. The researchers used predefined data (load/PV profiles) to carry out the experiment; however, they did suggest in future deploying predictive analytics to improve the reliability of the system.

Conclusions and relation to present work

Next, we summarize important conclusions drawn from the literature review and explain how these are related to the present research work:

- **Value stacking is possible with peak shaving:** There are indications from previous works that a battery storage system used in peak shaving applications is underutilized and consequently there is potential to combine peak shaving with other services to increase the economic profitability of the investment [106, 109, 110, 113, 115, 116]. Nevertheless, the majority of such studies refer to unique use cases (i.e., peak shaving combined with UPS) [109, 110, 115, 116] while in other studies the data used to conduct the simulation is very limited to draw any meaningful conclusions [106, 113].
 - Present study: In this research work, we conducted simulations for 40 different users, 3 years of historic load profiles at 15 min resolution. We quantify the battery utilization in terms of SoC active time and cycles. Our results validate previous findings that batteries in peak shaving applications are indeed underutilized and there is potential to consider additional revenue streams depending on the predictability of the load profile.
- **No concrete methodology on sizing the battery capacity:** Previous research works have focused on the control strategy of the BESS suggesting the use of adaptive peak thresholds in order to maximize the profitability of the investment [107, 108, 114, 117]. Given the availability of accurate load forecasts the user can increase the profits by dynamically adapting his peak threshold (e.g., day-ahead – setting a new threshold every day) instead of setting a fixed threshold over a long term horizon (e.g., year-ahead).

- **Present study:** In this study, we follow the fixed threshold concept. We strongly believe that adaptive threshold strategies are not reliable in the context of peak shaving applications. A battery that is deployed for peak shaving must be prepared for worst case scenario's (e.g., bad forecast); a single failure, missing a quarter peak, can result in losing the entire revenue on the long term (months – years)²⁸. This study presents a methodology for sizing the battery capacity in fixed threshold applications.
- **Lack of data to draw generalizable conclusions:** In general, there has not been a comprehensive study to derive broadly applicable conclusions primarily because of data limitations. The available data is often restricted in terms of time duration (typically no more than 2 – 3 months), and studies often focus on individual users, resulting in quantitative results that lack generalizability.
 - **Present study:** To the best of our knowledge, the present study is the first to consider such large dataset: 40 load profiles, each one with 3 full years of historic load power. Knowing the difficulties of finding qualitative data, we decided to make this dataset publicly available (see relevant publication). In our sensitivity analysis we summarize quantitative results for several key performance metrics such as the battery utilization, peak reduction and consumption increase in function of the installed battery capacity.

Research core, key questions & contributions

[Figure 40](#) shows the topology of our system comprising the battery storage system, the load (enterprise user) and the grid. The grid serves as the only power supply since there are no renewable energy sources. In general, for peak shaving, the energy storage system should have high energy efficiency as well as high power capacity (C rate) [29]. For these reasons, we selected a Lithium-ion battery to carry out our analysis (See [Table 12](#)). The battery is exclusively used for peak shaving (no other services are considered); given a predefined peak threshold the battery is charged when the load power is lower than the threshold and vice versa it is discharged when the load power is higher than the threshold. Next, we present the key research questions addressed in this work including the delivered contributions:

- What is a suitable power flow model for peak shaving applications?
In Section [5.2.2](#) we present the power flow model developed in Matlab Simulink. The model is based on the version introduced in Chapter 4. In this version (Chapter 5), we consider

²⁸ DSOs applying peak demand tariffs typically define peaks in monthly or yearly resolutions.

non-linearity in the efficiency curve of the DC/AC converter which improves the model accuracy especially regarding the energy losses of the BESS.

- How do I calculate the battery capacity (kWh) needed to achieve a certain peak power reduction?

In Section [5.2.3](#) we present the algorithm (dichotomy method) used for sizing the battery capacity in peak shaving applications (fixed threshold). The algorithm is written in pseudocode; it can be used separately from the power flow model in other (than Matlab) programming environments.

- How much is the peak reduction in function of the battery capacity?
Section [5.3.1](#) presents the results of a comparative study for 40 low voltage enterprise profiles, showing the peak reduction, battery utilization and energy consumption increase in function of the battery capacity.
- Can peak shaving be a profitable business case for enterprises in Flanders?
This question is addressed in Section [5.3.2](#). It is shown that peak shaving can be economically interesting for several users in Flanders, Belgium given the real market data (e.g., electricity price, battery quotations, DSO tariff tables) of that time.
- What is the battery utilization, can we combine peak shaving with other services?
This question is addressed in Section [5.3.1](#) where we summarize the results (in terms of cycles and SoC active time) for all 40 enterprise users. Furthermore, we elaborate on this topic in Section [5.5](#).

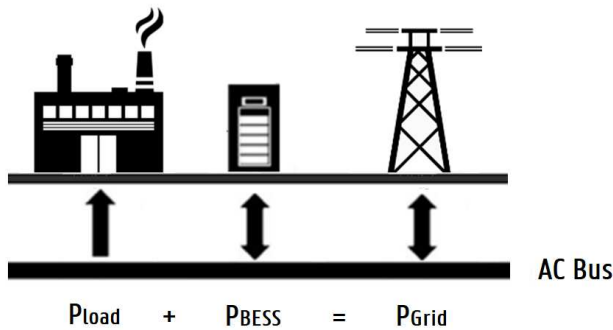


Figure 40: System topology

Table 12: LFP Cell Characteristics, according to [79]

Characteristics	Specifications
Chemistry	LiFePO ₄
Battery capacity	2.28 Ah (7.52 W h)
Nominal voltage	3.3 V
Operating voltage	2.5 to 3.6 V
Operating temperature	-30 °C to +60 °C
Cell weight	70 g

The rest of the chapter is structured as follows. In Section 5.2, the data of the study are presented (Section 5.2.1). Then, we proceed with the methodology; the power flow model is explained (Section 5.2.2) and the dichotomy method is proposed as an optimization algorithm for sizing the battery capacity (Section 5.2.3). Section 5.2 closes with the definition of performance metrics (Section 5.2.4). Next, Section 5.3 shows the results of the simulation (Section 5.3.1) and explains how to interpret those from an economic perspective (Section 5.3.2). Finally, Section 5.4 and 5.5 summarize the most important conclusions and makes suggestions for future research objectives.

5.2 METHODOLOGY

5.2.1 Data

We received 40 load profiles from the Flemish distribution grid operator (Fluvius) Each profile is the active power (in kW) of an enterprise for the 3-year period between 1 January 2014, 00:00 and 31 December 2016, 23:45. All enterprises are low-voltage users with peak demand pricing and a connection capacity above 56 kVA and lower than 1 MVA. The data was logged through automatic measurement reading (AMR) devices with a time resolution of 15 min. The mean power of the users varied between 1.92 and 53.75 kW (Figure 41 a). The peak-to-mean power ratio was between 1.5 and 40; however, for 90 % of the users, the ratio is lower than 10 (Figure 41 b).

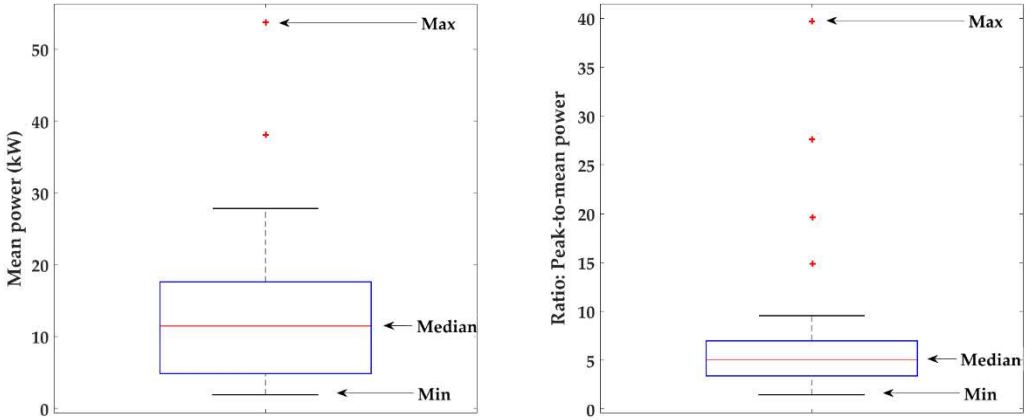


Figure 41: Boxplots, 40 load profiles: (a) Mean power (left), (b) Ratio: Peak-to-mean power (right).

5.2.2 Power flow model

The simulation model, built in Matlab/Simulink is shown in [Figure 43](#). Here, it is worth noting that a part of the present model used for peak shaving was based on the model described in [\[2\]](#). Therefore, in this study, we will only detail the new model components, which are blocks 1 and 5 (See [Figure 43](#)). For the remaining blocks 2, 3 and 4, we provide a generic description, but for more information, the reader is referred to [\[2\]](#). For the development of the model, we relied heavily on a real test-setup—microgrid emulator²⁹ comprising: (i) a low-voltage grid (250 kVA power source), (ii) a 90 kVA DC/AC converter, (iii) a 20 kWh LiFePO4 battery, (iv) a 30-kW programmable load. The behavior of each component and the interaction between them was studied analytically and converted into simulation models using information from test measurements, scientific papers and commercial datasheets.

To begin with, the model has three variables: (i) the time resolution of the load profile, (ii) the battery capacity (kWh) and (iii) its C rate. Furthermore, it receives two data inputs: (i) the load profile and (ii) a power threshold. The load profile is simply a time series of the active power in kW at 15 min resolution. The power threshold is a constant specifying the ‘desired’ maximum power. This value must be lower than the peak power but also higher than the mean power. Given the time step (resolution) and the 3-year period, in total, there are 105216 simulation steps (1096 days × 96 quarters/day). At each step, the model reads the load power of that moment and the current State-of-Charge (SoC). Then, it undergoes three sequential processes (1, 2 and 3) to calculate the battery power P_{bat} (inverter’s DC side), the inverter power P_{inv}

²⁹ The microgrid emulator makes part of the laboratory infrastructure of EELab/Lemcko, an expertise center of Ghent University, specialized in Renewable Energy System applications.

(inverter's AC side) and the power of the grid P_{grid} . Next, after updating the State-of-Charge (SoC) of the battery, it proceeds to the next simulation step and hence, the simulation progresses. [Figure 42](#) shows the DC/AC conversion efficiency of the inverter in charging mode. Additionally, all the equations that were used to calculate the inverter power P_{inv} and battery power P_{bat} in charging and discharging mode are given below:

$$P_{\text{bat}} = f(x) \cdot P_{\text{inv}}$$

$$\frac{P_{\text{bat}}}{P_{\text{nom}}} = f(x) \cdot \frac{P_{\text{inv}}}{P_{\text{nom}}}$$

$$\frac{P_{\text{bat}}}{P_{\text{nom}}} = f(x) \cdot x = g(x)$$

$$\frac{P_{\text{inv}}}{P_{\text{nom}}} = g^{-1}\left(\frac{P_{\text{bat}}}{P_{\text{nom}}}\right)$$

$$P_{\text{bat}} = \frac{P_{\text{inv}}}{f(x)}$$

$$\frac{P_{\text{bat}}}{P_{\text{nom}}} = \frac{P_{\text{inv}}}{P_{\text{nom}}} \cdot \frac{1}{f(x)}$$

$$\frac{P_{\text{bat}}}{P_{\text{nom}}} = \frac{x}{f(x)} = h(x)$$

$$\frac{P_{\text{inv}}}{P_{\text{nom}}} = h^{-1}\left(\frac{P_{\text{bat}}}{P_{\text{nom}}}\right)$$

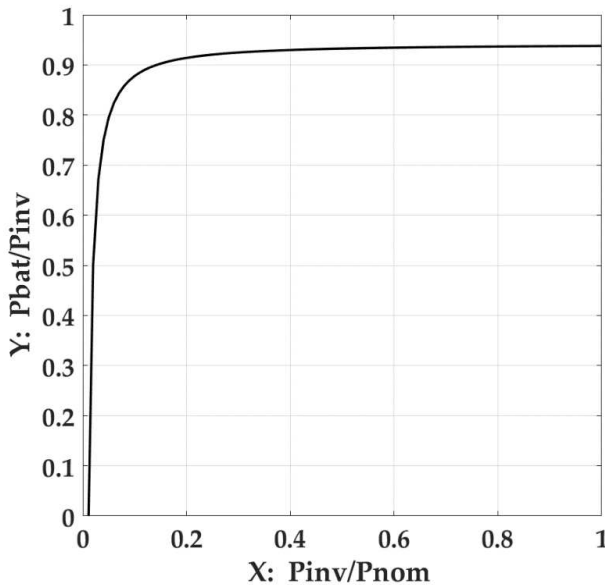


Figure 42: DC/AC efficiency, $Y = f(x)$

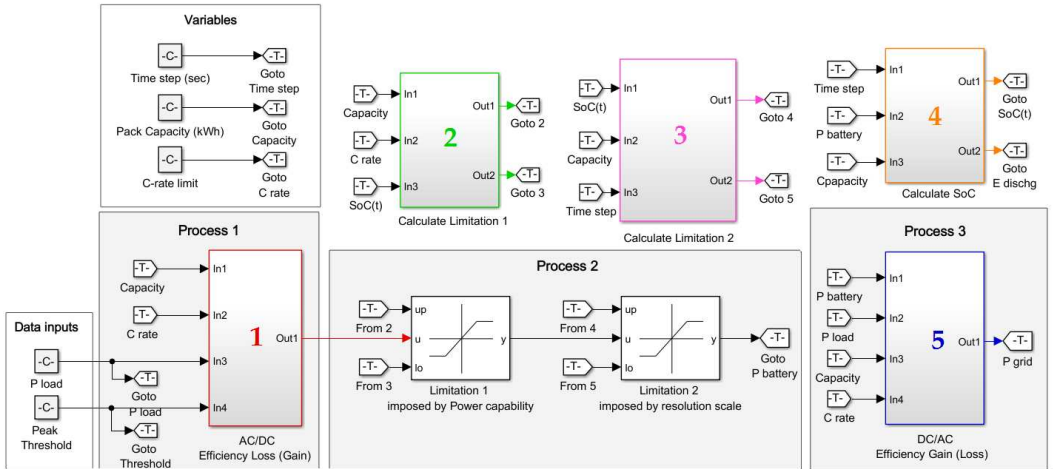
With respect to the sequential processes, process 1 performs the power conversion from AC to DC compensating for the efficiency losses (AC to DC). Process 2 applies two saturation

constraints to the battery power: one for the given C rate and one for the given time resolution. Finally, process 3 performs the reverse conversion from DC to AC considering the inverse (DC to AC) efficiency losses. In the following paragraph, we describe with more detail those processes.

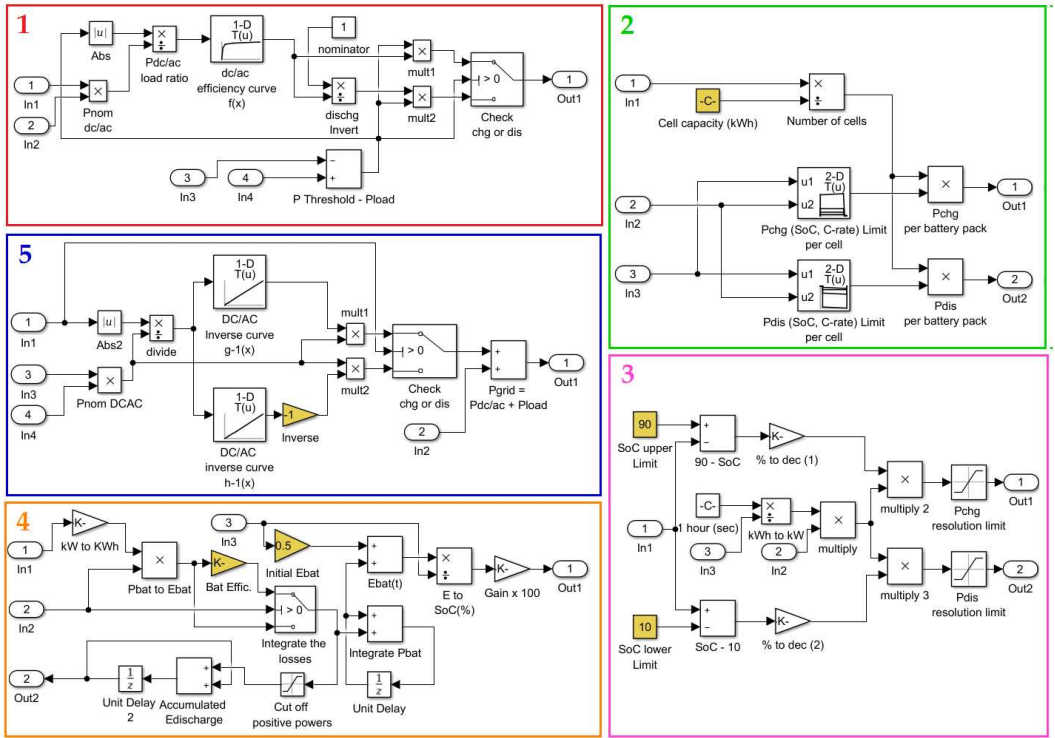
Process 1—AC/DC power conversion (Figure 43, block 1): Initially, we set the inverter power equal to the difference $P_{\text{Threshold}} - P_{\text{load}}$. In case of a power surplus (positive difference), the inverter is in charging mode to restore the battery's energy capacity, otherwise, in case of a power deficit (negative difference), the inverter is in discharging mode to shave the peak. After setting the inverter power, next, we calculated the battery power compensating for the efficiency losses. In charging mode, the battery power is always lower than the inverter power (See Equation 5-1) and vice versa in discharging mode the battery power is always higher than the inverter power (See Equation 5-5).

Process 2—Power saturation constraints (Figure 43, block 2, 3, 4): Here, we impose two constraints to the battery power. First (block 2), the battery power can never exceed its power capacity as specified by its C rate limit and the SoC level. For this battery technology, the recommended C rate is 1. How we calculate exactly the power from the C rate limit, has been explained in [2]. (As an approximation, we can state that the power capacity is equal to the battery's nominal voltage times the C rate, times its energy capacity in Ah: $P_{\text{bat max}} = U_{\text{nom}} \cdot C_{\text{rate}} \cdot C_{\text{Ah}}$). Second (block 3), we must take into account also the time resolution of our data (15 min). This constraint comes into effect when the SoC level is very close either to its upper or lower limit (90 % and 10 % respectively) (10–90 % is the recommended by the manufacturer SoC range to maximize the lifetime of the battery). Since our simulation is executed in discrete steps of 15 min, we need to consider how much energy is left inside the battery and saturate its power accordingly (see [2]). Afterwards, at the output of the second constraint, the battery power was finally defined and hence the SoC can be updated (block 4).

Process 3—DC/AC power conversion (Figure 43, block 5): Knowing the final value of the battery power, it is then possible to calculate the final value of the inverter power. At this point, the DC/AC efficiency function $f(x)$ needs to be inverted. In charging mode, we make use of Equation 5-4 (function g^{-1}) and in discharging mode Equation 5-8 (function h^{-1}). As a result, we finally know both the load power P_{load} and the inverter power P_{inv} . Therefore, we can also calculate the power of the grid P_{grid} ($P_{\text{grid}} = P_{\text{load}} + P_{\text{inv}}$) and proceed to the next simulation step.



(a) Main model



(b) Subsystem components

Figure 43: Power flow model for peak shaving designed in Matlab/Simulink.

5.2.3 Dichotomy method

As already mentioned in Section 5.2.2, the Simulink model receives both the battery capacity (as variable) and a peak threshold (as data input). To find out whether or not that threshold will be met, all we have to do is run the simulation and check the maximum load power $\text{Max}(P_{\text{load}})$. On the one hand, if the threshold is too low, the system will be unreliable ($\text{Max}(P_{\text{load}}) > P_{\text{Threshold}}$) due to insufficient battery capacity, whereas, on the other hand, if the threshold is too high ($\text{Max}(P_{\text{load}}) \leq P_{\text{Threshold}}$) the system will be reliable but the battery is overdimensioned. Consequently, for each load profile and a given battery capacity, there is only one threshold that minimizes the load power (See Figure 44). To find the solution for our optimization problem we deployed the 'dichotomy method'. In the next paragraph, follows a short description of the algorithm.

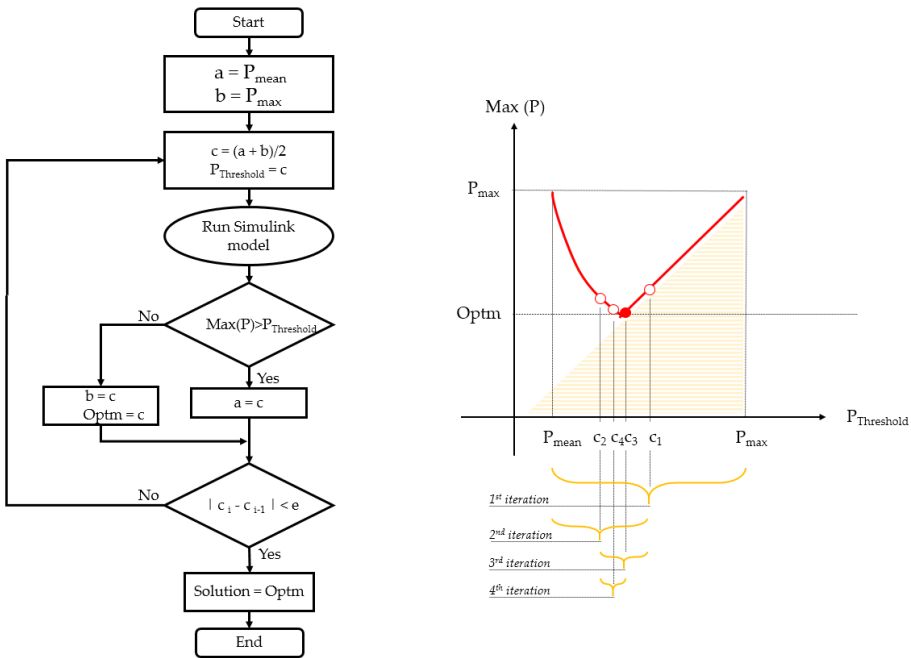


Figure 44: Flow chart—Dichotomy method: (a) Pseudocode (left), (b) Midpoint evolution (right).

Dichotomy method (Figure 44):

1. Initialize the lower and upper threshold limit at $a = P_{\text{mean}}$ and $b = P_{\text{max}}$, respectively.
2. Enter dichotomy loop: Calculate the midpoint at $c = (a + b)/2$ and set the peak threshold equal to that value.
3. Run the Simulink model.

4. Check the maximum load power. If the load power exceeds the threshold update the lower limit at $a = c$. Otherwise, update the upper limit at $b = c$ and store that value as the current solution.
5. Check convergence criterion. If the distance between the current and previous midpoint is lower than a constant, exit the loop, otherwise, go to step 2 and recalculate the new midpoint.

5.2.4 Definition of performance metrics

Before continuing with the presentation of the simulation results, first, we need to give the definitions of our performance metrics, based on which we evaluated the peak shaving potential of the users. In our approach, we would rather associate the word 'potential' explicitly to energetic assessments. The extent to which these can be translated into economic terms (e.g., revenues, expenses, ROIs) depends certainly on the tariff structure under consideration as well as the cost for the battery storage system. Although, as shown in Section 5.3, we do provide some insights specifically for Belgium, preferably, each reader ought to make his own reflections.

Peak reduction (%): It is the percentual difference between the initial peak power and the final peak power after peak shaving:

$$A_{\text{peak red}} = \frac{P_{\text{max } i} - P_{\text{max } f}}{P_{\text{max } i}} \cdot 100$$

where $A_{\text{peak red}}$ is the peak reduction, $P_{\text{max } i}$ is the initial peak power, $P_{\text{max } f}$ is the final peak power after peak shaving.

Peak reduction-to-capacity. It is the difference between the initial peak power and the final peak power after peak shaving divided by the battery capacity. This metric can serve us as a rough estimation of the profitability of the installation if we can express the revenue and costs linearly proportional to the peak reduction and battery capacity respectively.

$$R_{\text{peak red-to-cap}} = \frac{P_{\text{max } i} - P_{\text{max } f}}{C_{\text{kWh}}}$$

where $R_{\text{peak red-to-cap}}$ is the ratio peak reduction-to-capacity, $P_{\text{max } i}$ is the initial peak power, $P_{\text{max } f}$ is the final peak power after peak shaving, C_{kWh} is the battery capacity.

SoC active time (%). It is the average percentage of time per year that the battery is deployed for peak shaving. This metric can be very useful, especially when our intention is to combine peak shaving with other services (e.g., increasing the self-sufficiency of PV, ancillary services, Time-of-Use (ToU) prices).

$$\text{SoC}_{\text{act time}} = \sum_{i=1}^{1096 \cdot 96} \text{OnOff}_i \cdot \frac{100}{1096 \cdot 96}$$

$$\text{OnOff}_i = \begin{cases} 1, & |P_{\text{bat } i}| > 0 \\ 0, & P_{\text{bat } i} = 0 \end{cases}$$

where $\text{SoC}_{\text{act time}}$ is the SoC active time, P_{bat} is the battery power at quarter i , i is the quarter index of the simulation, 1096×96 is the total number of quarters within the 3 years period (1st January 2014–31st December 2016).

Battery utilization (cycles/year). It is the average total energy discharged by the battery within a year divided by the battery capacity. This metric can be used to assess how fast the battery reaches the end of its lifetime. Particularly for peak shaving applications, it is desirable that the battery be utilized as low as possible since our cost savings are exclusively dependent on the power component (cost in function of kW). Conversely, when the aim is to increase the self-sufficiency of the installation (PV or wind), the battery utilization should be as high as possible, since our cost savings are mainly dependent on the energy component (cost in function of kWh).

$$U_{\text{battery}} = \frac{E_{\text{dis tot}}}{C_{\text{kWh}} \cdot 3}$$

where U_{battery} is the battery utilization, $E_{\text{dis tot}}$ is the total discharged energy (kWh) within the 3 years period, C_{kWh} is the battery capacity.

Consumption increase (%). It is the percentage of energy consumption increase due to efficiency losses of the battery storage system. In addition to the initial capital expenditures for the battery, the additional energy consumption should be taken into account as operating cost.

$$A_{\text{incr}} = \frac{E_{\text{load f}} - E_{\text{load i}}}{E_{\text{load i}}} \cdot 100$$

where A_{incr} is the consumption increase, $E_{\text{load f}}$ and $E_{\text{load i}}$ is the total energy consumed within the 3-year period after and before peak shaving, respectively.

5.3 RESULTS

As mentioned in Section 5.2, the power flow model receives three variables: battery capacity, C rate, and time step. For each load profile in our dataset, we carried out multiple simulations by varying only the battery capacity, whereas both the time step and the C rate were set at constant values. The peak threshold was calculated using the dichotomy method after defining the battery capacity.

The time step was set at 15 min which is the time resolution of the dataset. The C rate was set at 1 C; higher values are not recommended for the chosen battery technology because this would negatively impact its lifetime. Furthermore, based on our experience, for most applications, 1 C is sufficiently high to meet a given peak threshold. In general, the extent to which we can reduce the peak power depends on the battery's energy capacity rather than its power capacity. Nevertheless, we do suggest for future research to investigate the impact of the C rate as well, but in this study, it will not be addressed. Regarding the battery capacity, since we deal with several users, in order to maintain a common reference of comparison between the users, we normalized the battery capacity by dividing it by the mean power of the user. Finally, the ratio battery capacity-to-mean power was varied within 0.1–10.

5.3.1 Energetic assessments

The simulation results are presented in [Figure 45](#) and [Figure 46](#). Knowing that our dataset consists of 40 users, it would be ineffective to illustrate 40 individual plots into the same figure. Instead, we selected five quantile elements at which the cumulative probability becomes 5 %, 25 %, 50 %, 75 % and 95 %. This gives us a better view of the statistical distribution of each performance metric.

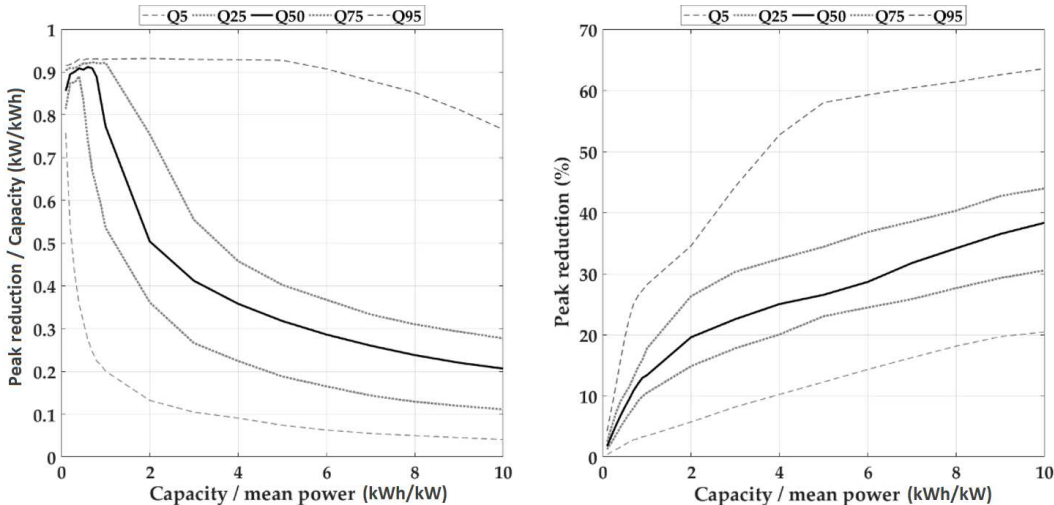


Figure 45: Simulation results: (a) Peak reduction-to-capacity (left), (b) peak reduction (right).

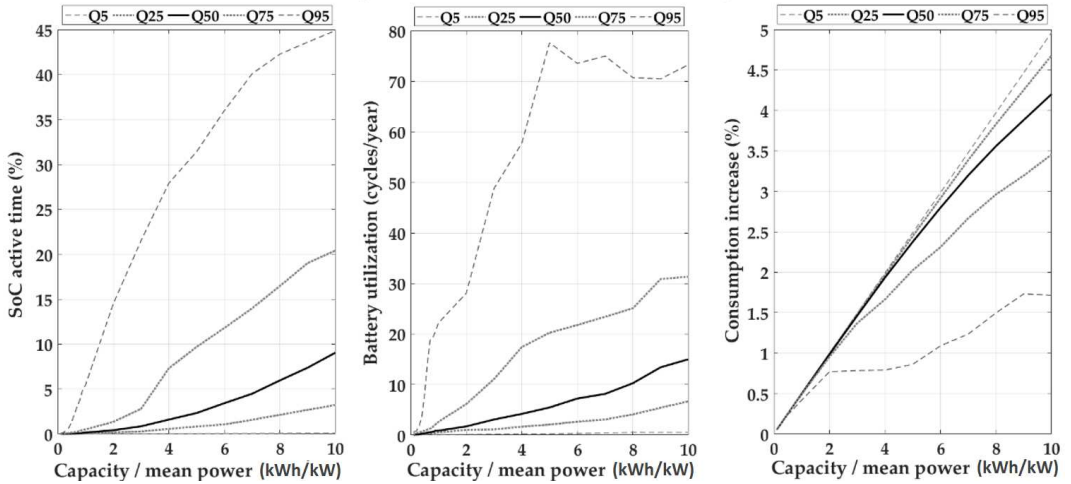


Figure 46: Simulation results: (a) SoC active time (left), (b) Battery utilization (middle), (c) Consumption increase (right).

From both [Figure 45a](#), [Figure 45b](#), it can be concluded that the peak reduction increase decreases with the battery capacity (second derivative of the function in [Figure 45b](#) is negative) or in other words: as the battery capacity increases, peak shaving becomes more difficult. For a battery capacity 2 times the mean power (e.g., a user with 30 kW mean power installs a 60 kWh battery) seventy percent of the users between Q5 and Q75 achieve peak reduction in the range 0.26–1.5 times their mean power ([Figure 45a](#)). The same group of users achieves peak reduction up to 6–27 % of their peak power ([Figure 45b](#)). For a battery capacity of 10 times the mean power (e.g., a user with 30 kW mean power installs a 300 kWh battery) the peak reduction for that group (Q5–Q75) varies within 0.4–2.8 times their mean power ([Figure 45a](#)) and 20–44 % of their peak power ([Figure 45b](#)).

Regarding the SoC active time ([Figure 46a](#)), it increases with the battery capacity. The reason is that as the battery capacity increases, the peak threshold is reduced and consequently, the battery is used more frequently. An important conclusion to note is that, for most users, the SoC active time remains very low, even for large battery capacities. Seventy percent of the users between Q5 and Q75 with a battery capacity 10 times the mean power deploy their battery in the range of 0–20 %, or in other words the battery stays idle for at least 80 % of the time during the year. This fact in itself opens up new research opportunities.

If peak shaving does occur rarely, then we could possibly hybridize our energy management system including other services as well (e.g., ancillary services, increasing the self-sufficiency of renewable energy installations). [Figure 46b](#) provide another indication that the battery is underutilized, here, however in terms of lifetime expectancy. Over the entire battery capacity

dimension, for ninety-five percent of the users (Q0–Q95), the battery does not deliver more than 80 cycles per year. This number is considerably lower compared to the cycle lifetime of nowadays' state-of-the-art Lithium-ion technologies (above 5000 cycles) [29]. At such low utilization rates, the battery can endure several years of use (more than a decade). Finally, it will be due to another reason why the battery was decommissioned such as a maintenance issue or simply because the battery has reached the end of its calendar lifetime.³⁰

The consumption increase is shown in [Figure 46c](#). It is worth noting once more that the battery technology in the present study exhibits a very high energy efficiency. Undoubtedly, if other technologies were used (e.g., lead acid, flow batteries), the consumption increase would be higher. As can be seen from the figure, obviously, the higher the battery capacity, the higher the absolute energy losses. One reason why this happens is due to the increase of the battery utilization (see [Figure 46b](#)) and another reason is because both the battery and the dc/ac converter become bigger in size. Consider, for instance, a user with 30 kW mean power and a battery capacity of 300 kWh (capacity-to-mean power is 10). Only the converter losses to (dis)charge the battery at 1 C are approximately 15 kW (at 95% dc/ac efficiency). If the battery capacity was 30 kWh (capacity-to-mean power is 1), those losses would be significantly lower (1.5 kW).

5.3.2 Economic evaluations

Let us now consider a case study of how to interpret those results from an economic perspective. [Table 13](#) lists the parameters used for our economic analysis:

- The electricity price is an average for Belgium energy invoices in the considered capacity connection range. The electricity price lies in the range of 0.2–0.25 €/kWh [119]. Here, it must be noted that our analysis is exclusively applicable for end users with fixed electricity prices during the year; there is no Time-of-Use (ToU) dependency (e.g., day/night tariff, dynamic pricing schemes).³¹
- Regarding the peak shaving compensation, for the DSO in Belgium, peak demand is defined as the highest 15 min load power measured by the user's AMR meter over the last 12 months. The compensation ranges approximately within 87.6–131 €/kW per year

³⁰ The capacity fade effect of Lithium-ion batteries is both time-dependent (calendar lifetime) and cycle-number dependent (cycle lifetime). Regardless of its utilization, after a certain time period the battery loses a part of its initial capacity. Usually, the End of Life (EoL) of a battery is defined when its initial capacity is reduced by 20 %, in many critical applications (e.g., EVs) this is the time when the battery needs to be either decommissioned or repurposed for another application.

³¹ In case of ToU dependency, the control strategy of the battery is different. Peak demand pricing coexists with ToU pricing and therefore, we need to solve the economic optimization problem first.

depending on the geographical location. By dividing by the total number of hours per year (8760 h), this equals 0.01–0.015 €/kWh/h.³²

- With respect to the battery storage system, we consider capital expenditures at 500 €/kWh (per kWh of energy capacity). The consumption increase can be approximated as linear function of the battery capacity (See [Figure 46c](#)) at 0.4 %/capacity-to-mean power. The battery cycle lifetime is estimated at 5000 cycles (at 80 % EoL) considering normal operating conditions: (i) Ambient temperature 25 °C, (ii) SoC within 10–90 %, (iii) (dis)charge current at 1C. Given that our battery utilization is very low (80 cycles/year worst case), we will consider only calendar aging at 2 % capacity loss per year. To calculate the battery’s cycle lifetime and calendar aging, under those conditions (25 °C, 10–90 % SoC, 1C) we received information from the manufacturer. For those interested in analytic methods to calculate the battery cycle lifetime and calendar aging, we refer to noteworthy research works [[120](#), [121](#)]. The payback period of our investment is 10 years and we do not consider any option to resell the battery; after this period the battery is recycled.

Table 13: Peak Shaving, Parameters for Economic Feasibility.

Parameters	Values
Payback period	10 Years
Peak shaving compensation	0.01–0.015 €/kWh
Battery capex	500 €/kWh
Consumption increase rate	0.4 %/capacity-to-mean power
Electricity price	0.20–0.25 €/kWh
Battery capacity fade	2 % per year

In order for the system to be profitable, the total peak shaving compensation has to be higher than the total cost (incl. battery and losses) over the payback period; this condition is expressed in Equation [5-15](#). Next, as shown in Equation [5-16](#), the peak reduction-to-capacity ratio can be expressed in function of all economic parameters. Finally, by replacing with the values of [Table 13](#), it can be concluded that the ratio needs to be higher than 0.43–0.67 (Equation [5-16](#)).

³² These values have been defined using a cost simulation tool from the distribution grid operator. The values apply exclusively to those users connected to the low-voltage grid with peak demand pricing.

$$\text{Rev} \cdot 8760 \cdot \text{ROI} \cdot \Delta P_{\text{peak}} > C_{\text{kWh}} \cdot (\text{Cost}_{\text{bat}} + \text{Rate}_{\text{cons incr}} \cdot P_{\text{elect}} \cdot 8760 \cdot \text{ROI})$$

$$\frac{\Delta P_{\text{peak}}}{C_{\text{kWh}}} > \frac{\text{Cost}_{\text{bat}} + \text{Rate}_{\text{cons incr}} \cdot P_{\text{elect}} \cdot 8760 \cdot \text{ROI}}{\text{Rev} \cdot 8760 \cdot \text{ROI}}$$

$$\frac{\Delta P_{\text{peak}}}{C_{\text{kWh}}} > 0.43 - 0.67$$

where ΔP_{peak} is the peak reduction, ROI is the return of investment (payback period), Rev is the peak compensation (revenue), C_{kWh} is the battery capacity, Cost_{bat} is the battery capex, $\text{Rate}_{\text{cons incr}}$ is the rate of consumption increase and P_{elect} is the electricity price.

Over the 10-year period, the total capacity loss of the battery will be 20 %. Consequently, to ensure that the peak threshold will always be met, we have to oversize the battery capacity. Finally, the results of the economic feasibility study are illustrated in [Figure 47](#). [Figure 47](#) can be made easily from [Figure 45a](#) (see Section [5.3.1](#)) by adding a 20 % margin to the minimum battery capacity requirement. The color at each point $[x,y]$ represents the total number of users whose peak reduction-to-capacity exceeds the y value (similarly to the quantile plots of [Figure 45a](#)). The yellow and green dashed lines represent the profitability thresholds 0.43 and 0.67, respectively (see Equation [5-16](#)). As can be seen, there are several positive use cases; of course the number of positive cases depends on the battery size. To give an example, when the ratio capacity/mean power equals 2, there are 15–20 users exceeding the value 0.43 (lower profitability threshold), whereas when the ratio capacity/mean power becomes 10, there are only 0–5 users exceeding that value (0.43). With that being said, we do now have an estimation of the profitability margins for the Belgian use cases.

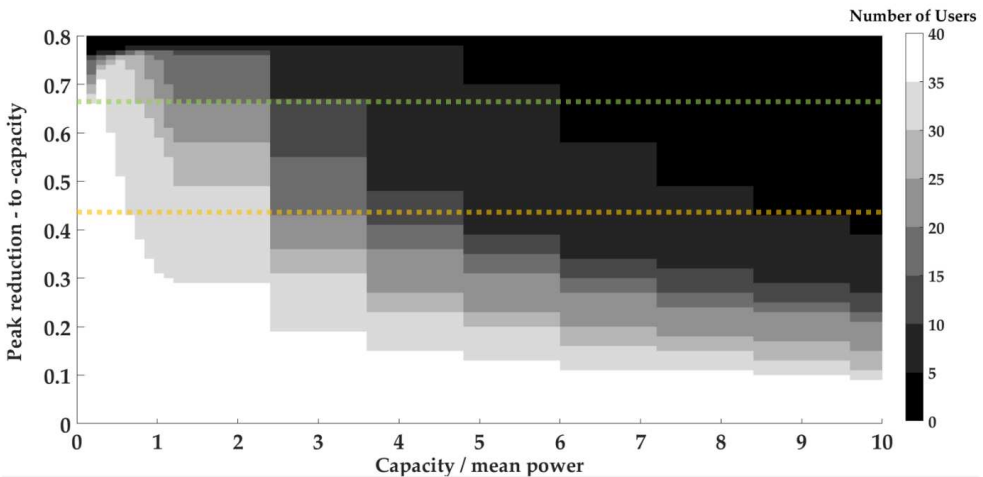


Figure 47: Peak shaving—results of economic feasibility study. At each point $[x, y]$, the color represents the total number of users whose peak reduction-to-capacity exceeds the y value. The yellow and green dashed lines represent the profitability thresholds 0.43

Here, it is worth noting that the battery capex at 500 €/kWh is very realistic for the time being and it is expected to decline further in the coming years [122].³³ As a general conclusion, we can note that given the current electricity prices (fixed, no ToU dependency) and capital expenditures, particularly for Belgium, peak shaving through battery storage seems to be interesting from an economic perspective for several low-voltage enterprises.

5.4 CONCLUSIONS

To summarize briefly what has been done, a model was developed in Matlab/Simulink for peak shaving. The dichotomy method was proposed as an optimization algorithm to find the minimum threshold above which we are 100 % certain that the peak will never be exceeded. The model was tested for 40 low-voltage users with peak demand charge derived from the Belgian grid operator. We introduced five performance metrics to evaluate the simulation results. Furthermore, we gave an example how to interpret the results from economic perspective and explored the profitability of the application in Belgium. Below is a summary of the most important conclusions resulting from our analysis:

- The SoC active time is limited for almost all cases. Even with an over-dimensioned battery (capacity-to-mean power is 10), for seventy-five percent of the users (Q0–Q75), the battery remains idle for at least 80 % for the time. Consequently, peak shaving could possibly be hybridized with other services (e.g., increasing PV self-sufficiency, ancillary services) in order to accelerate the return of investment of the battery storage system. (By adding more revenue streams (stacked services) the payback period of the investment can be reduced.)
- The battery utilization is very low, up to 80 cycles per year in worst case. This number is significantly lower compared to the cycle lifetime of nowadays' lithium-ion batteries. In other words, peak shaving does not impact negatively the battery in terms of cycle degradation. The battery can serve 10 years of peak shaving provided that capacity is appropriately sized to compensate for the unavoidable calendar degradation (here 2 %).
- The consumption increase gets higher with the battery capacity. It lies in the range 0 % to 5 % and does not substantially impact the operating cost of the system.
- From an economic perspective, peak shaving is interesting as a business case for several low-voltage users located in Flanders, Belgium under the real market data (electricity prices, DSO tariff tables and battery quotations) of that time.

³³ To define the battery capex we consulted manufacturers and received offers.

5.5 DISCUSSION

One of our main conclusions is that the battery utilization (SoC active time and number of cycles) is very low for almost all users. Consequently, there seems to be enough potential to let our battery provide additional services during those inactive periods in order to accelerate the payback period of our investment. Which services can be combined and how efficiently this can be done is certainly a topic to be addressed by future research works.

As an initial step, we suggest studying the predictability of the load profile. In our study, we consider the battery to be available for peak shaving 100 % of the time; therefore, there is no need to know in advance when the peak occurs. However, in hybrid applications, time must be allocated appropriately and as a result load prediction plays an important role. To better explain this argument, let us consider two different load profiles derived from our dataset, user A and B ([Figure 48](#) and [Figure 49](#) respectively). Although the battery utilization is in both cases very low (peak occurs rarely), user A is by far more predictable than the user B. For user A, the peak occurrence is dependent on the day, the time of use and the temperature, whereas for user B, there seem to be no clear explanatory variables. Consequently, user B cannot know how to allocate his inactive time to other services; hence, the battery remains underutilized solely reserved for peak shaving. Closing this paragraph, we note that, so far, most research works on battery storage have addressed only single applications. In our view, the concept of hybridization will gain more attention in the coming years as users gradually acquire more incentives to interact with the grid. Next, in the final chapter of the thesis, we present a case study for value stacking where we combine peak shaving with dynamic pricing arbitrage under forecasting uncertainty.

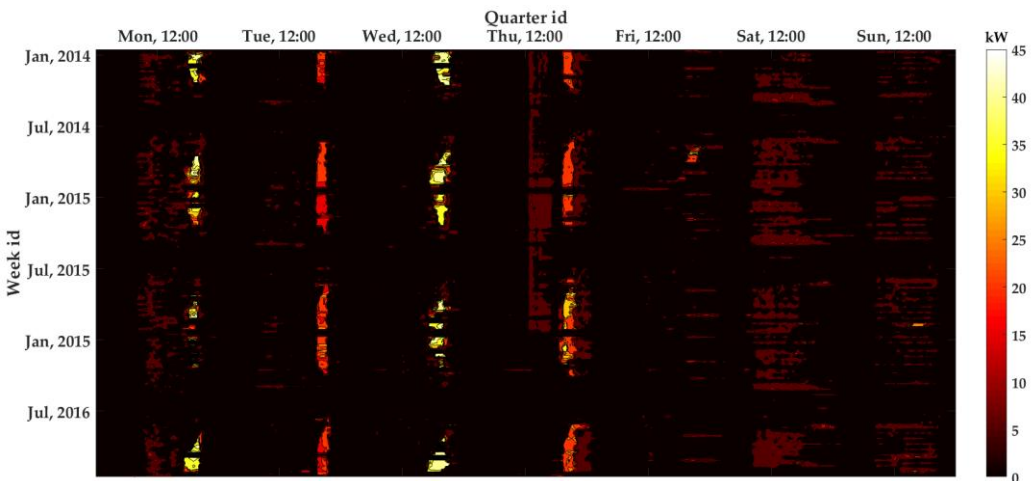


Figure 48: Thermal image, predictable load profile

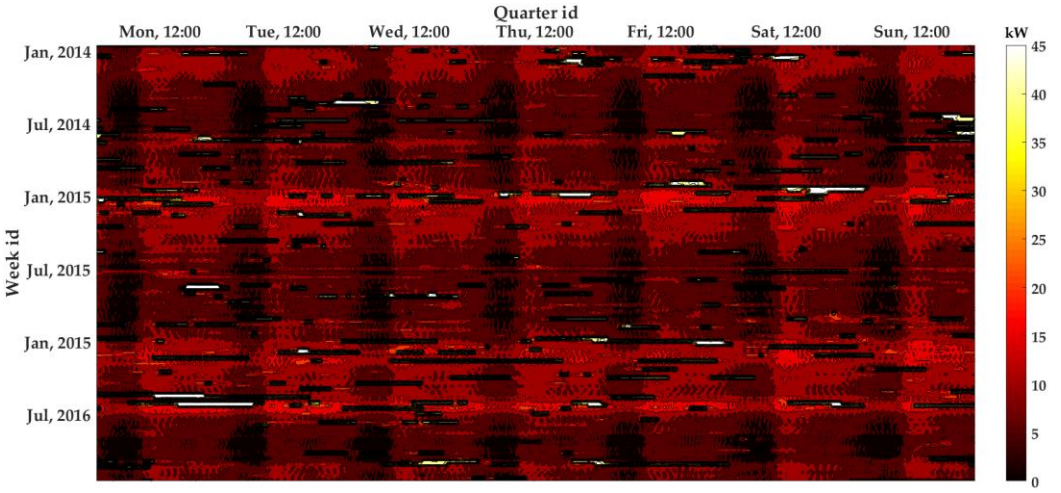


Figure 49: Thermal image, unpredictable load profile

6 Day-ahead pricing arbitrage & peak shaving

6.1 INTRODUCTION

In layman's terms, pricing arbitrage is the practice of buying low and selling high. In the context of electricity market this can refer to different things depending on the end user perspective. As mentioned in Chapter 2, we distinguish three main categories of pricing arbitrage for battery storage: (i) day-ahead, (ii) intraday, (iii) imbalance. Furthermore, we concluded that from those categories, in particular, day-ahead arbitrage through dynamic pricing retail contracts offers the biggest potential for widespread adoption from a prosumer's perspective.

Moreover, in Chapter 5, we developed a methodology for dimensioning the battery storage system in peak shaving applications. We also carried a techno-economic study on 40 enterprise users and proved that peak shaving can be a lucrative investment choice for some of those users. What is more, we showed that in most cases, the battery storage system stays idle for most of the time – underutilized. This fact makes peak shaving very interesting in value stacking applications. Nevertheless, the forecasting uncertainty of the load and power source imposes challenges to the application developer. Before further elaborating on our work, we will give in the next paragraph a brief overview of previous studies found on literature with respect to pricing arbitrage. Afterwards, we will introduce our problem statement and explain which are the main contributions delivered by this work.

The problem of pricing arbitrage optimization through battery storage has been addressed in the past by the research community. Different optimization techniques have been proposed, each one with its advantages and disadvantages. In the simplest case study, the battery storage can be modelled as a linear model. Both the electricity prices and the load profile are assumed deterministic; the user has perfect insight what the load profile will be over the next day. In such case, the optimization objective can be solved with linear programming [123, 124]. Linear programming has the advantage of finding a solution to the problem very fast. Linear programming is interesting in cases where advanced solvers cannot be considered due to time limitations e.g., conducting multiple day-ahead optimizations to estimate the annual cost of the system. Nevertheless, the trade-off here is that very often we oversimplify the problem. In most cases, the power flow model cannot be linearized and due to the inherent forecasting uncertainty of various system variables (e.g., load, power source, prices) linear programming is not suitable. Dynamic programming is another category of optimization algorithms that can be used to tackle the problem of pricing arbitrage in non-linear environments under forecasting uncertainty. Here, the problem usually is formulated as a finite Markov Decision Process (MDP). The optimization horizon is split into a set of discrete time steps [00:00, 01:00,

..., 23:00, 24:00]. At each time step, the battery controller takes a decision to (dis)charge the battery based on the current state input (e.g., $S_t = (S_{t_load}, S_{t_pv}, S_{t_soc})$). The MDP is solved through recursive backward induction starting from the last time step t , then calculating the value function (accumulated expected reward) at $t-1$ then moving to $t-1$ etc. Dynamic programming algorithms can be divided in two categories depending on the sampling technique used for exploring the state space: (i) discretised sampling, (ii) continuous sampling. In (i), the state space is discrete and therefore there is a finite total number of states [125, 126]. Consequently, in (i) the value function can be accurately calculated through full exploration of the state space. To calculate the value function a table is used; at each state we store the respective cumulative reward separately. The disadvantage of discretised sampling is that it fails to scale up efficiently in complex problems with large multidimensional states. In (ii), the state space is continuous, thus there is an infinite number of states to be explored and the use of tables is not feasible. In such situations, most research works follow a value function approximation technique [127-132]. A model is trained to fit the state-action space against the cumulative reward. Although such techniques typically result in suboptimal solutions, the model can still be very representative given sufficient sampling and a good function approximator.

In this study, we consider forecasting uncertainty for the load and power source forecast. Furthermore, both the load and power source profiles are modelled as continuous variables. Consequently, our problem falls under the category of dynamic programming with continuous sampling on the state space. Based on our literature review and after experimenting with different techniques we concluded to focus on Reinforcement Learning (RL) algorithms and in particular the Deep Q Network (DQN) architecture. Next, we summarize relevant previous works on the DQN architecture for applications in pricing arbitrage problems through battery storage.

In general, we note as a conclusion that there is not a fixed environment setting (e.g., system topology, optimization horizon, uncertainty on data inputs) to draw clear comparisons between the different studies. Regarding the system topology we distinguish two types of studies: (i) single end user systems [129, 130, 133], (ii) microgrids – community level systems [131, 134]. With respect to the algorithm used, over the time different variants have been introduced (e.g., Dueling DQN, Double DQN, Categorical DQN, Noisy Net DQN, Multistep DQN and Replay DQN) to mitigate the shortcomings of the standard DQN architecture [129, 130, 134]. In [129], a BESS was used for reducing the electricity bill in a datacenter with dynamic pricing contract. The researchers investigated different variants of the DQN architecture: (i) DQN, (ii) DQN dueling, (iii) Double DQN, (iv) Replay DQN. Experiments showed that Replay DQN

outperformed all other algorithms in terms of total annual revenue in different case studies having as input electricity prices from USA and Beijing. In [131], a BESS is installed at community level to reduce the total operating cost of a microgrid in grid-connected and island mode. The researchers argue that Double DQN is a better choice compared to the standard DQN architecture especially in very noisy environments with multidimensional state spaces; by decoupling the action selection from the action evaluation in separate networks, Double DQN is less prone to the phenomenon known as maximization bias which results in overestimating the Q values. In [130], the researchers propose a Noisy Net DQN algorithm for solving the pricing arbitrage problem based on wholesale electricity prices in UK. Here, the forecasting uncertainty is exclusively on the electricity price. A combined Convolutional Neural Net (CNN) and Long Short Term Memory (LSTM) is used to forecast the electricity price. No load or power sources are considered. The study puts in comparison different algorithms: (i) Mixed Integer Linear Programming (MILP), (ii) standard DQN, (iii) Dueling DQN and (iv) proposed Noisy Net DQN. It is concluded that Noisy Net DQN outperforms all other algorithms. In [134], a BESS is used to reduce the total operating cost of a microgrid including PV and wind power sources. The researchers propose the Rainbow algorithm integrating characteristics from other popular DQN variants (i.e., standard DQN, Dueling DQN, Double DQN, Categorical DQN, Noisy Net DQN, Multistep DQN and Replay DQN). They consider forecasting uncertainty on the electricity price and load. The results showed that the proposed algorithm clearly outperforms all other variants mentioned above.

Regarding the time resolution of the Markov Decision Process (MDP), most studies typically consider hourly time steps [130, 131, 133, 134]; every hour the agent takes a single action given the latest input from the state space (e.g., price, SoC, load and/or power source yield). The time resolution is the same with that of the electricity price based on the day ahead market; in most countries the price is cleared at hourly resolution. In all studies, the action space is modelled as a discrete set of (dis)charging power commands (e.g., full power charge, full power discharge, idle). The battery controller will follow a constant power reference during the hour. The number of actions varies within 3 – 9 depending on how the battery's power capacity is discretized (e.g., a five action space reflects to $[-P_{\max}, -0.5P_{\max}, 0, +0.5P_{\max}, +P_{\max}]$). On the reward function, the basic approach is considering only the energy cost (e.g., Price x P_{BESS} x 1h). Another approach, like in the context of microgrid applications, is including also a penalty term to prevent the battery from reaching critical SoC levels [131]. Finally, a more advanced version of the reward function would require also modelling the battery cycle degradation as a cost [130].

Conclusions and relation to present work

Next, we summarize important conclusions drawn from the literature review and explain how these are related to the present research work:

- **There is no best algorithm:** From our literature review we conclude that there is no clear consensus which algorithm is best suitable in the context of pricing arbitrage applications. The choice depends a lot not only on the specific environment settings but also on the individual preferences of those conducting the study.
 - Present study: In the present study, we use the standard DQN architecture to solve a problem that has not been addressed by previous works. As shown, the proposed algorithm succeeds in solving the optimization problem given sufficient exploration of the state space and low forecasting uncertainty on the load and power source profiles.
- **Peak shaving is out of scope:** None of the studies mentioned above addressed peak shaving. All studies have treated pricing arbitrage as a single application. The methodologies presented so far do not suffice to provide a solution to our problem.
 - Present study: To the best of our knowledge, this is one of the very few (if not the first) to consider peak shaving combined with pricing arbitrage. Compared to previous works on the DQN architecture, here, the presence of a peak threshold constraint necessitates a different design approach regarding the reward function, state and action space.
- **The MDP is directly coupled to the power flow simulation:** A major issue, never noted before by previous works, is that the power flow simulation is directly coupled to the MDP. Since both the MDP and the power flow simulation have the same time resolution there is always a trade-off to be made; sacrificing accuracy of the power flow model to achieve a more efficient learning process. Another problem is that the algorithm is not suitable in the context of “value stacking” combining pricing arbitrage with other applications (here peak shaving). Analytic explanation is given in Section [6.2.1](#) (see Action space).
 - Present study: In this study, we construct the state and action space in such way that allows us to decouple the MDP from the power flow simulation. By abstracting the action space in control strategy decisions (instead of constant (dis)charging power commands) we maintain an hourly step for the MDP while the power flow simulation works at 15 min. This practice is a fundamental requirement for deploying the algorithm in a real time peak shaving application.

Research core, key questions & contributions

The system topology is shown in [Figure 50](#). Behind the meter the user has a battery, the load and a renewable energy power source (usually PV). The user has a meter (e.g., digital meter or AMR) recording his energy offtake and injection at 15 minutes resolution. Every year, the user pays a fee to the DSO based on his peak demand; this is the highest 15 minute offtake (kW) measured by the meter over the past 12 months. To avoid high costs imposed by the DSO, the user has deployed a battery for peak shaving. The battery has to be discharged whenever the user's load exceeds a certain peak threshold. Furthermore, the user has a dynamic pricing contract with an energy supplier following the Belpex index. This means that each hour of the day (8760 hours per year) the user has a different electricity price for his offtake and injection. At each hour, the user pays his energy supplier if he offtakes energy from the grid or he is paid by the energy supplier if he injects energy to the grid. Every day (D-1), the energy supplier publishes the electricity prices (i.e. 24 prices for offtake, 24 prices for injection) for the next day (D). The user has installed the battery to take advantage from two revenue streams: (i) pricing arbitrage, (ii) peak shaving. The problem statement is expressed as: How do I (dis)charge the battery during the day to maximize the total daily profit without violating the peak threshold constraint ?

Next, we present the key research questions addressed in this work including the delivered contributions:

- Which algorithm can be used to solve the combined problem of pricing arbitrage with peak shaving?
In Section [6.2](#) we present the methodology used to solve the optimization problem. The proposed algorithm is based on the standard DQN architecture trained through backward induction.
- Is there a solution to the trade-off: efficient training vs power flow model accuracy ?
A novel design approach (see Section [6.2](#)) is presented showing how to decouple the MDP from the power flow simulation. This allows to achieve an efficient learning process while not sacrificing the accuracy of the power flow model
- How do I construct the reward function ?
This is addressed in Section [6.2](#). The reward function comprises three components: (i) energy cost, (ii) battery degradation cost and (iii) peak punishment.
- How does the algorithm perform under different scenarios of forecasting uncertainty ?
In Section [6.3](#), we present the results from a sensitivity analysis on the forecasting uncertainty of the combined load and power source (here PV) forecast.

- Are there any suggestions to improve the reliability of the system under bad forecast days ?
This question is addressed in Section [6.3](#) and [6.4](#).

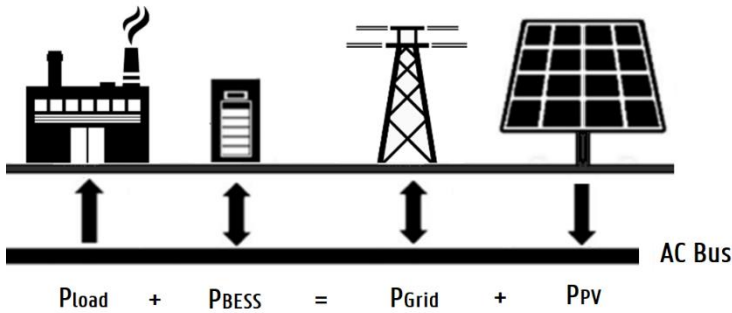


Figure 50: System topology

The rest of the chapter is organized as follows: Section [6.2](#) presents the methodology. Next, section [6.3](#) provides results from a sensitivity analysis considering different scenarios of forecasting uncertainty (PV and load). Finally section [6.4](#) summarizes important conclusions and key notes to be addressed in future works.

6.2 METHODOLOGY

6.2.1 Introduction to Markov Decision Process (MDP)

To begin with, our optimization objective is applied over a time horizon of 24 hours from (day D, 00:00 h) until (day D+1, 00:00 h). We divide our time horizon in 24 time steps as [00:00, 01:00, 02:00, ..., 23:00]. At each time step, the battery controller has to choose among a set of actions (e.g., charge to 100 % SoC, discharge to 50 % SoC, turn off) given its current SoC and the latest forecast for the load and power source profile. Our problem can be expressed as a finite Markov decision process (MDP). An MDP is a tuple (S, A, P_a, R_a) where:

- S is a set of states called the state space,
- A is a set of actions called the action space
- $P_a(s, s') = \Pr(S_{t+1} = s' \mid S_t = s, A_t = a)$ is the probability that action a in state s at time step t will lead to state s' at time step $t+1$.
- $R_a(s, s')$ is the expected immediate reward received after transitioning from state s to state s' due to action a .

A policy function π is a mapping from state space (S) to action space (A). The objective is to choose a policy π that will maximize the cumulative reward received over the time horizon of the process (24 hours in our case):

$$E \left[\sum_{t=0}^{24} \gamma^t R_{A_t} (S_t, S_{t+1}) \right] \quad 6-1$$

where

- γ is a discount factor typically $0 < \gamma < 1$
- $A_t = \pi(S_t)$ the action chosen by the policy at time step t and state S_t

State space

[Figure 51](#) illustrates the MDP. We assume that we have at our disposal two stochastic forecasting models: (i) one for the load and (ii) one for the power source (PV) profile. The forecast data is available the day before the start of the optimization horizon. The forecast horizon is 24 hours ahead at 15 min resolution. Consequently, there are totally 96 forecasted quarters, 4 quarters per time step of the MDP. The forecasted output is expressed as follows:

$$P_{\text{forecast}} = P_{\text{load}_i} - P_{\text{pv}_i} \quad 6-2$$

where

- P_{load_i} is the continuous random variable of the load power (kW) at quarter q_i . The load power is sampled according to f_{q_i} , the probability density function of the load power at quarter q_i .
- P_{pv_i} is the continuous random variable of the PV power (kW) at quarter q_i . The load power is sampled according to g_{q_i} , the probability density function of the pv power at quarter q_i .
- i is the quarter index ranging within $[0, 1, \dots, 95]$.

At each time step t the state is a five dimensional continuous variable:

$$S_t = (\text{SoC}_t, q_{t-1,m=0}, q_{t-1,m=1}, q_{t-1,m=2}, q_{t-1,m=3}) \quad 6-3$$

where

- SoC_t is the state of charge of the battery $0 < \text{SoC}_t < 100$ at the start of the time slot $[t, t + 1]$
- $q_{t-1,m}$ is the real power measurement of $P_{\text{load}} - P_{\text{pv}}$ in quarter m of time step $t - 1$.

- m is the quarter index $[0, 1, 2, 3]$ per time step

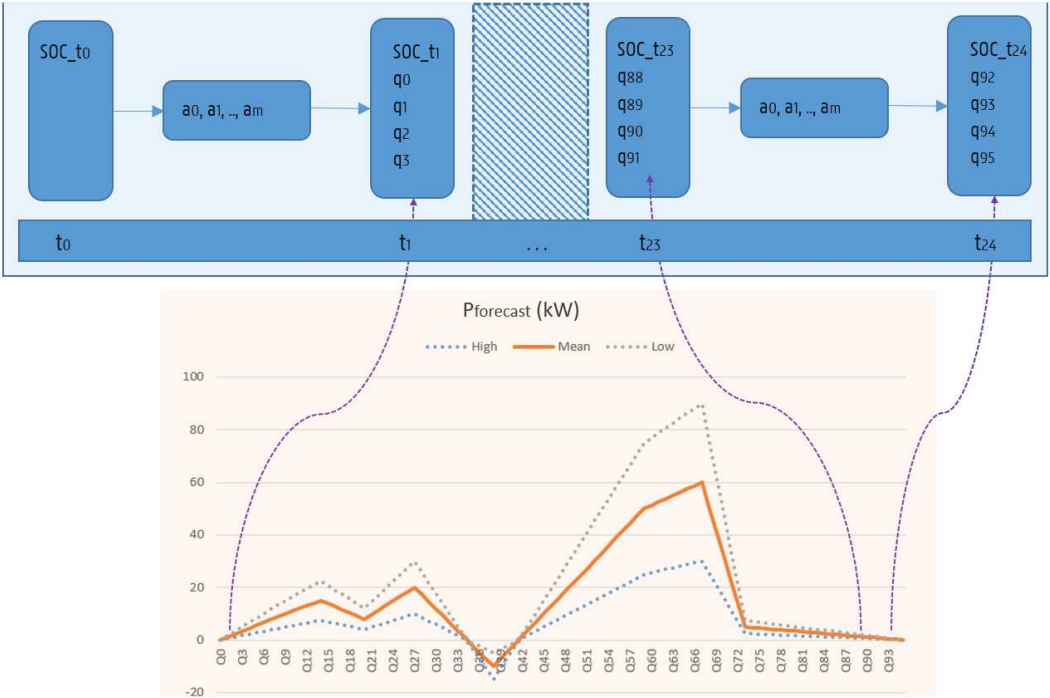


Figure 51: MDP in day-ahead optimization

Action space

Regarding the action space, at each time step t we consider a set of discrete actions (a_0, a_1, \dots, a_m) . Here, we keep our approach as generic as possible. As mentioned in the introduction section, a major issue of all previous studies is that the MDP is coupled to the power flow simulation; the action space is mapped directly to constant (dis)charging power commands. This approach results in two problems. First, the algorithm is exclusively applicable to pricing arbitrage application. Second, there is always a trade-off to be made; sacrificing the power flow model accuracy against improving the learning efficiency during the training the algorithm. We address those problems in the next two paragraphs respectively.

Regarding the first problem, by mapping the action space directly to (dis)charging power commands we restrict the generalizability of the algorithm for other than pricing arbitrage applications. In the context of “value stacking”, we need to combine different applications together; each application has its own controller. A controller that works at hourly resolution (a fixed power command during the entire hour) may suffice for a pricing arbitrage application but it is undoubtedly not suitable for a peak shaving application. For peak shaving applications,

the controller needs to output commands in real time (sec – min) during the hourly quarter (15 min). To check whether or not the peak threshold is exceeded, the controller calculates continuously the running average of the load power within the hourly quarter. In other words, the power commands are calculated in real time, therefore there is no way to pre-determine these in a day-ahead optimization. In another example, if ancillary services (e.g., aFRR) were considered, the control of the battery is even more stochastic; the power commands are not only calculated in real time but they are also specified by the TSO; the battery owner has no control of the system during the time slot of the reserved capacity.

With respect to the second problem, on the one hand, for a given optimization horizon (usually 24 – 48 h in pricing arbitrage problems) the learning process becomes less efficient as we increase the resolution of the MDP (number of time steps increases to reach terminal state); for instance given a 24 h horizon, a 15 min resolution (96 time steps) is more difficult to train compared to 1 h (24 time steps). On the other hand, as explained in Chapter 4, the accuracy of the power flow simulation gets worse as we decrease the time resolution; we argued that power flow simulations at hourly resolutions (the great majority of DQN studies reviewed above) can result in significant errors in the context of renewable energy applications.

To tackle the above problems, we need a different design approach. In this study, the action space is mapped to a discrete set of control strategies. By abstracting the action space to control strategies (instead of using fixed power commands) we decouple the MDP from the power flow simulation. Consequently, this practice enables us to deploy the best for different (other than pricing arbitrage) applications and also maintain a decent accuracy on the power flow simulation (15 min resolution). The environment for our reinforcement learning algorithm is the power flow model developed in Chapter 5. We define five actions as mentioned in [Table 14](#). Every hour the agent takes a single control strategy decision; this is fixed during the 60 min time slot from t to $t+1$. We recall that the time resolution of the power flow simulation is 15 min and consequently, the same decision applies for all 4 quarters ($q_{m=0}, q_{m=1}, q_{m=2}, q_{m=3}$) of the hour. The purpose of actions a_0 and a_4 is mainly to facilitate the pricing arbitrage application. Moreover, we need another action, a_3 , for recovering the SoC to its initial value ($SoC_{t=0} = SoC_{t=24}$). We assume that the SoC at the start of the day is 50 %. Furthermore, we need a_1 to facilitate the peak shaving application. Finally, we define action a_2 for turning off the BESS to eliminate the energy losses in situations where the battery stays idle doing nothing.

Table 14: Action space

Action id	Name	Description
a_0	Discharge to 10 % SoC	The controller will discharge the battery during the hour as fast as possible (constrained by the C-rate) until the SoC reaches 10 %.
a_1	Peak threshold	The controller charges (discharges) the battery in function of the power deficit (surplus) $P_{BESS} = P_{Threshold} - (P_{load} - P_{pv})$. Here, charging corresponds to the positive sign ($P_{BESS} > 0$) and discharging to negative ($P_{BESS} < 0$).
a_2	Turn off	The BESS is turned off. This is useful for eliminating the energy losses present when the BESS is in idle state.
a_3	(Dis)charge to 50 % SoC	The controller will charge or discharge the battery during the hour as fast as possible (constrained by the C-rate and the peak threshold) until the SoC reaches 50 %.
a_4	Charge to 90 % SoC	The controller will charge the battery during the hour as fast as possible (constrained by the C-rate and the peak threshold) until the SoC reaches 90 %.

Regarding the reward, at each time step t the following equations apply:

$$R_t = E_t + P_t + D_t \quad 6-4$$

$$E_t = 0.25 \cdot \sum_{m=0}^{m=3} (P_{net\ t,m}^{inj} \cdot Pr_t^{inj} - (C_{DSO}^{off} + Pr_t^{off}) \cdot P_{net\ t,m}^{off}) \quad 6-5$$

$$P_t = -(\max(P_{net\ t,m=0}^{off}, P_{net\ t,m=3}^{off}, P_{peak\ thres}) - P_{peak\ thres}) \cdot C_{punish} \quad 6-6$$

$$D_t = -C_{BESS} \cdot \min(\text{SoC}_{t+1} - \text{SoC}_t, 0) \quad 6-7$$

where

- E_t is the cost (remuneration) paid to (by) the energy supplier for the energy offtake (injection). This term also includes the cost paid to the DSO for the energy offtake
- P_t is the punishment accounted for exceeding the peak threshold if peak shaving is applicable. The cost is proportional to the power surplus.
- D_t is the cost accounted for the battery cycle degradation. This is a linear function of the battery Depth of Discharge (DoD). For more advanced degradation models, we refer to [126].

- $P_{\text{net } t,m}^{\text{off (inj)}}$ is the power of the grid at quarter m i.e. the real power measurement recorded by the meter. This is equal to $P_{\text{inv } t,m} + P_{\text{load } t,m} - P_{\text{pv } t,m}$ where $P_{\text{inv } t,m}$ is the power of the inverter output at the AC side of the battery storage system. When the power is positive (negative) the meter records an energy offtake (injection).
- $P_r^{\text{off (inj)}}$ is the electricity price applied by the energy supplier for the energy offtake (injection).

6.2.2 Solution – Deep Q network

At the core of the optimization objective we have the Bellman equation. The goal is to solve this equation for each time step t of the MDP. At each time step t , knowing our current state S_t (i.e. historic 15 min power measurements during the (hourly) time slot $[t-1, t]$ and SoC at time step t), we select a certain action A_t (i.e. control strategy) and end up in a random state S_{t+1} (15 min power measurements during the (hourly) time slot $[t, t+1]$ and SoC at time step $t+1$).

$$Q(S_t, A_t) = E[R_t(S_t, A_t, S_{t+1}) + \gamma \cdot \max_A Q(S_{t+1}, A_{t+1})] \quad 6-8$$

where

- $Q(S_t, A_t)$ is the state-action value function at time step t . This is the expected cumulative reward given state S_t and action A_t .
- γ is a discount factor within $0 < \gamma < 1$
- $R_t(S_t, A_t, S_{t+1})$ is reward received after taking action A_t and transitioning from S_t to S_{t+1} .

The Bellman equation can be solved recursively through backward induction. We start from the terminal time step and move one step backward $[t_{24}, t_{23}, \dots, t_0]$ until we reach the start of the MDP. The value function $Q(S_t, A_t)$ can be approximated by an artificial neural network as shown in [Figure 52](#). The neural network used in this study is a feed forward network. For each time step we use a different network. Each neural network receives as input the five dimensional (continuous) state variable and outputs the Q value per action. Once the network has been trained sufficiently over the state-action space, the calculation of the term $\max_A Q(S_{t+1}, A_{t+1})$ is straightforward; given the state input S_{t+1} the network returns a Q tuple $(Q_{a_0}, Q_{a_1}, \dots, Q_{a_m})$ by action and we take the max of it. Next, in [Table 15](#) we present the pseudocode of the day-ahead optimization algorithm written in Python.

Table 15: Pseudocode of Day-Ahead optimization problem

```

# Initialize variables and properties
bess = Bess(efficiency=0.9, Sinv=100, capacity=50, crate=1) # initialize bess
actionSpace = {0: 'Charge to 90%', 1: 'Discharge to 0%', 2: 'Turn Off', 3: 'Peak shaving'} # set action space
actionSize = len(actionSpace)
date = '2024-02-05' # select date
reward = Reward(getElectricityPrices(date), bess) # initialize reward
forecast = Forecast(date) # get forecast as an array (24 hours x 4 quarters per hour) of tuples (mean, std)
Nsamples = 10000 # set how many state samples to collect per time step
nets = emptyArray(24) # initialize empty array of neural nets, one for each time step
timesteps = [t for t in range(23, -1, -1)] # build a list of 24 steps [23, 22, ..., 1, 0]

# Optimize
for t in timesteps:
    # Collect samples from state space at t and t+1
    St = {'soc': None, 'Q_m0': None, 'Q_m1': None, 'Q_m2': None, 'Q_m3': None} # initialize state dictionary at t
    St_plus1 = {'soc': None, 'Q_m0': None, 'Q_m1': None, 'Q_m2': None, 'Q_m3': None} # initialize state dictionary at
    t+1
    St['soc'] = collectSamples(Nsamples, 'uniform', [0, 100])
    for S, j enumerate([St, St_plus1]): # loop over the state dictionaries
        for m in range(4): # loop over the quarter index
            state = 'Qm_' + m
            (mean, std) = forecast[t-j][m]
            s = collectSamples(Nsamples, 'normal', mean, std) # returns a vector of (Nsamples x 1)
            samples
            samples = concatenate([s]*actionSize, axis = 1) # makes actionSize copies, one for each
            action
            S[state] = reshape(samples, (-1, 1)) # reshape to vector and update state dictionary

    # collect rewards, calculate SoCt+1 and update state dictionary at t+1
    Rt = emptyArray(Nsamples * actionSize)
    St_plus1['soc'] = emptyArray(Nsamples * actionSize)
    for i in range(len(Rt)):
        (r, SoC_plus1) = reward.calculateReward(St, St_plus1, actionSpace)
        Rt[i] = r
        St_plus1['soc'][i] = SoC_plus1

    # Initialize neural net
    If t==23: # if this is the last time step
        net = neuralNet() # initialize an empty neural net
        QTarget = Rt # build q values targets
    else:
        net = copy(nets[t+1]) # initialize neural net by copying parameters from previous net
        QTarget = Rt + nets[t+1].getMaxQ(St_plus1) # build q value targets

    # Start training
    net.train(St, QTarget) # train network to minimize the Mean Square Error

```

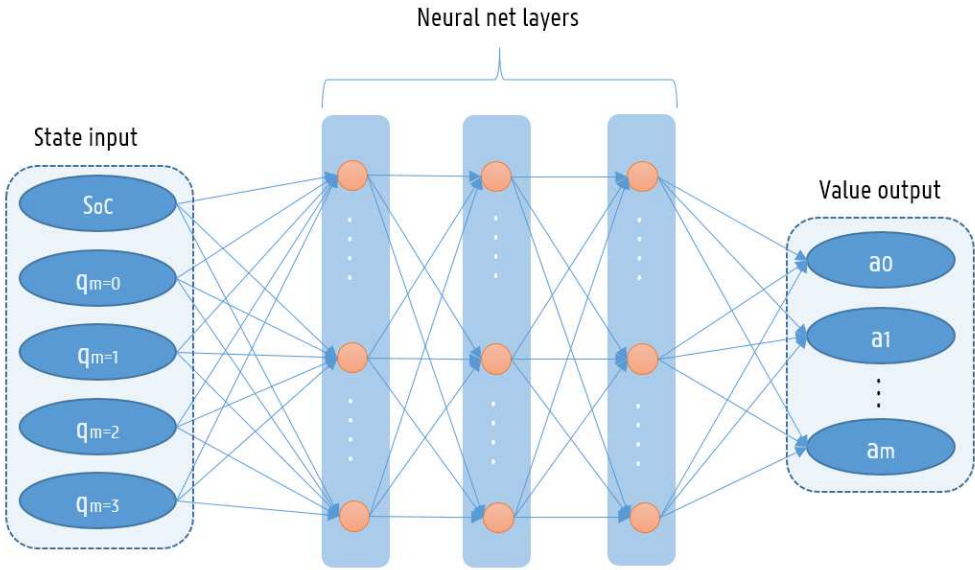


Figure 52: Feed Forward Neural Network

6.3 RESULTS

In this section, we put the algorithm to the test. We conduct a sensitivity analysis investigating the impact of the forecasting uncertainty on the performance of the model. Let us first introduce the reader to the environment settings of our experiment. We have an enterprise user located in Flanders, Belgium connected to the low voltage grid. The user has a dynamic pricing contract with an energy supplier. The user is interested to deploy a battery storage system for pricing arbitrage and peak shaving. In [Figure 53](#), we give an example how the user's load profile looks like over a weekly time period at 15 min resolution.

The power profile is mainly a function of two variables: (i) day of the week, (ii) time of use within the day. It has a peak usually early in the morning between 05:00 and 10:00 a.m. The highest annual peak is 28 kW. The user has installed a battery energy storage system (BESS) in order to reduce his peak demand to 20 kW. The specifications of the battery storage system are displayed in [Table 16](#).³⁴ The BESS has been dimensioned for peak shaving using the methodology developed in Chapter 5.

³⁴ See chapter 5 for analytic information regarding the battery cell properties and DC/AC efficiency curve.

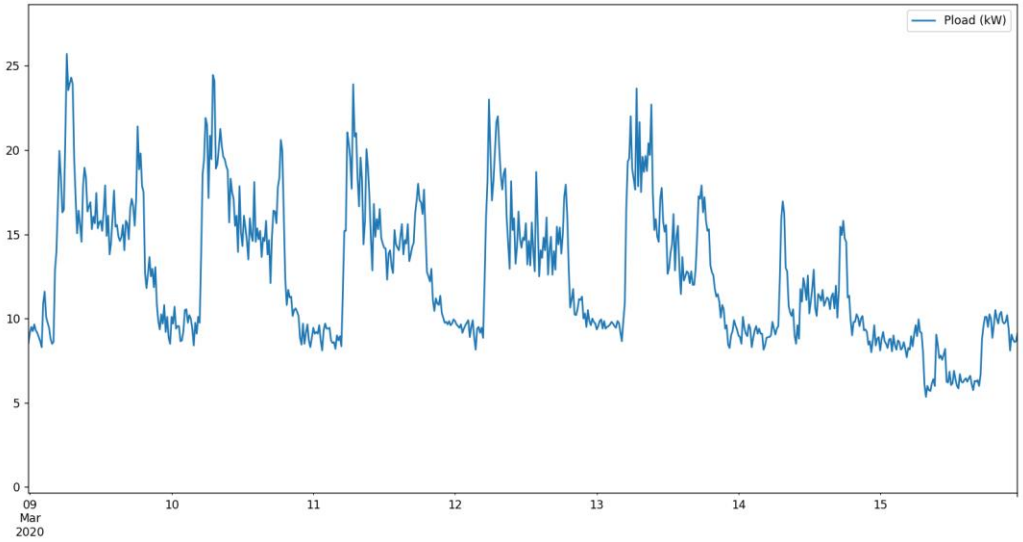


Figure 53: Weekly load profile

Table 16: BESS specifications

Characteristics	Specifications
Chemistry	LiFePO ₄
Battery capacity	25 kWh
C-rate	1
DC/AC converter power	25 kVA
Cycles	8000 at 80 % DoD
CAPEX	5000 €

Regarding the reward function (see Equations [6-4](#), [6-5](#), [6-6](#), [6-7](#)) C_{DSO}^{off} is 0.008 €/kWh. This constant has been calculated based on the electricity tariff structure of Flanders as of 2023, given the location and type of connection of the user. We set the peak punishment constant C_{punish} at 1 €/kW. In general, the peak punishment constant must be big enough so that the peak punishment term P_t can persist the reward against the energy compensation term E_t at all times. A very high value however would impact negatively the training of the function approximator and therefore it should be avoided. All experiments were done considering the same date 2023-07-03. We selected this date because it has a good potential for the pricing arbitrage application due to the high variability of the day-ahead price. Finally the degradation

constant C_{BESS} was set at 0.0078 € / %. To calculate this constant we simply divide the cost of the system (capex) by the equivalent number of battery cycles ($8000 \times 0.8 / 100$). With respect to the neural network, at each time step we initialize a feed forward network (see [Figure 52](#)) with 3 layers where each layer has 50 neurons. All neurons are relu (rectified linear unit) functions. The optimization method used for the training of the neural network is Adam [135]. We employ random mini-batch training at 5 % of the training samples and we use MSE (Mean Square Error) as the loss function. All experiments are programmed in Python 3.8. Pytorch is used for the implementation and training of the neural networks.

Scenario A – Deterministic load, no PV: In this scenario we assume that we have perfect insight of the load profile over the optimization horizon. We know what the load will be for each and every quarter of the next day. This assumption does not apply in most use cases due to the inherent stochasticity of the load. Nevertheless, there are still use cases where the load can be predicted accurately e.g., many factories that plan their production process in advance exhibit high correlations on the day of the week and time of use within the day. What is more, we assume that there is no PV yield on this date. Note that the dimensioning of the BESS for peak shaving is done without consideration of the PV yield in order to account for worst case scenarios. Scenario A serves as a benchmark because it provides the best solution. [Figure 54](#) illustrates the optimization output. The electricity price curve (axis 3 | Belpex) presents two pairs of valley–peaks. The SoC trajectory is illustrated with the blue curve (axis 2 | Bess SoC). The battery is charged during the valleys and it is discharged when peaks occur. The green curve (axis1 | Pnet with bess) indicates the grid power. As shown, the peak threshold constraint is never violated.

Scenario B – Probabilistic load, no PV: In this scenario we consider a real forecasting model of the load. To build the forecasting model, we trained an artificial neural network³⁵ on historic data from 2020 – 2023. Also in scenario B, we consider no PV yield. Scenario B serves as real use case; no perfect insight of the load is available. The performance of the algorithm is subject to the accuracy of the forecasting model. [Figure 55](#) illustrates the optimization output. The power forecast ($P_{\text{load}} - P_{\text{pv}}$) is given by the three quantile curves (Q25, Q50, Q75) while the power target is given by the dashed red curve (axis 1 | Pnet no bess). Also here, the peak threshold is always respected (see green curve). However, due to the forecasting uncertainty the battery controller decides to give priority to the peak shaving application during the second valley of the price curve (10:00 – 18:00).

³⁵ We trained a feed forward network with 2 layers of 40 neurons (sigmoid functions), Adam optimizer and MSE as the loss function

Scenario C – Probabilistic load and PV: In this scenario, we consider also the power profile generated by the PV installation. The PV source can generate up to 10 kW of peak power over the year. We developed a forecasting model for the PV power profile based on historic data and weather forecast of the next day. We employ the same model architecture both for the load and PV forecast based on artificial neural networks. The optimization output is given in [Figure 56](#). Compared to scenario B, we clearly see that the presence of PV has decreased the grid power profile. In other words, having PV in general reduces the risk of exceeding the peak threshold and therefore the amount of energy allocated for the pricing arbitrage application is bigger. Nevertheless, having PV has the disadvantage that we need to develop an additional forecasting model and unavoidably the total forecasting uncertainty is higher compared to scenario B.

Scenario D – Probabilistic load and PV, bad forecast: In scenario D, we maintain the same topology as in scenario C (load and PV). However, we assume that for some reason the forecast models failed to deliver an accurate prediction. This can be due to several reasons e.g., fast intermittent clouds creating power spikes in sub-hourly resolution, errors on calendar plan inputs impacting the load forecast. As can be seen in [Figure 57](#), this time the algorithm failed to respect the peak threshold. Our forecast underestimated the grid power offtake. Scenario D can have catastrophic effects on our value stacking application; missing the peak on a single day would punish the total cost over an annual time period. The question is how big is the likelihood of having such bad forecasts? The only way to guarantee 100 % that the peak threshold is respected all the time is to put a circuit breaker behind the meter (e.g., a number of non-critical loads are automatically disconnected whenever the peak threshold is exceeded). This could be acceptable depending on the user and provided that the occurrence of such bad days is very rare. Here, we note once more (see Chapter 5) the DSO in Flanders, Belgium calculates the user's peak power as the highest hourly-quarter (15 min) offtake power (kW) over the past 12 months. This peak demand cost is expressed in €/kW/year (e.g., 87 – 130 €/kW/year, see Chapter 5 → Section [5.3.2](#)). To give an idea how a bad forecast day impacts our revenue, considering a peak demand cost at 100 €/kW/year, in this example, we missed the peak approximately by 3 kW (20 → 23 kW) which reflects to 300 €/year. To compensate this amount from pricing arbitrage with our 25 kWh battery, considering a very optimistic Belpex valley-peak at 0.1 €/kWh per day, it would take at least 120 days (1 full discharging cycle per day ³⁶). It is obvious that the revenue stream from peak shaving (yearly cycle) is much higher

³⁶ 120 days = $\frac{300 \text{ €}}{25 \text{ kWh} \cdot 0.1 \frac{\text{€}}{\text{kWh-day}}}$, at 100 % DoD, ignoring efficiency losses.

than the revenue stream from pricing arbitrage (daily cycle) and consequently peak shaving must be prioritized when co-optimizing those two together.

Scenario E – Probabilistic load, increased forecasting uncertainty: In the last scenario, we give an example of a load forecast with increased uncertainty. In this case there is no PV. This is a virtual forecast profile created from the real target sampling from a ‘normal’ distribution where the tuple (mean, std) corresponds to $(P_{load} - P_{pv}, 10 \text{ kW})$. [Figure 58](#) shows the output of the optimization algorithm. As can be seen, the battery controller prioritizes peak shaving against pricing arbitrage and the peak threshold is never violated. Scenario E is interesting from the point of view that in situations with high uncertainty the battery controller, under the proposed algorithm, will always prioritize peak shaving. As we overestimate the grid power, relatively to the peak threshold, the chance to allocate the battery capacity for peak shaving grows also. As conclusion, we note that in situations where the user is not sure what the load (and PV) power will be, it is suggested to adjust in a way the forecast to overestimate the power profile and consequently prioritize the peak shaving application. Nevertheless, in any case, with or without a good forecast, the circuit breaker must always have the last word to guarantee 100 % compliance with the peak threshold.

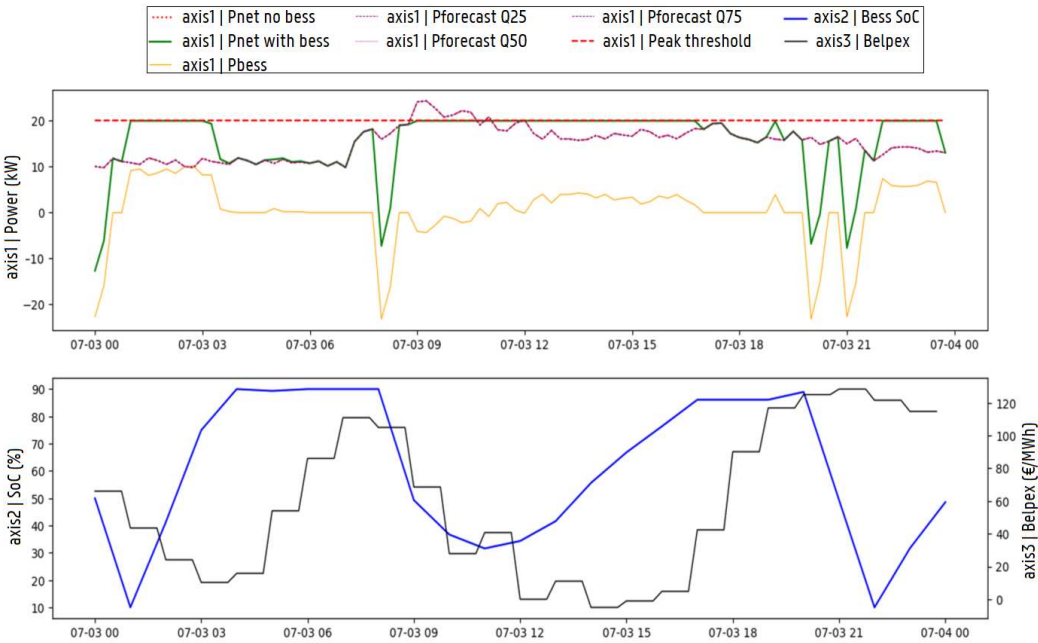


Figure 54: Scenario A - optimization output

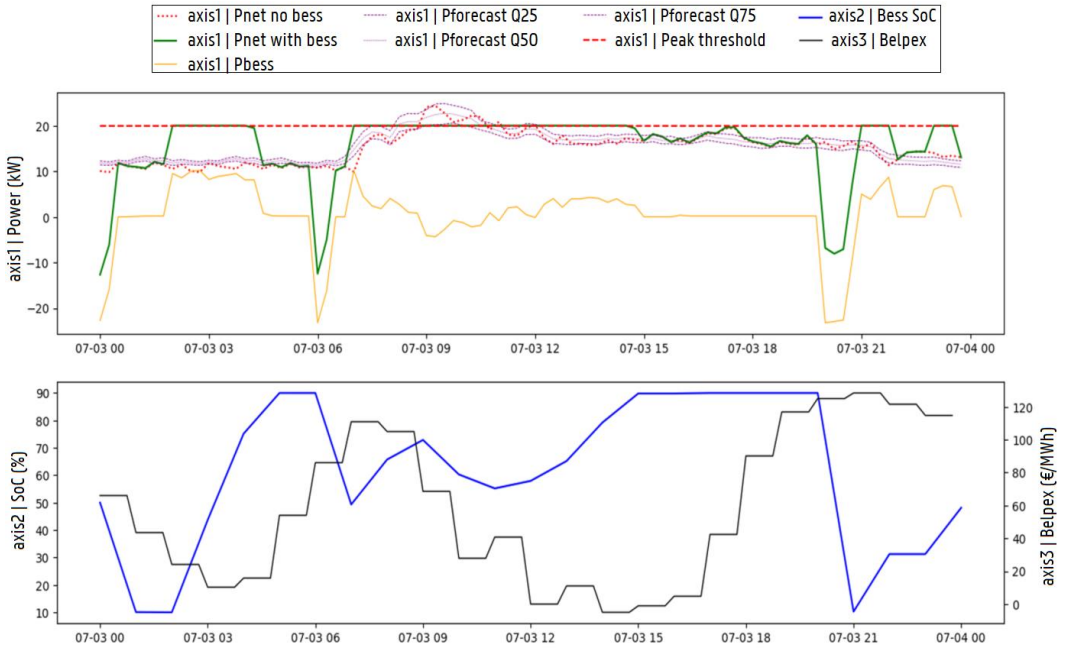


Figure 55: Scenario B – optimization output

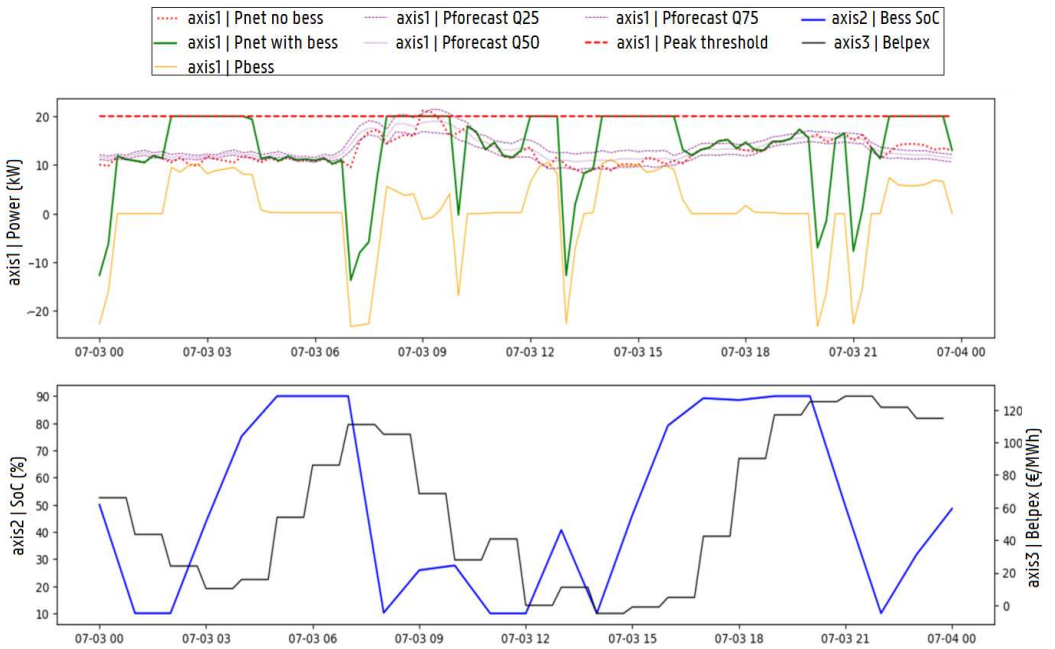


Figure 56: Scenario C – optimization output

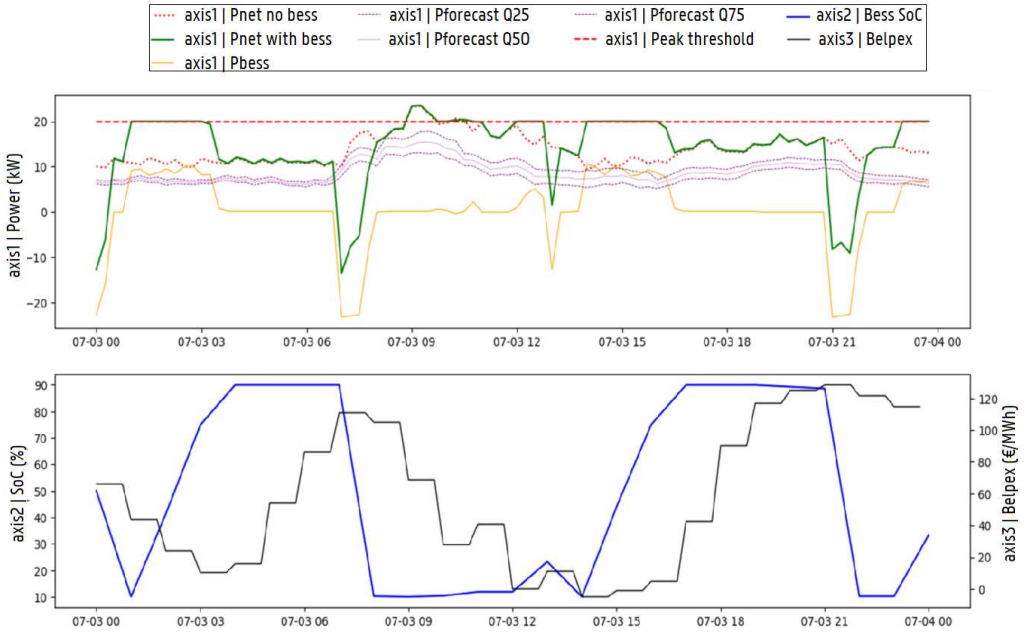


Figure 57: Scenario D – optimization output

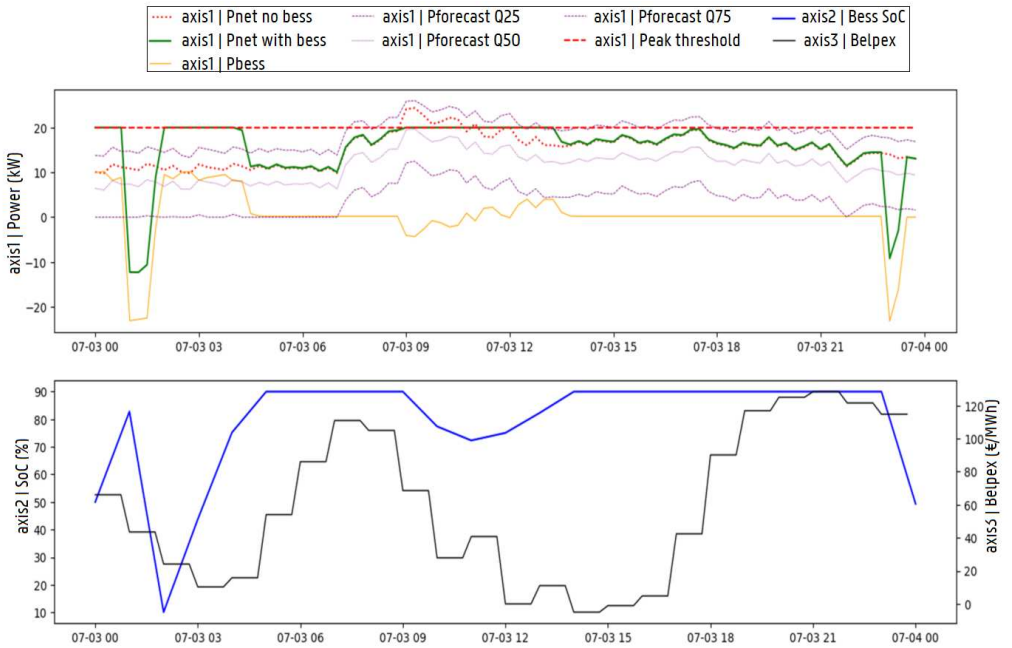


Figure 58: Scenario E – optimization output

6.4 CONCLUSIONS

In this research work, we developed an algorithm for solving the day-ahead problem co-optimizing pricing arbitrage and peak shaving through battery storage systems. The algorithm can be applied for enterprise users with dynamic pricing contracts. The algorithm is based on the standard DQN architecture which is suitable for solving MDPs having a continuous state space and a discrete action space. We tested the algorithm in different scenarios by changing the system topology (no PV, with PV) and varying the forecasting uncertainty (deterministic, probabilistic). The algorithm finds the optimal solution in deterministic environments. Furthermore, it finds a suboptimal solution in a probabilistic environment provided that the load (and PV) forecast are sufficiently accurate as not to violate the peak threshold constraint. What is more, we showed that in occasions where the forecast is not good, co-optimizing peak shaving with pricing arbitrage could fail and lead to catastrophic effects for the total annual cost of the system. Inevitably, the use of a circuit breaker is recommended to guarantee 100 % no violation of the peak threshold constraint. Finally, we explained how to adjust the forecasting profile as a safeguard to prioritize the peak shaving application in occasions where there is high uncertainty on the load (and/or PV) forecast.

7 Final thoughts, discussion for future work

This PhD thesis is a contribution to the ongoing research field of battery storage systems in stationary applications. At the beginning of this PhD, back in 2018, the ultimate goal was to develop a master Energy Management System (EMS) that would allow the BESS to operate in value stacking mode by co-optimizing several revenue streams from applications such as ancillary services, PV self-sufficiency, peak shaving, pricing arbitrage etc. We started with a review of the electricity market landscape in Belgium and we showed how these market mechanisms open up opportunities for batteries to deliver value to end users such as enterprises and households. We evaluated the potential of each possible application taking into account different factors. Is it a special non-reproducible application or can it be generalized to multiple use cases? What is the current regulatory framework under consideration, how stable is it and where are we heading to? How does the revenue formula work e.g., electricity tariff structure, auction trading platform? We opted to leave ancillary services out of scope given the ongoing transition phase to integrate the balancing reserves at pan-European level but also due to its limited market size. We decided to explore the value of battery storage on three applications: (i) increasing the self-sufficiency of renewable energy installations, (ii) peak shaving and (iii) pricing arbitrage. In Chapter 3, we investigated how the battery increases the self-sufficiency in a hybrid PV-wind plant powering a hydrogen electrolyzer. From there, we decided to further explore the impact of time resolution in Chapter 4 where we introduced the first version of our BESS power flow model. Afterwards, in Chapter 5, we moved our focus on peak shaving where we analyzed the techno-economic potential of peak shaving on 40 enterprise users; there we introduced the dichotomy method for dimensioning the BESS and we also upgraded the power flow model by integrating non-linearity in the dc/ac efficiency curve. An important conclusion was that the BESS is underutilized in most cases indicating that peak shaving can be combined with another application. Finally in Chapter 6, we proposed and tested an optimization algorithm for peak shaving and pricing arbitrage considering forecasting uncertainty on the load and PV forecast. We tested different scenarios by changing the system topology and by varying the forecasting accuracy of the model.

After having explored in depth the battery storage landscape, we conclude that the development of a multi-objective EMS is quite a challenging task especially when the different applications are served concurrently. First of all, one would argue that the electricity market in general is constantly in transition. A BESS is not like a PV or a wind installation that once it is commissioned it injects power to the grid for the next 20 years. To serve a customer on the long term, the EMS of a BESS must be sufficiently flexible to adapt to new regulatory conditions, market prices and changes inside the end user's infrastructure. The more applications we

consider, the higher the maintenance effort we exert. Another issue to consider is the need for accurate power forecasts. When we first started with this thesis, we were in a sense preoccupied that forecasting would not be a problem; big data and deep learning were taking over the research world and given the latest breakthroughs on that field we believed that sooner or later this would apply in the energy sector as well. We were wrong in this assumption. The main challenge in electric power forecasts has nothing to do with the algorithm under consideration. It is the quality of the data inputs. A simple parametric regression model would beat the most advanced deep learning model if the first has a much better dataset input. Unfortunately, the acquisition of such datasets is quite a difficult task if not infeasible. In the great majority of use cases, the data input of the forecaster is retrieved from the energy meter (AMR or digital meter) possibly combined with a weather forecast. Unless the user has a crystal clear correlation in function of datetime indexes (e.g., day of the week, hour of the day, month of year) there is inevitably a non-negligible stochasticity in his power profile.

One of the priorities in our research work was to consider whenever possible real market data in our case studies. We developed a full electricity invoice model applicable in Flanders, Belgium and updated it according to the latest evolutions. As already mentioned, an important cost component of the electricity invoice in retail markets is imposed by the DSO for using the distribution grid infrastructure. At this point it is worth mentioning, starting from 2024, the DSO in Flanders (Fluvius) is planning to integrate a new time-of-use (ToU) factor in his tariff structure. As the number of wind and PV installations increases, the distribution grid becomes more prone to congestion issues that exhibit ToU characteristics. The highest peaks on the distribution grid occur due to large power offtakes during the winter for a few hours in the evening. So far, the distribution grid tariffs are mainly offtake-based rather than injection-based. Nevertheless, studies show, that in the future, high peaks can happen also due to power injection especially during the summer in the midday, primarily caused by PV. It would be interesting for future research in the field to investigate the impact of ToU on BESS applications, especially with respect to pricing arbitrage. Another important evolution introduced by Fluvius is the upcoming flex market for managing local congestion issues [136]. Although generally speaking the hosting capacity of the grid is still large enough to support the ongoing electrification the DSO has expressed its concerns especially after 2030. To avoid expensive infrastructure upgrades the DSO is willing to engage into bilateral or multilateral agreements with flex providers. Similarly to the balancing market mechanism, users with flexible assets such as EVs and batteries can make a contract with the DSO to sell their power capacity for specific time slots during the day. It would be interesting to address this topic also in future research works; how does it work and what does it mean for a BESS operating in value stacking mode ?

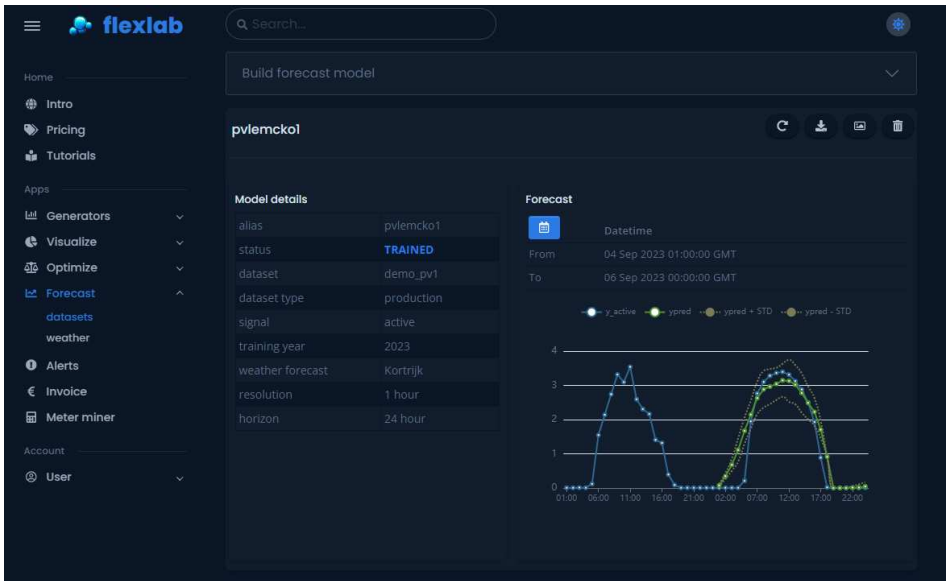
As the electricity market evolves with the increased penetration of renewables, our planning is shifted closer to real time. The day-ahead market is an important pillar for pricing arbitrage. What is more, the procurement of balancing reserves occurs through daily auctions. The load and power source profiles exhibit periodicities of daily cycles. With respect to multi-objective BESS EMS, all the above indicate that a day-ahead planning is becoming the norm. Our recommendation for future research in the field of multi-objective EMS is to approach the problem in daily segments. In a first phase, the user has to decide which applications will be considered for the next day. Here, the user allocates the BESS resource based on a priority ranking from the most to the least critical application. For instance when combining peak shaving with any other application, peak shaving has the highest priority; violating the peak threshold on a single sub-hourly quarter would affect the total annual electricity cost. In another example, combining ancillary services with the self-sufficiency of PV, the ancillary services have the highest priority; the BSP is obliged to follow the Elia activation signal as specified in the BSP contract and any serious deviation from is subject to fines. In a second phase, after selecting the applications, the EMS would conduct intra-day optimizations following the latest forecasts and unforeseen events.

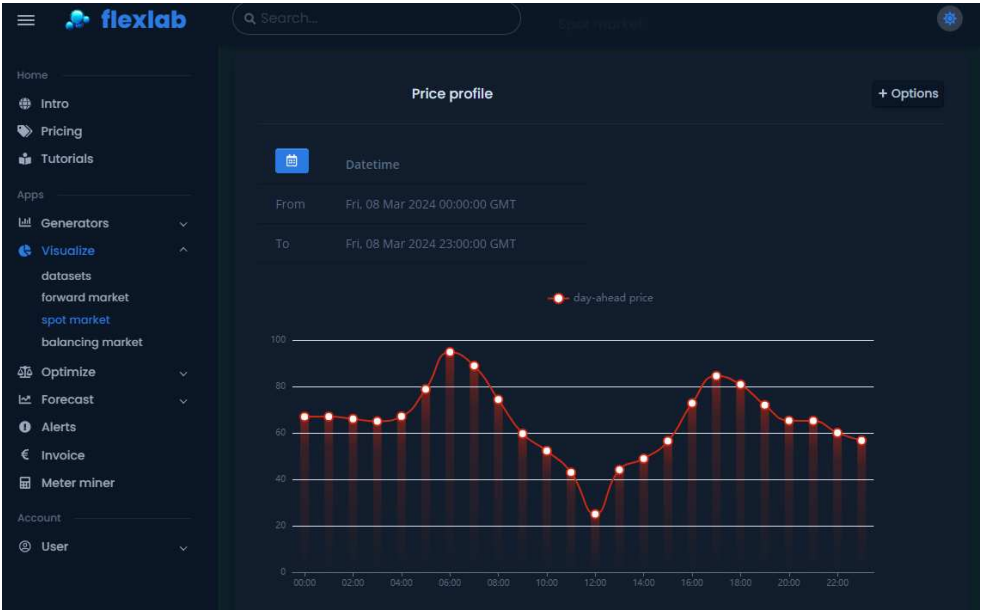
8 Annex – FlexLab

Over the past 2 years (2022–2024) this PhD has been the foundation towards the development of what we call “FlexLab” (Flexible Laboratory), a SaaS (Software as a Service) web application for electricity end users. FlexLab comes with a suite of energy tools designed for the non-expert user providing insights in different areas of interest. At this moment, FlexLab consists of seven main tool categories:

1. Visualize: A dashboard for visualizing the user's datasets and prices from the Belgian electricity market including day-ahead, forward and balancing market of Elia.
2. Meter miner: A natural language chat-GPT powered bot that runs queries on the user data retrieved from his digital meter.
3. Generators: A tool for generating synthetic load and PV profiles.
4. Forecast: A tool that trains power forecasting models based on artificial neural networks, weather forecast and historic measurements.
5. Alerts: A tool that generates alerts on selected by the user signals (e.g., market prices, power profiles) and informs when critical thresholds have been violated.
6. Invoice: An electricity invoice model, currently applies only in Flanders, Belgium. The user can specify his offtake and/or injection, type of connection and energy supply contract then getting an estimation of the total bill in annual, monthly and sub-hourly (15 min) resolution.
7. Optimize: A suite of optimization modules for BESS. Currently two modules are included: (i) a peak shaving sizing tool, (ii) day-ahead pricing arbitrage under peak threshold constraints

The entire programming stack has been built using open source tools (Python, JavaScript and HTML). The cloud architecture was implemented in Microsoft Azure. At this moment, FlexLab is in valorization phase. Different stakeholders (e.g., consultants, energy suppliers, research fellows) have expressed interest for our web application. So far, the feedback we received is very positive and gives validation to its conceptualization. In the future, there are plans to upgrade the application adding new tools including flexible assets such as electric vehicles and heat pumps. We also plan to integrate a REST framework to allow further compatibility with third party hardware devices. Closing this section, we give some illustrations how the web application looks like.





Bibliography

- [1] V. Papadopoulos, J. Desmet, J. Knockaert, and C. Develder, "Improving the utilization factor of a PEM electrolyzer powered by a 15 MW PV park by combining wind power and battery storage - Feasibility study," *International Journal of Hydrogen Energy*, vol. 43, no. 34, pp. 16468-16478, Aug 23 2018, doi: 10.1016/j.ijhydene.2018.07.069.
- [2] V. Papadopoulos, J. Knockaert, C. Develder, and J. Desmet, "Investigating the need for real time measurements in industrial wind power systems combined with battery storage," *Applied Energy*, vol. 247, pp. 559-571, Aug 1 2019, doi: 10.1016/j.apenergy.2019.04.051.
- [3] V. Papadopoulos, J. Knockaert, C. Develder, and J. Desmet, "Peak Shaving through Battery Storage for Low-Voltage Enterprises with Peak Demand Pricing," *Energies*, vol. 13, no. 5, 2020, doi: 10.3390/en13051183.
- [4] Sibelga. www.sibelga.be
- [5] Fluvius. www.fluvius.be
- [6] ORES. www.ores.be
- [7] N. Kraftwerke. www.next-kraftwerke.be
- [8] Elia. www.elia.be
- [9] "The current electricity market design in Europe," KU Leuven, 2015. [Online]. Available: https://set.kuleuven.be/ei/images/EI_factsheet8_eng.pdf
- [10] A. Phung, "Forward Contracts vs Futures Contracts: What's the Difference?." [Online]. Available: <https://www.investopedia.com/ask/answers/06/forwardsandfutures.asp>
- [11] "Les marchés de l'électricité - Comprendre les différents marchés et les différents prix de l'électricité," ENGIE, 2023.
- [12] "What is Day-Ahead trading of Electricity," Next Kraftwerke. [Online]. Available: <https://www.next-kraftwerke.com/knowledge/day-ahead-trading-electricity>
- [13] "Basics of the Power Market," EPEXSPOT. [Online]. Available: <https://www.epexspot.com/en/basicspowermarket>
- [14] "Trading at EPEXSPOT," EPEXSPOT, 2022. [Online]. Available: https://www.epexspot.com/sites/default/files/2022-07/22-07-12_TradingBrochure.pdf

- [15] "Single Day-Ahead Coupling (SDAC)," ENTSO-E. [Online]. Available: https://www.entsoe.eu/network_codes/cacm/implementation/sdac/
- [16] "What does intraday trading mean?," Next Kraftwerke. [Online]. Available: <https://www.next-kraftwerke.com/knowledge/intraday-trading>
- [17] "Single Intraday Coupling (SIDC)," ENTSO-E. [Online]. Available: https://www.entsoe.eu/network_codes/cacm/implementation/sidc/
- [18] Elia, "MFRR 2020 PRODUCT DESIGN NOTE," 2020. [Online]. Available: <https://www.elia.be/en/publications>
- [19] Elia, "Rules for the compensation of the quarter-hourly imbalances," 2020. [Online]. Available: <https://www.elia.be/en/publications>
- [20] "Frequency Containment Reserve (FCR)," ENTSO-E. [Online]. Available: https://www.entsoe.eu/network_codes/eb/fcr/
- [21] "Platform for the International Coordination of Automated Frequency Restoration and Stable System Operation (PICASSO)," ENTSO-E. [Online]. Available: https://www.entsoe.eu/network_codes/eb/picasso/
- [22] "Manually Activated Reserves Initiative (MARI)," ENTSO-E. [Online]. Available: https://www.entsoe.eu/network_codes/eb/mari/
- [23] J. Baetens, J. Laveyne, G. Van Eetvelde, and L. Vandeveldel, "Imbalance Pricing Methodology in Belgium: Implications for Industrial Consumers," presented at the 17th International Conference on the European Energy Market (EEM), Stockholm, Sweden, 2020.
- [24] Elia, "2019 Design Note FCR for 2020," 2019. [Online]. Available: <https://www.elia.be/en/publications>
- [25] J. Engels, "Integration of Flexibility from Battery Storage in the Electricity Market," 2020.
- [26] S. O. Amrouche, D. Rekioua, T. Rekioua, and S. Bacha, "Overview of energy storage in renewable energy systems," *International Journal of Hydrogen Energy*, vol. 41, no. 45, pp. 20914-20927, Dec 7 2016, doi: 10.1016/j.ijhydene.2016.06.243.
- [27] IEA, "Technology Roadmap: Energy Storage," 2014. [Online]. Available: <https://www.iea.org/reports/technology-roadmap-energy-storage>
- [28] M. Aneke and M. H. Wang, "Energy storage technologies and real life applications - A state of the art review," *Applied Energy*, vol. 179, pp. 350-377, Oct 1 2016, doi: 10.1016/j.apenergy.2016.06.097.

- [29] M. S. Guney and Y. Tepe, "Classification and assessment of energy storage systems," *Renewable & Sustainable Energy Reviews*, vol. 75, pp. 1187-1197, Aug 2017, doi: 10.1016/j.rser.2016.11.102.
- [30] T. A. Hamad *et al.*, "Hydrogen recovery, cleaning, compression, storage, dispensing, distribution system and End-Uses on the university campus from combined heat, hydrogen and power system," *International Journal of Hydrogen Energy*, vol. 39, no. 2, pp. 647-653, Jan 13 2014, doi: 10.1016/j.ijhydene.2013.10.111.
- [31] S. Singh *et al.*, "Hydrogen: A sustainable fuel for future of the transport sector," *Renewable & Sustainable Energy Reviews*, vol. 51, pp. 623-633, Nov 2015, doi: 10.1016/j.rser.2015.06.040.
- [32] G. Aparicio, Z. Andreas, C. Francesco, M. Fabio, H. Thomas, and B. Jake, "EMHIREs dataset Part I: Wind power generation," JRC Science Hub, 2016. [Online]. Available: https://setis.ec.europa.eu/emhires-dataset-part-i-wind-power-generation_en
- [33] M. Momirlan and T. N. Veziroglu, "The properties of hydrogen as fuel tomorrow in sustainable energy system for a cleaner planet," *International Journal of Hydrogen Energy*, vol. 30, no. 7, pp. 795-802, Jul 2005, doi: 10.1016/j.ijhydene.2004.10.011.
- [34] C. A. Cottrell, S. E. Grasman, M. Thomas, K. B. Martin, and J. W. Sheffield, "Strategies for stationary and portable fuel cell markets," *International Journal of Hydrogen Energy*, vol. 36, no. 13, pp. 7969-7975, Jul 2011, doi: 10.1016/j.ijhydene.2011.01.056.
- [35] A. Isenstadt and N. Lutsey, "Developing hydrogen fueling infrastructure for fuel cell vehicles: A status update," The International Council on Clean Transportation, 2017. [Online]. Available: https://theicct.org/sites/default/files/publications/Hydrogen-infrastructure-status-update_ICCT-briefing_04102017_vF.pdf
- [36] A. A. Agll, T. A. Hamad, Y. M. Hamad, S. G. Bapat, and J. W. Sheffield, "Development of design a drop-in hydrogen fueling station to support the early market buildout of hydrogen infrastructure," *International Journal of Hydrogen Energy*, vol. 41, no. 10, pp. 5284-5295, Mar 16 2016, doi: 10.1016/j.ijhydene.2016.01.138.
- [37] D. Celik and M. Yildiz, "Investigation of hydrogen production methods in accordance with green chemistry principles," *International Journal of Hydrogen Energy*, vol. 42, no. 36, pp. 23395-23401, Sep 7 2017, doi: 10.1016/j.ijhydene.2017.03.104.
- [38] I. Dincer and C. Acar, "Review and evaluation of hydrogen production methods for better sustainability," *International Journal of Hydrogen Energy*, vol. 40, no. 34, pp. 11094-11111, Sep 14 2015, doi: 10.1016/j.ijhydene.2014.12.035.
- [39] F. Suleman, I. Dincer, and M. Agelin-Chaab, "Comparative impact assessment study of various hydrogen production methods in terms of emissions," *International Journal*

of Hydrogen Energy, vol. 41, no. 19, pp. 8364-8375, May 25 2016, doi: 10.1016/j.ijhydene.2015.12.225.

- [40] P. Nikolaidis and A. Poullikkas, "A comparative overview of hydrogen production processes," *Renewable & Sustainable Energy Reviews*, vol. 67, pp. 597-611, Jan 2017, doi: 10.1016/j.rser.2016.09.044.
- [41] S. B. Walker, D. van Lanen, M. Fowler, and U. Mukherjee, "Economic analysis with respect to Power-to-Gas energy storage with consideration of various market mechanisms," *International Journal of Hydrogen Energy*, vol. 41, no. 19, pp. 7754-7765, May 25 2016, doi: 10.1016/j.ijhydene.2015.12.214.
- [42] M. Kopp, D. Coleman, C. Stiller, K. Scheffer, J. Aichinger, and B. Scheppat, "Energiepark Mainz: Technical and economic analysis of the worldwide largest Power-to-Gas plant with PEM electrolysis," *International Journal of Hydrogen Energy*, vol. 42, no. 19, pp. 13311-13320, May 11 2017, doi: 10.1016/j.ijhydene.2016.12.145.
- [43] M. Felgenhauer and T. Hamacher, "State-of-the-art of commercial electrolyzers and on-site hydrogen generation for logistic vehicles in South Carolina," *International Journal of Hydrogen Energy*, vol. 40, no. 5, pp. 2084-2090, Feb 9 2015, doi: 10.1016/j.ijhydene.2014.12.043.
- [44] L. Viktorsson, J. T. Heinonen, J. B. Skulason, and R. Unnthorsson, "A Step towards the Hydrogen Economy-A Life Cycle Cost Analysis of A Hydrogen Refueling Station," *Energies*, vol. 10, no. 6, Jun 2017, doi: 10.3390/en10060763.
- [45] D. Parra and M. K. Patel, "Techno-economic implications of the electrolyser technology and size for power-to-gas systems (vol 41, pg 3748, 2016)," *International Journal of Hydrogen Energy*, vol. 41, no. 18, pp. 7527-7528, May 18 2016, doi: 10.1016/j.ijhydene.2016.03.114.
- [46] S. H. Siyal, D. Mentis, and M. Howells, "Economic analysis of standalone wind-powered hydrogen refueling stations for road transport at selected sites in Sweden," *International Journal of Hydrogen Energy*, vol. 40, no. 32, pp. 9855-9865, Aug 24 2015, doi: 10.1016/j.ijhydene.2015.05.021.
- [47] A. Khalilnejad and G. H. Riahy, "A hybrid wind-PV system performance investigation for the purpose of maximum hydrogen production and storage using advanced alkaline electrolyzer," *Energy Conversion and Management*, vol. 80, pp. 398-406, Apr 2014, doi: 10.1016/j.enconman.2014.01.040.
- [48] P. Hou, P. Enevoldsen, J. Eichman, W. H. Hu, M. Z. Jacobson, and Z. Chen, "Optimizing investments in coupled offshore wind -electrolytic hydrogen storage systems in Denmark," *Journal of Power Sources*, vol. 359, pp. 186-197, Aug 15 2017, doi: 10.1016/j.jpowsour.2017.05.048.

- [49] A. Al-Sharafi, A. Z. Sahin, T. Ayar, and B. S. Yilbas, "Techno-economic analysis and optimization of solar and wind energy systems for power generation and hydrogen production in Saudi Arabia," *Renewable & Sustainable Energy Reviews*, vol. 69, pp. 33-49, Mar 2017, doi: 10.1016/j.rser.2016.11.157.
- [50] M. Gökcek and C. Kale, "Techno-economical evaluation of a hydrogen refuelling station powered by Wind-PV hybrid power system: A case study for Izmir-Cesme," *Int.J. Hydrogen Energy*, vol. 43, no. 23, pp. 10615-10625, 7 June 2018 2018, doi: 10.1016/j.ijhydene.2018.01.082.
- [51] R. Shandarr, C. A. Trudewind, and P. Zapp, "Life cycle assessment of hydrogen production via electrolysis - a review," *Journal of Cleaner Production*, vol. 85, pp. 151-163, Dec 15 2014, doi: 10.1016/j.jclepro.2013.07.048.
- [52] W. S. M Kaltschmitt, A Wiese, *Renewable energy: technology, economics and environment*. 2007.
- [53] M. Uhrig, S. Koenig, M. R. Suriyah, and T. Leibfried, "Lithium-based vs. Vanadium Redox Flow Batteries - A Comparison for Home Storage Systems," *10th International Renewable Energy Storage Conference, Ires 2016*, vol. 99, pp. 35-43, 2016, doi: 10.1016/j.egypro.2016.10.095.
- [54] P. Alotto, M. Guarnieri, and F. Moro, "Redox flow batteries for the storage of renewable energy: A review," *Renewable & Sustainable Energy Reviews*, vol. 29, pp. 325-335, Jan 2014, doi: 10.1016/j.rser.2013.08.001.
- [55] J. Eichman, "Hydrogen Energy Storage: Experimentnal Analysis and Modeling," National Renewable Energy Laboratory (NREL), 2014. [Online]. Available: <https://www.energy.gov/eere/fuelcells/articles/increasing-renewable-energy-hydrogen-storage-and-fuel-cell-technologies>
- [56] K. Abdulla, K. Steer, A. Wirth, J. de Hoog, and S. Halgamuge, "The Importance of Temporal Resolution in Evaluating Residential Energy Storage," *2017 Ieee Power & Energy Society General Meeting*, 2017, doi: 10.1109/PESGM.2017.8274019.
- [57] M. Gotz *et al.*, "Renewable Power-to-Gas: A technological and economic review," *Renewable Energy*, vol. 85, pp. 1371-1390, Jan 2016, doi: 10.1016/j.renene.2015.07.066.
- [58] CREG, "Nota over de opvallende evoluties op de Belgische groothandelsmarkten voor elektriciteit en aardgas in 2017," 2018. [Online]. Available: <https://www.creg.be/nl/publications>
- [59] "De prijs van water," Vlaamse Milieumaatschappij 2018. [Online]. Available: <https://www.vmm.be/waterloket/de-waterfactuur/de-prijs-van-water>

- [60] R. Luthander, J. Widen, D. Nilsson, and J. Palm, "Photovoltaic self-consumption in buildings: A review," *Applied Energy*, vol. 142, pp. 80-94, Mar 15 2015, doi: 10.1016/j.apenergy.2014.12.028.
- [61] K. L. Zhou, S. L. Yang, and Z. Shao, "Energy Internet: The business perspective," *Applied Energy*, vol. 178, pp. 212-222, Sep 15 2016, doi: 10.1016/j.apenergy.2016.06.052.
- [62] M. F. Zia, E. Elbouchikhi, and M. Benbouzid, "Microgrids energy management systems: A critical review on methods, solutions, and prospects," *Applied Energy*, vol. 222, pp. 1033-1055, Jul 15 2018, doi: 10.1016/j.apenergy.2018.04.103.
- [63] J. Apt, "The spectrum of power from wind turbines," *Journal of Power Sources*, vol. 169, no. 2, pp. 369-374, Jun 20 2007, doi: 10.1016/j.jpowsour.2007.02.077.
- [64] A. Mills *et al*, "Dark Shadows," *Ieee Power & Energy Magazine*, vol. 9, no. 3, pp. 33-41, May-Jun 2011, doi: 10.1109/Mpe.2011.940575.
- [65] S. Shedd, B.-M. Hodge, A. Florita, and K. Orwig, "A Statistical Characterization of Solar Photovoltaic Power Variability at Small Timescales," in *2nd Annual International Workshop on Integration of Solar Power into Power Systems Conference*, Lisbon, Portugal, 2012.
- [66] J. Van de Vyver, "Modellering en Emulatie van Kleine Windturbines," Diss. Master in de ingenieurswetenschappen: werktuigkunde-elektrotechniek, Faculty of Engineering and Architecture, Ghent University, 2012. [Online]. Available: <http://lib.ugent.be/catalog/ruq01:001887195>
- [67] T. Beck, H. Kondziella, G. Huard, and T. Bruckner, "Assessing the influence of the temporal resolution of electrical load and PV generation profiles on self-consumption and sizing of PV-battery systems," *Applied Energy*, vol. 173, pp. 331-342, Jul 1 2016, doi: 10.1016/j.apenergy.2016.04.050.
- [68] S. Ried, P. Jochem, and W. Fichtner, "Profitability of Photovoltaic Battery Systems Considering Temporal Resolution," *2015 12th International Conference on the European Energy Market (Eem)*, 2015, doi: 10.1109/EEM.2015.7216632.
- [69] A. Wright and S. Firth, "The nature of domestic electricity-loads and effects of time averaging on statistics and on-site generation calculations," *Applied Energy*, vol. 84, no. 4, pp. 389-403, Apr 2007, doi: 10.1016/j.apenergy.2006.09.008.
- [70] S. L. Cao and K. Siren, "Impact of simulation time-resolution on the matching of PV production and household electric demand," *Applied Energy*, vol. 128, pp. 192-208, Sep 1 2014, doi: 10.1016/j.apenergy.2014.04.075.
- [71] E. J. Hovenaars and C. A. Crawford, "Implications of temporal resolution for modeling renewables-based power systems," *Renewable Energy*, vol. 41, pp. 285-293, May 2012, doi: 10.1016/j.renene.2011.11.013.

- [72] L. Kools and F. Phillipson, "Data granularity and the optimal planning of distributed generation," *Energy*, vol. 112, pp. 342-352, Oct 1 2016, doi: 10.1016/j.energy.2016.06.089.
- [73] J. Widen, E. Wackelgard, J. Paatero, and P. Lund, "Impacts of different data averaging times on statistical analysis of distributed domestic photovoltaic systems (vol 84, pg 492, 2010)," *Solar Energy*, vol. 85, no. 1, pp. 214-214, Jan 2011, doi: 10.1016/j.solener.2010.11.015.
- [74] A. Hawkes and M. Leach, "Impacts of temporal precision in optimisation modelling of micro-combined heat and power," *Energy*, vol. 30, no. 10, pp. 1759-1779, Jul 2005, doi: 10.1016/j.energy.2004.11.012.
- [75] R. Tang, K. Abdulla, P. H. W. Leong, A. Vassallo, and J. Dore, "Impacts of temporal resolution and system efficiency on PV battery system optimisation," presented at the 2017 Solar Research Conference, 2017.
- [76] M. Lydia, S. S. Kumar, A. I. Selvakumar, and G. E. P. Kumar, "A comprehensive review on wind turbine power curve modeling techniques," *Renewable & Sustainable Energy Reviews*, vol. 30, pp. 452-460, Feb 2014, doi: 10.1016/j.rser.2013.10.030.
- [77] C. R. Birkl and D. A. Howey, "Model identification and parameter estimation for LiFePO₄ batteries," in *IET Hybrid and Electric Vehicles Conference (HEVC)*, 2013, doi: 10.1049/cp.2013.1889.
- [78] X. S. Hu, S. B. Li, and H. Peng, "A comparative study of equivalent circuit models for Li-ion batteries," *Journal of Power Sources*, vol. 198, pp. 359-367, Jan 15 2012, doi: 10.1016/j.jpowsour.2011.10.013.
- [79] D. Ansean, M. Gonzalez, J. C. Viera, V. M. Garcia, C. Blanco, and M. Valledor, "Fast charging technique for high power lithium iron phosphate batteries: A cycle life analysis," *Journal of Power Sources*, vol. 239, pp. 9-15, Oct 1 2013, doi: 10.1016/j.jpowsour.2013.03.044.
- [80] F. Baronti, W. Zanaboni, R. Roncella, R. Saletti, and G. Spagnuo, "Open-Circuit Voltage Measurement of Lithium-Iron-Phosphate Batteries," *2015 IEEE International Instrumentation and Measurement Technology Conference (I2MTC)*, pp. 1711-1716, 2015, doi: 10.1109/I2MTC.2015.7151538.
- [81] O. Palizban and K. Kauhaniemi, "Energy storage systems in modern grids-Matrix of technologies and applications," *Journal of Energy Storage*, vol. 6, pp. 248-259, May 2016, doi: 10.1016/j.est.2016.02.001.
- [82] M. C. Argyrou, P. Christodoulides, and S. A. Kalogirou, "Energy storage for electricity generation and related processes: Technologies appraisal and grid scale

- applications," *Renewable & Sustainable Energy Reviews*, vol. 94, pp. 804-821, October 2018 2018, doi: 10.1016/j.rser.2018.06.044.
- [83] T. M. U. N. Mohan, W.P. Robbins, *Converters, applications and design*. John Wiley and Sons Inc, 2003.
- [84] H. X. Wang, M. A. Munoz-Garcia, G. P. Moreda, and M. C. Alonso-Garcia, "Optimum inverter sizing of grid-connected photovoltaic systems based on energetic and economic considerations," *Renewable Energy*, vol. 118, pp. 709-717, Apr 2018, doi: 10.1016/j.renene.2017.11.063.
- [85] X. Fleury, M. H. Noh, S. Genies, P. X. Thivel, C. Lefrou, and Y. Bultel, "Fast-charging of Lithium Iron Phosphate battery with ohmic-drop compensation method: Ageing study," *Journal of Energy Storage*, vol. 16, pp. 21-36, Apr 2018, doi: 10.1016/j.est.2017.12.015.
- [86] X. Luo, J. Wang, M. Dooner, and J. Clarke, "Overview of current development in electrical energy storage technologies and the application potential in power system operation," *Applied Energy*, vol. 137, pp. 511 - 536, 1 January 2015, doi: 10.1016/j.apenergy.2014.09.081.
- [87] P. Keil and A. Jossen, "Charging protocols for lithium-ion batteries and their impact on cycle life-An experimental study with different 18650 high-power cells," *Journal of Energy Storage*, vol. 6, pp. 125-141, May 2016, doi: 10.1016/j.est.2016.02.005.
- [88] S. Ahmadi and S. Abdi, "Application of the Hybrid Big Bang-Big Crunch algorithm for optimal sizing of a stand-alone hybrid PV/wind/battery system," *Solar Energy*, vol. 134, pp. 366-374, Sep 2016, doi: 10.1016/j.solener.2016.05.019.
- [89] A. Fathy, "A reliable methodology based on mine blast optimization algorithm for optimal sizing of hybrid PV-wind-FC system for remote area in Egypt," *Renewable Energy*, vol. 95, pp. 367-380, Sep 2016, doi: 10.1016/j.renene.2016.04.030.
- [90] A. Maheri, "Multi-objective design optimisation of standalone hybrid wind-PV-diesel systems under uncertainties," *Renewable Energy*, vol. 66, pp. 650-661, Jun 2014, doi: 10.1016/j.renene.2014.01.009.
- [91] S. Sanajaoba and E. Fernandez, "Maiden application of Cuckoo Search algorithm for optimal sizing of a remote hybrid renewable energy System," *Renewable Energy*, vol. 96, pp. 1-10, Oct 2016, doi: 10.1016/j.renene.2016.04.069.
- [92] M. Tahani, N. Babayan, and A. Pouyaei, "Optimization of PV/Wind/Battery stand-alone system, using hybrid FPA/SA algorithm and CFD simulation, case study: Tehran," *Energy Conversion and Management*, vol. 106, pp. 644-659, Dec 2015, doi: 10.1016/j.enconman.2015.10.011.

- [93] M. Antonelli, U. Desideri, and A. Franco, "Effects of large scale penetration of renewables: The Italian case in the years 2008-2015," *Renewable & Sustainable Energy Reviews*, vol. 81, pp. 3090-3100, Jan 2018, doi: 10.1016/j.rser.2017.08.081.
- [94] J. O. Petinrin and M. Shaaban, "Impact of renewable generation on voltage control in distribution systems," *Renewable & Sustainable Energy Reviews*, vol. 65, pp. 770-783, Nov 2016, doi: 10.1016/j.rser.2016.06.073.
- [95] P. Simshauser, "Distribution network prices and solar PV: Resolving rate instability and wealth transfers through demand tariffs," *Energy Economics*, vol. 54, pp. 108-122, Feb 2016, doi: 10.1016/j.eneco.2015.11.011.
- [96] K. Lummi, A. Rautiainen, P. Jarventausta, P. Heine, J. Lehtinen, and M. Hyvarinen, "Cost-causation based approach in forming power-based distribution network tariff for small customers," *2016 13th International Conference on the European Energy Market (Eem)*, 2016, doi: 10.1109/EEM.2016.7521251.
- [97] W. Strielkowski, D. Streimikiene, and Y. Bilan, "Network charging and residential tariffs: A case of household photovoltaics in the United Kingdom," *Renewable & Sustainable Energy Reviews*, vol. 77, pp. 461-473, Sep 2017, doi: 10.1016/j.rser.2017.04.029.
- [98] VREG, "Consultatiedocument tariefstructuur periodieke distributienettarieven elektriciteit voor klanten met een kleinverbruiksmeterinrichting," 2019. [Online]. Available: <https://www.vreg.be/sites/default/files/document/cons-2019-02.pdf>
- [99] VREG, "Consultatiedocument tariefstructuur periodieke distributienettarieven elektriciteit voor klanten met een grootverbruiksmeterinrichting.," 2019. [Online]. Available: <https://www.vreg.be/sites/default/files/document/cons-2019-01.pdf>
- [100] V. Bertsch, J. Geldermann, and T. Luhn, "What drives the profitability of household PV investments, self-consumption and self-sufficiency?," *Applied Energy*, vol. 204, pp. 1-15, Oct 15 2017, doi: 10.1016/j.apenergy.2017.06.055.
- [101] E. Nyholm, J. Goop, M. Odenberger, and F. Johnsson, "Solar photovoltaic-battery systems in Swedish households - Self-consumption and self-sufficiency," *Applied Energy*, vol. 183, pp. 148-159, Dec 1 2016, doi: 10.1016/j.apenergy.2016.08.172.
- [102] G. E. Silva and P. Hendrick, "Lead-acid batteries coupled with photovoltaics for increased electricity self-sufficiency in households," *Applied Energy*, vol. 178, pp. 856-867, Sep 15 2016, doi: 10.1016/j.apenergy.2016.06.003.
- [103] J. Huvilina, "Value of Battery Energy Storage at Ancillary Service Markets " Master, Department of Electrical Engineering and Automation, Aalto University, 2015. [Online]. Available: <https://aaltodoc.aalto.fi>

- [104] M. Koller, T. Borsche, A. Ulbig, and G. Andersson, "Review of grid applications with the Zurich 1 MW battery energy storage system," *Electric Power Systems Research*, vol. 120, pp. 128-135, Mar 2015, doi: 10.1016/j.epsr.2014.06.023.
- [105] I. Staffell and M. Rustomji, "Maximising the value of electricity storage," *Journal of Energy Storage*, vol. 8, pp. 212-225, Nov 2016, doi: 10.1016/j.est.2016.08.010.
- [106] J. Leadbetter and L. Swan, "Battery storage system for residential electricity peak demand shaving," *Energy and Buildings*, vol. 55, pp. 685-692, Dec 2012, doi: 10.1016/j.enbuild.2012.09.035.
- [107] A. Oudalov, R. Cherkaoui, and A. Beguin, "Sizing and optimal operation of battery energy storage system for peak shaving application," *2007 IEEE Lausanne Powertech, Vols 1-5*, pp. 621-+, 2007, doi: 10.1109/Pct.2007.4538388.
- [108] M. Rowe, T. Yunusov, S. Haben, C. Singleton, W. Holderbaum, and B. Potter, "A Peak Reduction Scheduling Algorithm for Storage Devices on the Low Voltage Network," *IEEE Transactions on Smart Grid*, vol. 5, no. 4, pp. 2115-2124, Jul 2014, doi: 10.1109/Tsg.2014.2323115.
- [109] S. Govindan, D. Wang, A. Sivasubramaniam, and B. Urgaonkar, "Leveraging Stored Energy for Handling Power Emergencies in Aggressively Provisioned Datacenters," *Asplos XVII: Seventeenth International Conference on Architectural Support for Programming Languages and Operating Systems*, pp. 75-86, 2012, doi: 10.1145/2248487.2150985.
- [110] V. Kontorinis *et al.*, "Managing Distributed UPS Energy for Effective Power Capping in Data Centers," *2012 39th Annual International Symposium on Computer Architecture (ISCA)*, pp. 488-499, 2012, doi: 10.1109/ISCA.2012.6237042.
- [111] G. Fitzgerald, J. Mandel, J. Morris, and H. Touati, "The Economics of Battery Energy Storage: How multi-use, customer-sited batteries deliver the most services and value to customers and the grid," *Rocky Mountain Institute*, 2015.
- [112] S. Energy, "Making the commercial case for battery storage," 2016. [Online]. Available: <https://www.smartestenergy.com/media/1577/making-the-commercial-case-for-battery-storage-smartestenergy.pdf>
- [113] A. Lucas and S. Chondrogiannis, "Smart grid energy storage controller for frequency regulation and peak shaving, using a vanadium redox flow battery," *International Journal of Electrical Power & Energy Systems*, vol. 80, pp. 26-36, Sep 2016, doi: 10.1016/j.ijepes.2016.01.025.
- [114] K. H. Chua, Y. S. Lim, and S. Morris, "A novel fuzzy control algorithm for reducing the peak demands using energy storage system," *Energy*, vol. 122, pp. 265-273, Mar 1 2017, doi: 10.1016/j.energy.2017.01.063.

- [115] B. Aksanli, T. Rosing, and E. Pettis, "Distributed Battery Control for Peak Power Shaving in Datacenters," *2013 International Green Computing Conference (Igcc)*, 2013, doi: 10.1109/IGCC.2013.6604477.
- [116] D. S. Palasamudram, R. K. Sitaraman, B. Urgaonkar, and R. Urgaonkar, "Using batteries to reduce the power costs of internet-scale distributed networks," presented at the Proceedings of the Third ACM Symposium on Cloud Computing, San Jose, California, 2012.
- [117] K. H. Chua, Y. S. Lim, and S. Morris, "Energy storage system for peak shaving," *International Journal of Energy Sector Management*, vol. 10, no. 1, pp. 3-18, 2016, doi: 10.1108/Ijesm-01-2015-0003.
- [118] M. Garcia-Plaza, J. E. G. Carrasco, J. Alonso-Martinez, and A. P. Asensio, "Peak shaving algorithm with dynamic minimum voltage tracking for battery storage systems in microgrid applications," *Journal of Energy Storage*, vol. 20, pp. 41-48, Dec 2018, doi: 10.1016/j.est.2018.08.021.
- [119] "Evolutie energieprijzen en distributienettarieven," VREG, 2019. [Online]. Available: <https://www.vreg.be/nl/energiemarkt-cijfers>
- [120] K. Liu, Y. Li, X. Hu, M. Lucu, and D. Widanalage, "Gaussian Process Regression with Automatic Relevance Determination Kernel for Calendar Aging Prediction of Lithium-ion Batteries," *IEEE Transactions on Industrial Informatics*, vol. PP, pp. 1-1, 2019, doi: 10.1109/TII.2019.2941747.
- [121] K. L. Liu, X. S. Hu, Z. L. Yang, Y. Xie, and S. Z. Feng, "Lithium-ion battery charging management considering economic costs of electrical energy loss and battery degradation," *Energy Conversion and Management*, vol. 195, pp. 167-179, Sep 1 2019, doi: 10.1016/j.enconman.2019.04.065.
- [122] G. Berckmans, M. Messagie, J. Smekens, N. Omar, L. Vanhaverbeke, and J. Van Mierlo, "Cost Projection of State of the Art Lithium-Ion Batteries for Electric Vehicles Up to 2030," *Energies*, vol. 10, no. 9, Sep 2017, doi: 10.3390/en10091314.
- [123] L. T. Youn and S. Cho, "Optimal Operation of Energy Storage Using Linear Programming Technique," *Wcecs 2009: World Congress on Engineering and Computer Science, Vols I and II*, pp. 480-+, 2009.
- [124] W. H. Hu, Z. Chen, and B. Bak-Jensen, "Optimal Operation Strategy of Battery Energy Storage System to Real-Time Electricity Price in Denmark," *Ieee Pes General Meeting*, 2010, doi: 10.1109/PES.2010.5590194.
- [125] Y. Li *et al.*, "Optimal battery schedule for grid-connected photovoltaic-battery systems of office buildings based on a dynamic programming algorithm," *Journal of Energy Storage*, vol. 50, Jun 2022, doi: 10.1016/j.est.2022.104557.

- [126] K. Abdulla *et al.*, "Optimal Operation of Energy Storage Systems Considering Forecasts and Battery Degradation," *Ieee Transactions on Smart Grid*, vol. 9, no. 3, pp. 2086-2096, 2018, doi: 10.1109/TSG.2016.2606490.
- [127] L. Hannah and D. Dunson, "Approximate Dynamic Programming for Storage Problems.," presented at the Proceedings of the 28th International Conference on Machine Learning (ICML), 2011.
- [128] D. R. Jiang, T. V. Pham, W. B. Powell, D. F. Salas, and W. R. Scott, "A Comparison of Approximate Dynamic Programming Techniques on Benchmark Energy Storage Problems: Does Anything Work?," *2014 IEEE Symposium on Adaptive Dynamic Programming and Reinforcement Learning (ADPRL)*, pp. 140-147, 2014, doi: 10.1109/ADPRL.2014.7010626.
- [129] L. C. A. Yan, W. T. Liu, W. Jiang, Y. Li, R. X. Li, and S. L. Hui, "Deep Reinforcement Learning based Optimization of Battery Charging and Discharging Management for Data Center," *2021 International Joint Conference on Neural Networks (Ijcnnc)*, 2021, doi: 10.1109/Ijcnnc52387.2021.9533476.
- [130] J. Cao, D. Harrold, Z. Fan, T. Morstyn, D. Healey, and K. Li, "Deep Reinforcement Learning-Based Energy Storage Arbitrage With Accurate Lithium-Ion Battery Degradation Model," *Ieee Transactions on Smart Grid*, vol. 11, no. 5, pp. 4513-4521, Sept 2020, doi: 10.1109/Tsg.2020.2986333.
- [131] V.-H. Bui, A. Hussain, and H.-M. Kim, "Double Deep Q-Learning-Based Distributed Operation of Battery Energy Storage System Considering Uncertainties," *Ieee Transactions on Smart Grid*, vol. PP, pp. 1-1, 06 2019, doi: 10.1109/TSG.2019.2924025.
- [132] X. Xi, R. Sioshansi, and V. Marano, "A stochastic dynamic programming model for co-optimization of distributed energy storage," *Energy Systems*, vol. 5, no. 3, pp. 475-505, 2014/09/01 2014, doi: 10.1007/s12667-013-0100-6.
- [133] V. Francois, D. Taralla, D. Ernst, and R. Fonteneau, "Deep Reinforcement Learning Solutions for Energy Microgrids Management," 12 2016.
- [134] D. J. B. Harrold, J. Cao, and Z. Fan, "Data-driven battery operation for energy arbitrage using rainbow deep reinforcement learning," *Energy*, vol. 238, Jan 1 2022, doi: 10.1016/j.energy.2021.121958.
- [135] D. Kingma and J. Ba, "Adam: A Method for Stochastic Optimization," *International Conference on Learning Representations*, 12 2014.
- [136] "Specificaties voor de marktgebaseerde aankoop van flexibiliteitsdiensten voor het beheer van lokale congestie," Fluvius, 2023. [Online]. Available: <https://partner.fluvius.be/sites/fluvius/files/2023-04/marktbevraging-specificaties-voor-marktflexibiliteit.pdf>



Futuristic battery storage warehouse (generated by Bing AI).